2. Mesoproterozoic Geology of the Blue Ridge Province in North-Central Virginia: Petrologic and Structural Perspectives on Grenvillian Orogenesis and Paleozoic Tectonic Processes

By Richard P. Tollo,[1] Christopher M. Bailey,[2] Elizabeth A. Borduas,[1] and John N. Aleinikoff[3]

Introduction

This field trip examines the geology of Grenvillian basement rocks located within the core of the Blue Ridge anticlinorium in north-central Virginia over a distance of 64 kilometers (km) (40 miles (mi)), from near Front Royal at the northern end of Shenandoah National Park southward to the vicinity of Madison. This guide presents results of detailed field mapping, structural analysis, petrologic and geochemical studies, and isotopic investigations of Mesoproterozoic rocks directed toward developing an understanding of the geologic processes involved in Grenvillian and Paleozoic orogenesis in the central Appalachians. Stops included in this field guide illustrate the lithologic and structural complexity of rocks constituting local Blue Ridge basement, and demonstrate the type of integrated, multidisciplinary studies that are necessary to decipher the protracted Mesoproterozoic through Paleozoic geologic history of the region.

The field trip traverses the crest of the Blue Ridge along Skyline Drive and the adjacent foothills located east of the mountains. This largely rural area is characterized by locally steep topography and land-use patterns that are dominated by agriculture and recreation. In late June 1995, a series of tropical storms affected parts of the central Virginia Piedmont and adjacent Appalachian Mountains. These storms produced abundant rainfall, ranging from 75 to 175 millimeters (mm) (3–6.9 inches (in)) throughout the region, which increased the moisture content of the relatively thin soils and shallow rock debris that cover the mountains (Wieczorek and others, 2000). On June 27, following this extended interval of rainfall, an exceptionally intense, localized period of precipitation, resulting from the interaction of tropical moisture and a cold front that stalled over the region, produced up to 770 mm (30.3 in) of rain in the vicinity of Graves Mills (near Stops 18 and 19) in northwestern Madison County. During this storm, more than 1,000 shallow rock, debris, and soil slides mobilized into debris flows that were concentrated in northwestern Madison County (Morgan and others, 1999). The debris flows removed large volumes of timber, soil, and rock debris, resulting in locally widened channels in which relatively unweathered bedrock commonly was exposed. Stops 18 and 19 are located within such channels, and are typical of the locally very large and unusually fresh exposures produced by the event. Materials transported by debris flows were typically deposited at constrictions in the valley pathways or on top of prehistoric fans located at the base of many of the valleys that provided passageways for the flows. Water emanating from the debris flows typically entered streams and rivers located in the valley floors bordering the mountains, greatly increasing flow volume and resulting in flooding and scoured channels. The enormous exposures at Stops 17 and 20 were enlarged and swept clean by scouring during this flooding event. Analysis of this and other events suggests that such high-magnitude, low-frequency events are a significant means of delivering coarse-grained regolith from mountainous hollows and channels to the lowland floodplains (Eaton and others, 2003). Such events may happen in the Appalachian mountains of Virginia and West Virginia with a recurrence interval of 10 to 15 years (Eaton and others, 2003).

Geology of the Blue Ridge Anticlinorium

The Blue Ridge province is one of a series of thrust-bounded inliers that expose Laurentian basement within the Appalachians (Rankin and others, 1989a). The province consists of two massifs: the Shenandoah, located mostly in Virginia, and the French Broad, which extends from western North Carolina to southwestern Virginia (fig. 1). The Shenandoah massif, where the field trip area is located, constitutes part of an allochthonous, northwest-vergent, thrust-bounded sheet that, in central and

[1]Department of Earth and Environmental Sciences, The George Washington University, Washington, DC 20052.

[2]Department of Geology, College of William and Mary, Williamsburg, VA 23187.

[3]U.S. Geological Survey, Denver, CO 80225.

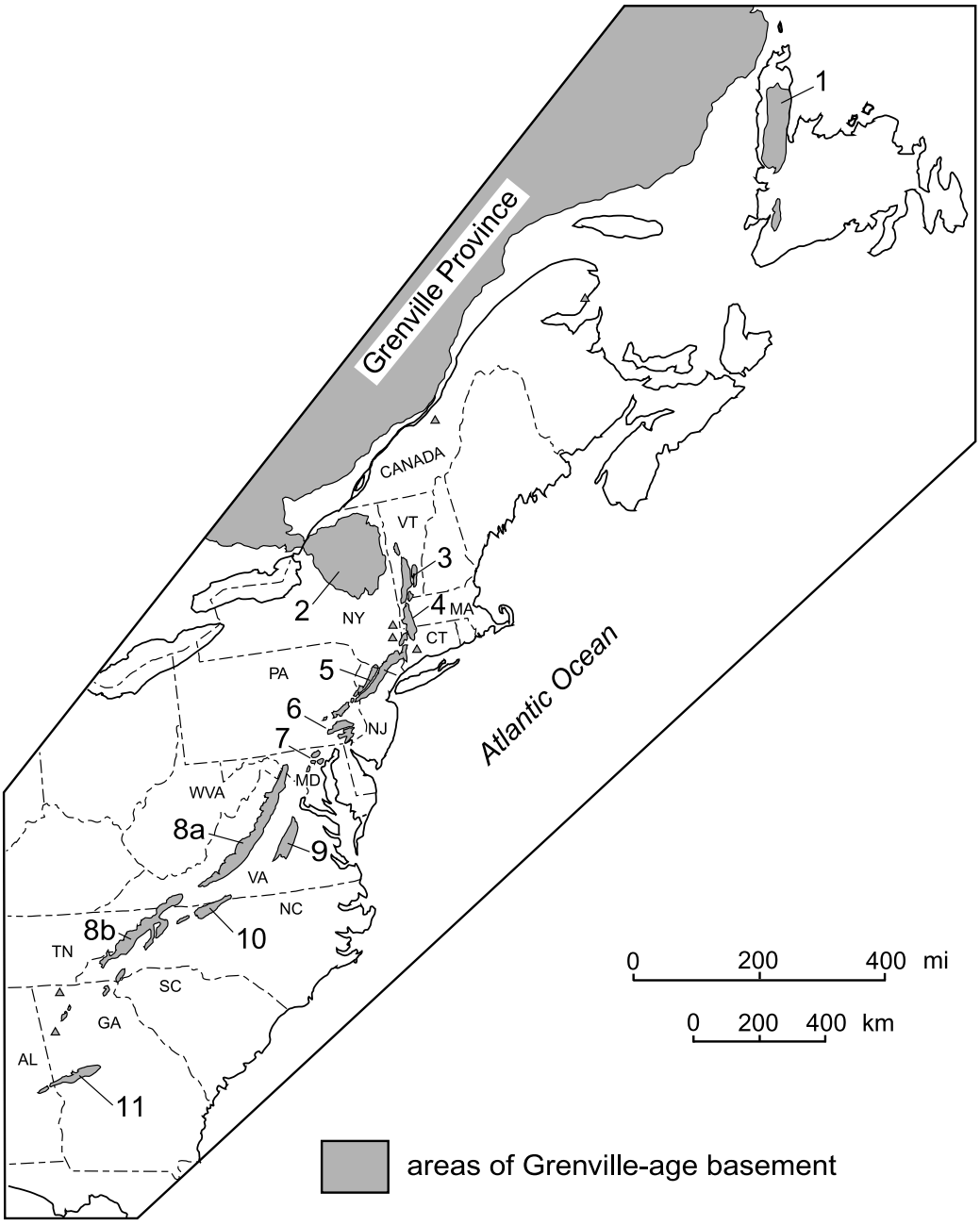

Figure 1. Map showing locations of major occurrences of Grenville-age basement in eastern North America. Labelled areas include: 1, Long Range massif; 2, Adirondack massif; 3, Green Mountains massif; 4, Berkshire massif; 5, Hudson Highlands–New Jersey Highlands–Reading prong; 6, Honey Brook upland; 7, Baltimore Gneiss antiforms; 8, Blue Ridge province, including Shenandoah (8a) and French Broad (8b) massifs; 9, Goochland terrane; 10, Sauratown Mountains anticlinorium; and 11, Pine Mountain belt. Map modified after Rankin and others (1989a).

northern Virginia, defines a northeast-trending anticlinorium that is overturned toward the northwest with Mesoproterozoic basement rocks constituting most of the core and a Neoproterozoic to lower Paleozoic cover sequence defining the limbs (Virginia Division of Mineral Resources, 1993) (fig. 2).

The igneous and high-grade metamorphic rocks of the basement preserve evidence of tectonic events associated with Grenvillian orogenesis at 1.2 to 1.0 Ga. These events resulted from a series of dominantly convergent tectonic events marking accretion of Laurentia and eventual assembly of the supercontinent Rodinia (Dalziel and others, 2000). Locally within the Blue Ridge massifs, as throughout much of the Grenville province of North America, Grenvillian orogenesis involved polyphase metamorphism, high-temperature deformation, and both synorogenic and postorogenic magmatism. In the Blue Ridge, these processes resulted in formation of a Mesoproterozoic terrane

composed of a wide range of plutonic rocks of largely granitic composition that contain screens and inliers of preexisting country rocks.

Eastern Laurentia and the Grenvillian orogen experienced two episodes of crustal extension during the Neoproterozoic (Badger and Sinha, 1988; Aleinikoff and others, 1995). Magmatic rocks formed during the first episode include granitoids and associated volcanic deposits of the 730- to 700-Ma Robertson River batholith (Tollo and Aleinikoff, 1996) and other smaller plutons that occur throughout the Blue Ridge province of Virginia and North Carolina. Collectively, these plutons were emplaced across the region during crustal extension at 760 to 680 Ma (Fetter and Goldberg, 1995; Su and others, 1994; Bailey and Tollo, 1998; Tollo and others, 2004). This earlier episode of encratonic rifting resulted in development of local-scale rift basins in which terrestrial and marine sedimentary deposits of the Fauquier, Lynchburg, and Mechum River, and Swift Run Formations were deposited (Wehr, 1988; Tollo and Hutson, 1996; Bailey and Peters, 1998). However, this episode of rifting did not lead to development of an ocean.

A second episode of Neoproterozoic extension at about 570 Ma produced extensive basaltic and relatively minor rhyolitic (only in the northern part of the anticlinorium) volcanism, ultimately resulting in creation of the pre-Atlantic Iapetus Ocean (Aleinikoff and others, 1995). The basaltic rocks produced during this latter episode constitute the Catoctin Formation, which includes a locally thick series of basaltic (now greenstone) lava flows and thin interlayered sedimentary deposits (Badger, 1989, 1999). Both the Catoctin basalts and sedimentary strata of the underlying and discontinuous Swift Run Formation were produced in a dynamic tectonic environment characterized by locally steep topography and local interaction between lava flows and stream systems, producing a series of complexly interlayered deposits that are well exposed on the western limb of the Blue Ridge anticlinorium (Simpson and Eriksson, 1989; Badger, 1999). Sedimentary deposits of the Lynchburg and Fauquier Formations, which underlie the Catoctin Formation on the east limb of the Blue Ridge anticlinorium, preserve a regional transition from braided-alluvial facies in the west to deeper-water facies in the east that is interpreted to result from a late Neoproterozoic hinge zone developed in response to extension-related crustal thinning (Wehr, 1988). The Catoctin Formation is overlain by rocks of the late Neoproterozoic to Early Cambrian Chilhowee Group and younger Paleozoic strata that were deposited on the rifted Laurentian margin during Iapetan onlap and represent local development of a tectonically passive margin (Simpson and Eriksson, 1989).

Blue Ridge basement rocks include igneous and metamorphic rocks containing orthopyroxene-bearing mineral assemblages (Rankin and others, 1989b; Bailey and others, 2003) that, in the latter, indicate that ambient metamorphic conditions reached granulite facies during Mesoproterozoic orogenesis (Spear, 1993). Many of these basement rocks and most of the overlying cover sequence display mineralogic evidence of metamorphism at upper greenschist-facies conditions that occurred as a result of Paleozoic orogenesis (Kunk and Burton, 1999). Paleozoic metamorphism is responsible for development of greenstone and chlorite-rich phyllite throughout the Catoctin Formation and some of the related cover rocks, and for production of retrograde minerals in the basement rocks such as biotite, chlorite, and uralitic amphibole.

Mesoproterozoic Basement Rocks

Introduction

Basement rocks of the Virginia Blue Ridge include a diverse assemblage of granitoids and gneissic lithologies that were emplaced in thickened crust and locally metamorphosed at high-grade conditions at about 1.2 to 1.0 Ga (Aleinikoff and others, 2000; Tollo and others, in press a). The oldest rocks, which include a compositionally variable group of gneisses and deformed granitoids, typically display widespread evidence of penetrative ductile deformation. These rocks occur both as regional map units and as smaller inliers that form screens and probable roof pendants within younger intrusive bodies (fig. 3). The younger, more areally extensive group is composed mostly of compositionally diverse granitoids that are variably deformed. Granitoids throughout the area vary widely in mineralogic composition, ranging from quartz monzonite to leucocratic alkali feldspar granite (fig. 4; table 1). Both age groups include orthopyroxene-bearing charnockitic types (table 2). Most rocks exhibit geochemical characteristics that indicate derivation from crustal sources and show compositional similarities to granitic rocks produced in within-plate tectonic settings (Tollo and others, in press a).

Blue Ridge basement rocks were historically divided into two regional suites based largely on mineralogy and inferred metamorphic grade. Bloomer and Werner (1955) grouped a wide spectrum of orthopyroxene-bearing rocks into the Pedlar Formation, distinguishing these mostly high-grade rocks from lower grade, biotite±amphibole-bearing varieties designated as the Lovingston Formation by Jonas (1928). Bartholomew and others (1981) extended this classification through definition of the areally extensive Pedlar and Lovingston massifs, wherein the former occurs west of the north-south-trending Rockfish Valley fault zone (and its along-strike extensions) and the latter occurs east of this structural feature. According to this model, rocks of the lower-grade Lovingston massif were juxtaposed against the Pedlar massif as a result of movement along the Rockfish Valley fault zone (Bartholomew and others, 1981; Sinha and Bartholomew, 1984). In proposing an alternative explanation for this lithologic juxtaposition, Evans (1991) suggested that the biotite-bearing assemblages of the Lovingston terrane were produced through fluid-enhanced retrograde metamorphic recrystallization of original orthopyroxene-bearing rocks. However, results from recent studies sug-

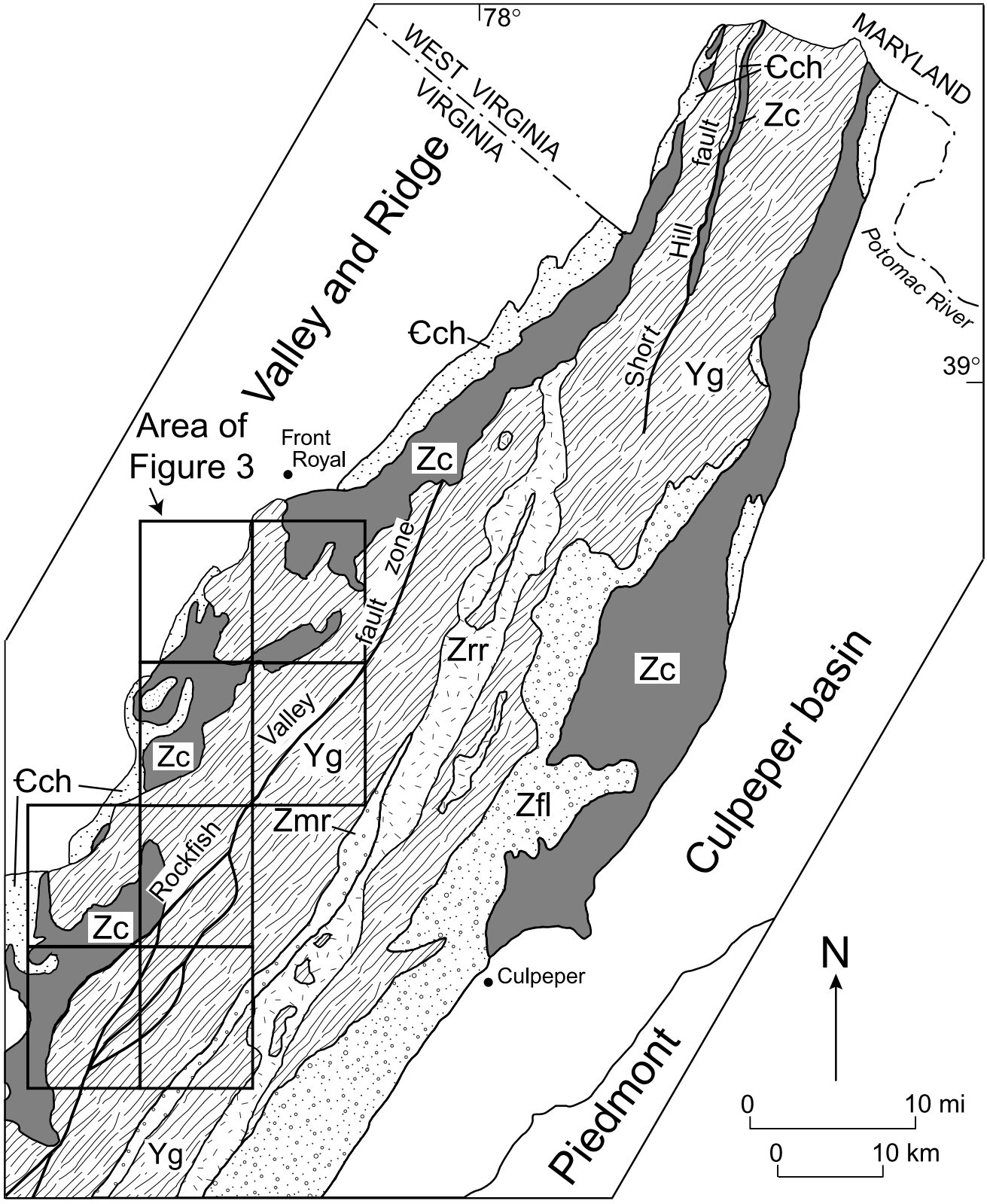
78°
WEST VIRGINIA
VIRGINIA
MARYLAND
Valley and Ridge
Cch
Zc
Hill fault
Potomac River
Short
Yg
39°
Area of Figure 3
Front Royal
Zc
fault zone
Zrr
Zc
Valley
Yg
Zc
Cch
Zmr
Zfl
Rockfish
Zc
Culpeper basin
Culpeper
N
Piedmont
Yg
0 10 mi
0 10 km

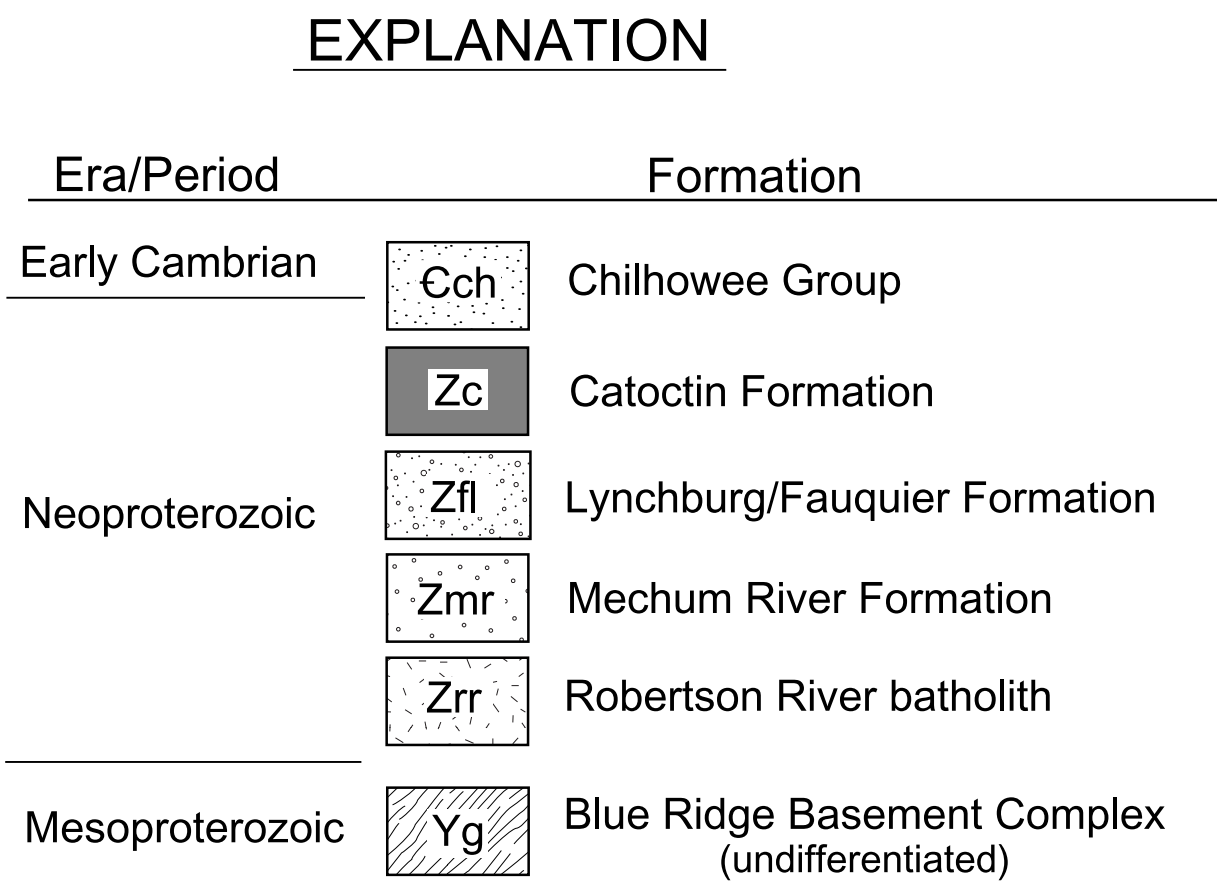

Figure 2 (this page and opposite page). Generalized geologic map of the northern Blue Ridge anticlinorium in Virginia. Outlined area corresponds to 7.5-minute quadrangles illustrated in figure 3. Map modified after Virginia Division of Mineral Resources (1993).

gest that neither model adequately accounts for the observed regional distribution of rocks. For example, recent detailed mapping and related structural studies indicate that the areal distribution of lithologies is more heterogeneous than indicated by the reconnaissance mapping that formed the basis of the earlier studies (Bailey and others, 2003; Tollo and others, in press b). Recent field-based studies also indicate that other ductile fault zones may have played a more significant role in the tectonic evolution of the north-central and northern Blue Ridge, thus diminishing the structural significance of the Rockfish Valley fault zone, especially in the north-central Blue Ridge (Bailey, 2003). Additionally, recent advances regarding the petrology of charnockitic rocks indicate that formation of orthorhombic pyroxene in the igneous systems that constitute the protoliths of most of the Blue Ridge Mesoproterozoic rocks is controlled by numerous characteristics of the original melt, such as aH_2O, pCO_2, Fe/(Fe+Mg), and depth of crystallization, and is thus not necessarily a reflection of ambient metamorphic grade (Frost and others, 2000).

U-Pb Geochronology

Zircons were extracted from seven samples of Mesoproterozoic basement rocks from the field area for U-Pb geochronology. In all samples, zircon generally is medium to dark brown, subhedral to euhedral, stubby to elongate prisms. Zircons in all samples contain multiple age components, a characteristic illustrated by igneous zircons in rocks from other studies of Grenvillian basement in the Blue Ridge and elsewhere (McLelland and others, 2001; Aleinikoff and others, 2000; Carrigan and others, 2003; Hamilton and others, in press). As a result, we decided to analyze the zircons using the high-spatial-resolution capabilities of spot analysis by the sensitive high-resolution ion microprobe (SHRIMP).

Areas on zircons about 25 microns in diameter by 1 micron in depth were dated using SHRIMP. Prior to isotopic analysis, all zircons were photographed in transmitted and reflected light, and imaged in cathodoluminescence (CL) on a scanning electron microscope. Analysis locations were chosen on the basis of crystal homogeneity (lack of cracks, inclusions, and other imperfections as shown by transmitted light photographs) and apparent age homogeneity (cores and overgrowths can usually be distinguished using CL). In all samples except SNP-02-197 (garnetiferous syenogranite, Ygg), igneous cores are distinct and obvious. Observed under CL illumination, cores typically contain concentric, euhedral, oscillatory, compositional zoning, consistent with crystalliza-

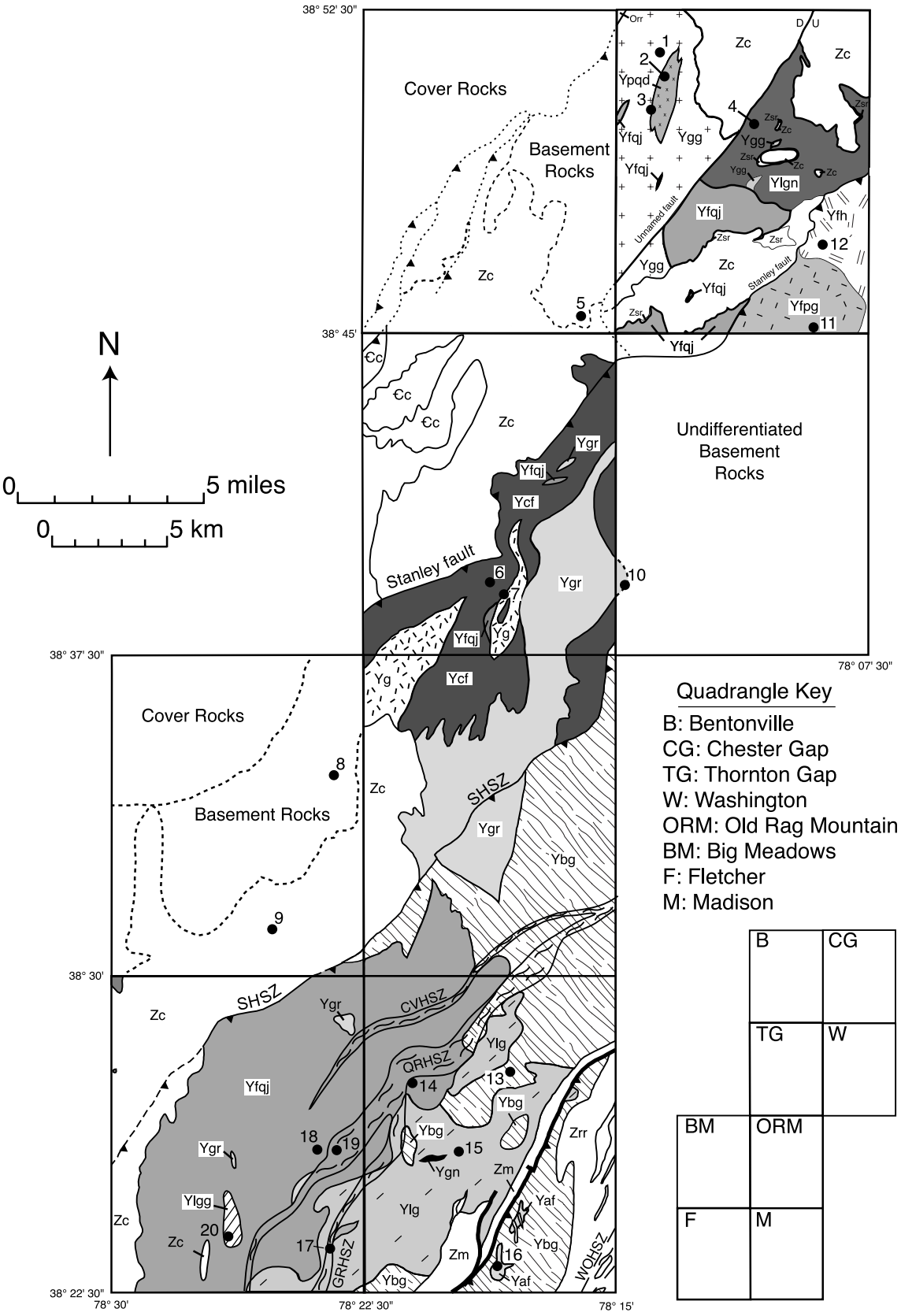
38° 52' 30"
38° 45'
38° 37' 30"
38° 30'
38° 22' 30"
78° 30'
78° 22' 30"
78° 15'
78° 07' 30"
N
0 5 miles
0 5 km
Cover Rocks
Basement Rocks
Undifferentiated Basement Rocks
Stanley fault
Unnamed fault
SHSZ
CVHSZ
QRHSZ
GRHSZ
WQHSZ
Zc
Ygr
Yfqj
Ycf
Yg
Ybg
Ylg
Ygn
Zm
Yaf
Zrr
Ylgn
Yfh
Yfpg
Ygg
Ypqd
Orr
Zsr
Ylgg
€c
Quadrangle Key
B: Bentonville
CG: Chester Gap
TG: Thornton Gap
W: Washington
ORM: Old Rag Mountain
BM: Big Meadows
F: Fletcher
M: Madison
B
CG
TG
W
BM
ORM
F
M

EXPLANATION TO FIGURE 3 AND SUMMARY OF LITHOLOGIC UNITS

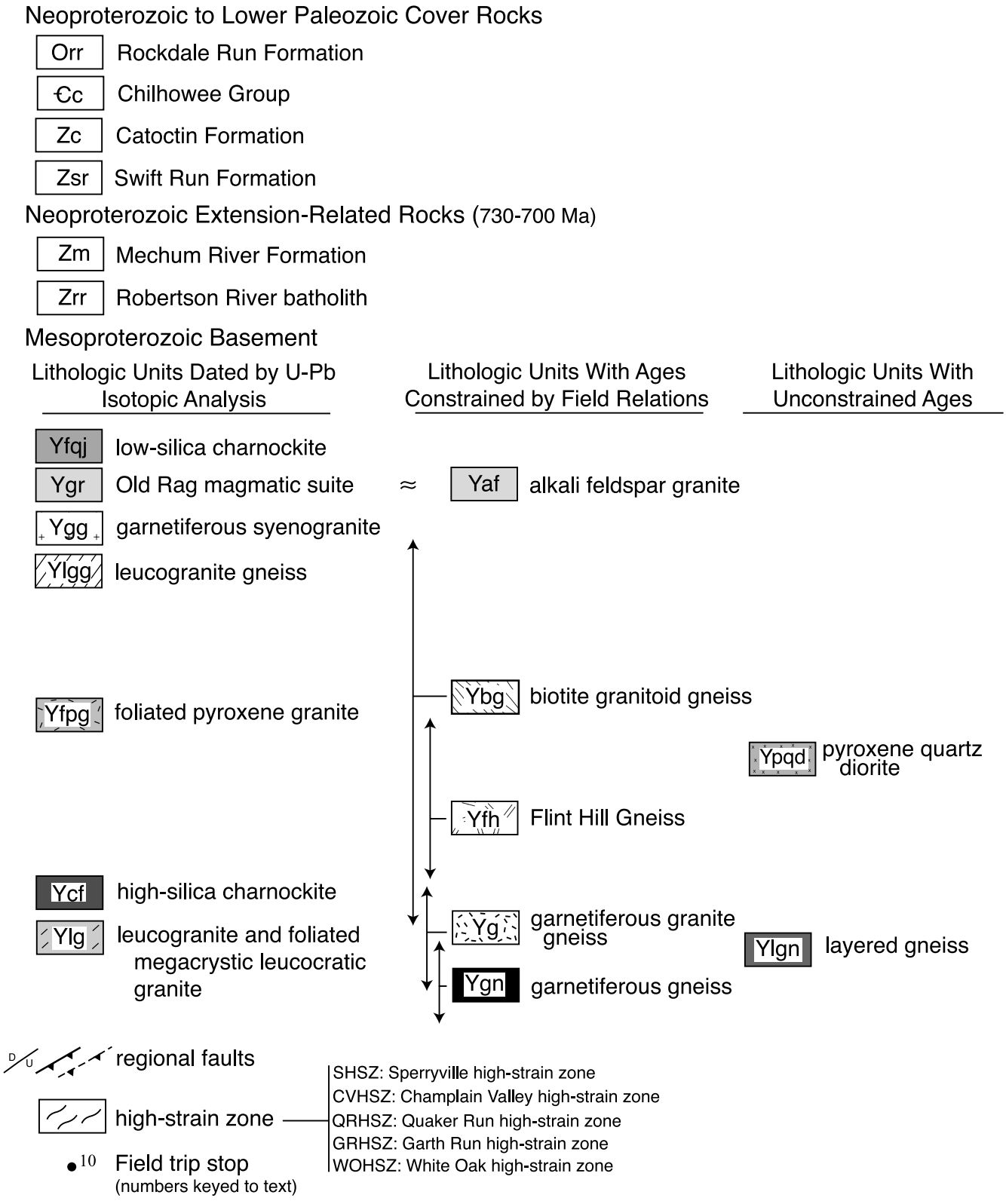

Figure 3 (this page and opposite page). Geologic map of basement rocks in the field trip area. Numbered locations refer to field trip stops described in the text. Geology is shown only where mapped in detail. Geology of the Madison 7.5-minute quadrangle is adapted from Bailey and others (2003).

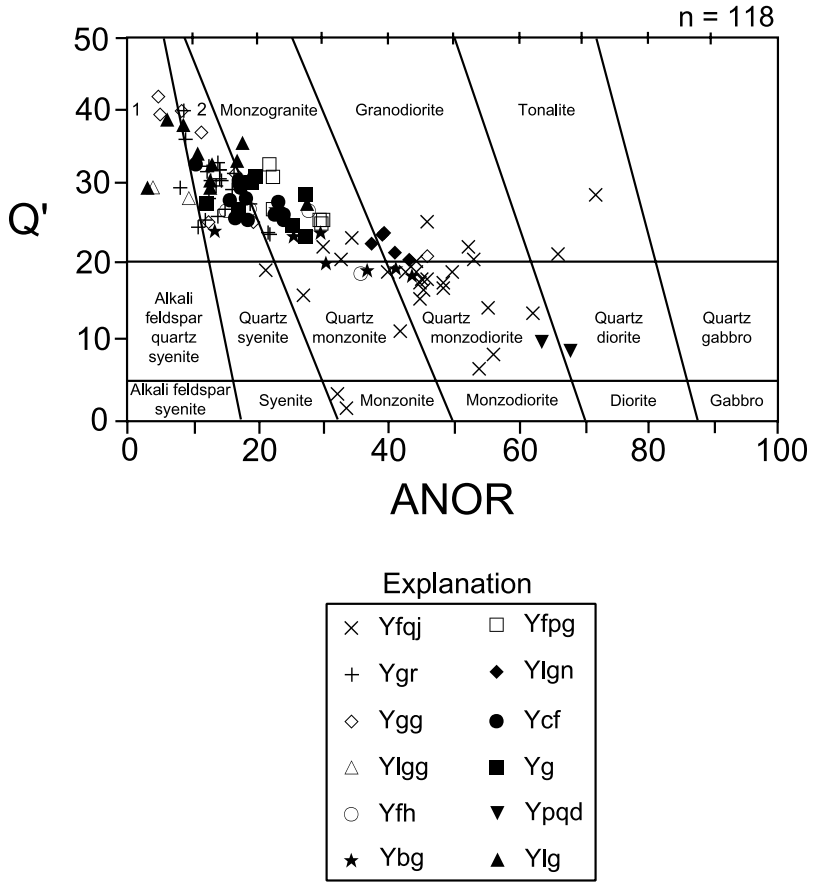

Figure 4. Plot of normative [anorthite/(orthoclase+anorthite)] × 100 versus normative [quartz/(quartz+orthoclase+albite+anorthite)] × 100 (ANOR versus Q′, after Streckeisen and Le Maitre, 1979). Normative compositions calculated with Fe^{2+}/Fe_{total}=0.9. Numbered field labels include (1) alkali feldspar granite, and (2) syenogranite. Abbreviations for lithologic units include: Yfqj, low-silica charnockite (*farsundite and quartz jotunite*); Ygr, Old Rag magmatic suite (after Hackley, 1999); Ygg, garnetiferous alkali feldspar granite and syenogranite; Ylgg, leucogranite gneiss; Yfh, Flint Hill Gneiss; Ybg, biotite granitoid gneiss; Yfpg, foliated pyroxene granite; Ylgn, layered granodiorite gneiss; Ycf, high-silica charnockite (*charnockite and farsundite*); Yg, garnetiferous granite gneiss; Ypqd, pyroxene quartz diorite; Ylg, leucocratic granitoid and megacrystic granite gneiss.

tion in a magma (Hanchar and Miller, 1993; Hanchar and Rudnick, 1995). Most cores typically have Th/U of about 0.3 to 0.6. Metamorphic overgrowths usually are unzoned and have distinctive, very low Th/U of 0.01 to 0.1. Rare xenocrystic cores can be distinguished by locally rounded morphology and truncated oscillatory zoning.

Igneous crystallization ages of the seven dated samples range from 1,183±11 Ma to 1,050±8 Ma (table 3). All samples contain younger overgrowths with ages of about 1,040 to 1,020 Ma; a few overgrowths that apparently formed during a younger, post-Grenville event(s) have ages of about 1,000 to 980 Ma. Compared to most zircons of igneous origin, zircons in the garnetiferous syenogranite (Ygg) have very unusual CL zoning patterns. Although crosscutting relations are observed, it is impossible to determine which zone formed during igneous crystallization because the typical igneous concentric zoning patterns are lacking. Four age groups were resolved for this sample (table 3). On the basis of field relations, we conclude that the age group at 1,064±7 Ma is the most likely time of crystallization of the garnetiferous syenogranite. Two older dates (1,135±6 Ma and 1,099±9 Ma) are interpreted as ages of inherited material; a younger age of 1,028±14 Ma probably represents the time of regional metamorphism, as indicated by overgrowth ages in other samples.

The age range of basement rocks in the study area is similar to ages of Grenville rocks elsewhere in the central and southern Appalachians. For example, in the northern Blue Ridge, Aleinikoff and others (2000) dated a series of gneisses and granitoids at about 1,150 to 1,050 Ma and noted three pulses of magmatic activity occurring at about 1,150 to 1,140 Ma, 1,110 Ma, and 1,075 to 1,050 Ma. In the southern Appalachians, Carrigan and others (2003) documented a regional pulse of granitic magmatism that occurred at ~1,165 to 1,150 Ma and presented evidence for nearly ubiquitous metamorphism at ~1,030 Ma. In the Adirondacks, McLelland and others (1996) recognized a similar geochronologic sequence for tectonomagmatic activity associated with Grenvillian orogenesis but including an older period, identify-

Table 1. Nomenclature for lithologic units within the field trip area.

Lithologic Unit	Descriptive Field Nomenclature*	General Petrologic Nomenclature†	Charnockitic Nomenclature‡
Yfqj	low-silica charnockite (5)	monzogranite to quartz monzodiorite	farsundite to quartz jotunite
Yaf	*alkali feldspar granite§ (4)*		
Ygr	*Old Rag magmatic suite (3)*	*alkali feldspar granite to syenogranite*	*alkali feldspar charnockite to charnockite*
Ygg	*garnetiferous alkali feldspar granite and syenogranite (1)*	*alkali feldspar granite to syenogranite*	
Ylgg	*leucogranite gneiss (5)*	*alkali feldspar granite*	
Ybg	biotite granitoid gneiss (3)	monzogranite to quartz monzonite and quartz monzodiorite	
Yfh	Flint Hill Gneiss (1)	syenogranite to monzogranite	
Yfpg	foliated pyroxene granite (1)	monzogranite	farsundite
Ylgn	layered granodiorite gneiss (1)	granodiorite	opdalite
Ypqd	pyroxene quartz diorite (1)	quartz diorite	orthopyroxene quartz diorite
Ycf	high-silica charnockite (2)	syenogranite to monzogranite	charnockite to farsundite
Yg	garnetiferous granite gneiss (2)	syenogranite to monzogranite	charnockite to farsundite
Ygn	garnetiferous gneiss (4)		
Ylg	*leucocratic granitoid and foliated megacrystic leucocratic granite (4)*	*alkali feldspar granite to syenogranite*	

* Number following nomenclature refers to the 7.5-minute quadrangle containing the reference locality within the area of new mapping: (1) Chester Gap, (2) Thornton Gap, (3) Old Rag Mountain, (4) Madison, and (5) Fletcher.
† Nomenclature determined using molar normative compositions calculated on basis of $Fe^{2+}/Fe_{(total)} = 0.9$ plotted on Q' vs ANOR plot of Streckeisen and Le Maitre (1979).
‡ Nomenclature following recommendations of Le Maitre and others (1989).
§ Leucocratic rocks are indicated by italics.

Table 2. Field and petrologic characterisitics for lithologic units within the field trip area.

Lithologic Unit	Rock Type(s)*	Primary Minerals†	Accessory Minerals†	Megascopic Field Characteristics†
low-silica charnockite Yfqj	monzogranite to quartz monzodiorite (*farsundite to quartz jotunite*)	Mipt (Mc), Pl, Qtz, Opx, Amph, Cpx,	Ap, Ilm, Mag, Zrn, Ep, Act	medium- to very coarse-grained, massive to weakly foliated, lenticular magnetite-rich xenoliths, Af megacrysts
alkali feldspar granite Yaf	alkali feldspar granite	Af, Pl, Qtz, Bt	Ttn, Fe-Ti Oxides	coarse-grained, porphyritic, massive
Old Rag magmatic suite Ygr	alkali feldspar granite to syenogranite	Pt (Mc), Pl, Qtz, Opx, Grt, Bt	Ap, Ilm, Mag, Zrn, Ep, Act	medium- to very coarse-grained, massive to weakly foliated
garnetiferous syenogranite Ygg	alkali feldspar granite to syenogranite	Or, Pl, Qtz, Grt, Bt, Opx	Ap, Ilm, Zrn	medium- to very coarse-grained, weakly to locally strongly foliated, medium-grained Af dikes, rare pegmatite dikes
leucogranite gneiss Ylgg	alkali feldspar granite	Mept (Mc), Pl, gray Qtz, Bt	Ilm, Mag, Zrn, Ep, Ms	coarse- to very coarse-grained, strongly foliated, Mept megacrysts
biotite granitoid gneiss Ybg	monzogranite to quartz monzonite and quartz monzodiorite	Mc, Pl, Qtz, Bt	Ap, Ilm, Ttn, Zrn, Ep, Chl	medium- to coarse-grained, strongly foliated
Flint Hill Gneiss Yfh	syenogranite to monzogranite	Mc, Pl, Qtz, Bt, Chl	Ap, Leux, Ilm, Zrn	medium- to very coarse-grained, strongly foliated
foliated pyroxene granite Yfpg	monzogranite (*farsundite*)	Mc, Pl, Qtz, Opx, Amph, Bt	Ap, Ilm, Zrn	medium- to coarse-grained, strongly foliated, pegmatitic dikes, Grt leucogranite dikes
layered granodiorite gneiss Ylgn	granodiorite (*opdalite*)	Mc, Or, Pl, Qtz, Amph, Opx	Ap, Ilm, Zrn	medium- to coarse-grained, strongly foliated, gneissic layers locally folded, massive leucogranite sheets, boudins
pyroxene quartz diorite Ypqd	quartz diorite (*orthopyroxene quartz diorite*)	Or, Pl, Qtz, Opx, Bt	Ap, Mag, Zrn	medium-grained, moderately to strongly foliated, gneissic layering
high-silica charnockite Ycf	syenogranite to monzogranite (*charnockite to farsundite*)	Mipt, Pl, Qtz, Opx, Amph, Cpx	Ap, Ilm, Mag, Zrn, Ep, Act	coarse- to very coarse-grained, moderately to strongly foliated, locally prominent gneissic layering, Af megacrysts
garnetiferous granite gneiss Yg	syenogranite to monzogranite	Mipt, Pl, Qtz, Opx, Grt, Bt, Cpx	Ap, Ilm, Mag, Zrn, Chl	medium- to coarse-grained, strongly foliated, prominent gneissic layering
garnetiferous gneiss Ygn	granodiorite (*opdalite*)?	Af, Pl, Qtz, Gt, Opx	Ttn, Fe-Ti Oxides	fine- to coarse-grained, layered
(1) foliated megacrystic leucocratic granite (2) leucogranite Ylg	alkali feldspar granite to syenogranite	1) Mept (Mc & Or), Pl, Qtz, intergrown Bt & Chl 2) Mc, Pl, Qtz, minor secondary Bt	Zrn, Ep, Ttn	(1): coarse-grained, strongly foliated (2): medium-grained, massive to weakly foliated Unit also includes coarse-grained leucogranite pegmatite

* Rock types determined using molar normative compositions calculated on basis of $Fe^{2+}/Fe_{(total)} = 0.9$ plotted on Q' vs ANOR diagram of Streckeisen and Le Maitre (1979). Charnockitic nomenclature included in parentheses following recommendations of Le Maitre and others (1989).

†Abbreviations: Af, alkali feldspar; Leux, leucoxene; Mipt, microperthite; Mept, mesoperthite; Pt, perthite. Other abbreviations after Kretz (1983): Act, actinolite; Aln, allanite; Amph, amphibole; Ap, apatite; Bt, biotite; Cal, calcite; Chl, chlorite; Cpx, clinopyroxene; Ep, epidote; Fl, fluorite; Grt, garnet; Ilm, ilmenite; Mag, magnetite; Mc, microcline; Or, orthoclase; Opx, orthopyroxene; Pl, plagioclase; Qtz, quartz; Ttn, titanite; Zrn, zircon.

Table 3. SHRIMP U-Pb isotopic ages of basement rocks in the field trip area.

Lithologic Unit	Sample Number	Igneous Crystallization Age (Ma) [± 2 sigma]	Metamorphic Ages (Ma) [± 2 sigma]	Inheritance Ages (Ma) [± 2 sigma]
low-silica charnockite (Yfqj)	SNP-99-93	1050 ± 8	1018 ± 14	
Old Rag magmatic suite (coarse-grained leucogranite) (Ygr)	OR-97-35	1060 ± 5	1019 ± 15	
			979 ± 11	
		*1059 ± 8**	*1027 ± 9*	
garnetiferous syenogranite (Ygg)	SNP-02-197	1064 ± 7	1028 ± 14	1135 ± 6
				1099 ± 9
leucogranite gneiss (Ylgg)	SNP-99-90	1078 ± 9	1028 ± 10	
			997 ± 19	
foliated pyroxene granite (Yfpg)	SNP-02-177	1117 ± 14	1043 ± 12	1175 ± 14
high-silica charnockite (Ycf)	SNP-96-10	1159 ± 14	1052 ± 14	
foliated megacrystic leucocratic granite (Ylg)	SNP-02-189	1183 ± 11	1110 ± 38	
			1043 ± 16	

* monazite ages indicated by italics; all other ages obtained from zircon.

ing episodes at 1,350 to 1,190 Ma, about 1,090 Ma, and 1,090 to 1,030 Ma. The Adirondack ages overlap episodes of major magmatic and metamorphic events recognized in the Grenville province of Canada (Gower and Krogh, 2002) and suggest that the two areas share some aspects of orogenic activity. However, extrapolation of these tectonic events to the Blue Ridge is tempered by the allochthonous nature of the Blue Ridge and the possibility that the terrane was separated from the Adirondack-New England region by a major tectonic boundary during Grenvillian orogenesis (Bartholomew and Lewis, 1988).

Lithologies and age relations

Textures, compositional characteristics, and field relations suggest that nearly all basement rocks within the study area were originally igneous in origin. Nomenclature was determined using normative compositions and standard procedures recommended by the International Union of Geological Sciences (IUGS) because the locally very coarse grain size and strongly preferred orientation of fabrics in some rocks hindered direct application of standard modal-based procedures. General petrologic nomenclature using parameters calculated from normative data are presented in table 1, with IUGS-recommended names for orthopyroxene-bearing varieties included where appropriate. The basement rocks collectively display a wide range of normative compositions; however, in most cases, individual lithologic units are characterized by relatively restricted compositional variation (fig. 4; table 4). Syenogranite to monzogranite compositions are most common, especially for the older rocks that predate local Grenvillian deformation. The low-silica charnockite (Yfqj), which includes numerous chemically consanguineous dikes of both similar and less-evolved composition, is characterized by the greatest internal variation, ranging from orthopyroxene-bearing monzogranite (*farsundite*[1]) to quartz monzodiorite (*quartz jotunite*). Older rocks that predate regional Grenvillian deformation are dominated by orthopyroxene-bearing, charnockitic granitoids, whereas rocks that postdate

[1]Nomenclature suggested for orthopyroxene-bearing rocks of probable igneous origin by Le Maitre and others (1989). Such terms are italicized wherever used throughout the text. Where charnockite is used to refer to orthopyroxene-bearing granitoids in general, it is not italicized.

Table 4. Geochemical data for basement rocks from the field trip area.

Stop	1	--	2	3	3	4
Map Unit	Ygg	Ygg	Ypqd	Ygg	Ypqd	Ylgn
Sample	SNP-03-197	SNP-01-164	SNP-01-175	SNP-01-174	SNP-01-155	SNP-01-150
SiO_2	64.10	68.94	55.29	72.51	63.51	66.49
TiO_2	0.23	0.51	1.71	0.45	1.20	0.79
Al_2O_3	18.44	16.13	16.49	14.63	15.18	15.83
Fe_2O_3*	6.59	3.02	9.33	1.92	9.19	5.08
MnO	0.26	0.03	0.14	0.03	0.13	0.07
MgO	0.28	0.42	4.78	0.40	4.54	1.04
CaO	2.92	1.30	6.54	1.17	1.93	3.43
Na_2O	4.13	2.59	3.00	2.14	1.85	2.95
K_2O	2.71	6.50	2.00	6.18	2.66	4.43
P_2O_5	0.11	0.16	0.52	0.14	0.05	0.20
Total	99.77	99.60	99.80	99.55	100.23	100.31
Rb	65.9	173.3	57.9	155.7	111.4	193.9
Ba	786	1524	1030	1198	726	896
Sr	511	327	993	308	194	213
Pb	39	44	11	49	17	26
Th†	38.20	21.68	0.59	50.9	5.9	3.6
U	1	0.8	0.63	1.9	1.1	n.d
Zr	331	305	188	286	259	388
Hf	10.38	10.98	6.55	9.30	7.88	11.37
Nb	7.8	7.9	6.7	4.4	12.1	12.5
Ta	0.42	0.47	0.70	0.60	1.10	1.28
Ni	1	3	32	3	35	5
Zn	41	54	130	23	192	87
Cr	20	24	144	30	139	34
Ga	27	24	25	17	22	23
V	1	17	161	11	168	45
La	103.2	100.6	39.2	120.2	35.0	45.7
Ce	323.4	203.1	79.4	264.1	70.0	108.7
Nd	121.4	79	47	102	32	54.5
Sm	16.83	9.55	8.43	17.12	6.56	10.85
Eu	2.02	2.48	2.66	2.00	1.91	2.01
Tb	1.65	0.71	1.04	1.37	1.51	1.77
Yb	5.21	1.1	1.80	2.0	5.7	4.6
Lu	0.79	0.16	0.28	0.25	0.92	0.65
Y	38.8	12.4	21.8	24.3	53.4	52.7
Sc	5.04	4.38	20.24	4.04	24.29	14.02
Ga/Al	2.77	2.81	2.86	2.20	2.74	2.75
A/CNK	1.23	1.18	0.87	1.19	1.61	1.00
FeOt/(FeOt+MgO)	0.95	0.87	0.64	0.81	0.65	0.81

* total iron expressed as Fe_2O_3. n.d.: not detected

† elements measured by instrumental neutron activation (INA) analysis noted in italics; all other elements measured by X-ray fluorescence.

Table 4. Geochemical data for basement rocks from the field trip area.—Continued

Stop	4	5	5	6	7	--
Map Unit	dike	Ycf	Ycf	Ycf	Yg	Yfqj
Sample	SNP-01-149	SNP-01-142	SNP-01-143	SNP-96-10	SNP-96-1	SNP-96-17
SiO_2	50.03	74.58	70.09	69.78	68.37	63.75
TiO_2	2.72	0.30	0.46	0.74	0.64	1.29
Al_2O_3	14.03	12.84	14.22	13.64	14.93	15.22
Fe_2O_3*	10.10	2.57	4.09	4.23	4.22	5.97
MnO	0.15	0.02	0.04	0.07	0.06	0.09
MgO	6.61	0.25	0.40	0.66	0.70	1.23
CaO	7.12	1.00	1.93	2.29	2.45	3.51
Na_2O	2.58	1.94	2.33	2.38	3.19	3.17
K_2O	4.71	6.90	6.50	5.63	4.94	5.30
P_2O_5	1.61	0.04	0.15	0.19	0.18	0.47
Total	99.65	100.45	100.23	99.60	99.66	99.99
Rb	276	238.7	212.6	199.3	170.3	181.2
Ba	2388	563	870	668	986	1650
Sr	611	85	107	128	175	579
Pb	39	49	39	28	30	38
Th†	7.2	40.0	10.93	2.3	12.0	2.2
U	2.0	3.5	1	0.7	n.d.	1.4
Zr	644	444	474	260	330	501
Hf	17.1	14.7	15.84	11.2	10.7	15.1
Nb	13.4	11.5	19.0	9.3	9.6	14.6
Ta	2.10	0.46	1.10	0.85	0.64	1.49
Ni	123	3	3	3	7	3
Zn	154	66	90	63	81	120
Cr	267	21	19	28	34	22
Ga	22	19	24	21	21	25
V	142	5	10	25	36	44
La	109.7	258.4	94.8	52.8	58.0	102.0
Ce	226.4	477.0	224.5	94.3	105.0	185.0
Nd	112	165	102	47	47	91
Sm	17.22	23.50	17.91	10.30	10.00	19.10
Eu	3.7	1.81	2.70	2.09	1.82	3.31
Tb	1.97	1.41	2.26	1.50	1.25	2.30
Yb	3.60	2.6	5.6	3.4	2.2	5.3
Lu	0.49	0.35	0.73	0.42	0.23	0.60
Y	42.3	31.4	72.6	38.2	26.2	63.5
Sc	20.88	2.44	8.75	8.90	9.08	11.30
Ga/Al	2.96	2.79	3.19	2.91	2.66	3.10
A/CNK	0.63	1.03	0.99	0.96	0.99	0.88
FeOt/(FeOt+MgO)	0.58	0.90	0.90	0.85	0.84	0.81

* total iron expressed as Fe_2O_3. n.d.: not detected

† elements measured by instrumental neutron activation (INA) analysis noted in italics; all other elements measured by X-ray fluorescence.

Table 4. Geochemical data for basement rocks from the field trip area.—Continued

Stop	--	--	11	12	13	14
Map Unit	Yor	Ygr-d	Yfpg	Yfh	Ybg	Yfqj
Sample	OR-97-35	OR-97-51	SNP-02-177	SNP-01-146	SNP-02-186	SNP-02-180
SiO_2	72.18	72.85	67.36	69.69	62.41	53.24
TiO_2	0.28	0.43	0.78	0.58	1.44	2.69
Al_2O_3	14.44	14.36	14.73	15.21	13.87	15.69
Fe_2O_3*	2.76	1.61	5.34	3.80	9.13	11.96
MnO	0.06	0.03	0.08	0.05	0.15	0.18
MgO	0.34	0.44	0.95	0.68	0.81	2.14
CaO	1.15	1.38	2.72	1.87	3.97	6.51
Na_2O	2.85	2.50	2.73	2.34	2.80	3.11
K_2O	6.04	5.69	4.83	6.13	4.43	2.72
P_2O_5	0.10	0.23	0.22	0.15	0.69	1.31
Total	100.19	99.53	99.74	100.49	99.70	99.55
Rb	305.1	240.6	186.2	166.7	109.1	52.8
Ba	425	746	863	951	2112	1926
Sr	80	151	161	170	314	633
Pb	65	53	28	28	28	19
Th†	75.1	53.8	15.00	3.19	1.40	1.4
U	9.5	4.2	1.5	n.d.	0.83	0.5
Zr	230	392	336	239	1354	988
Hf	9.0	12.1	13.07	9.26	43	22.90
Nb	10.9	12.6	10.4	8.6	25.2	35.5
Ta	0.72	0.68	1.1	0.50	1.4	1.57
Ni	2	2	8	5	1	2
Zn	70	48	77	64	249	241
Cr	25	18	39	27	11	21
Ga	25	24	22	20	25	30
V	8	10	49	33	39	95
La	112.0	170.9	69.5	46.2	83.6	117.8
Ce	202.0	339	129.2	100.4	170	250.2
Nd	81	130	61	42.9	106	127
Sm	20.80	23.70	10.82	7.06	18.87	28.61
Eu	0.91	1.49	1.72	1.83	5.0	4.51
Tb	3.61	1.45	0	0.85	1.9	3.24
Yb	10.2	1.5	3.9	1.9	4.6	5.40
Lu	1.10	0.22	0.57	0.27	0.73	0.8
Y	62.6	32.4	40.1	20.5	58.6	84.1
Sc	6.27	2.72	12.57	10.84	20.0	20.82
Ga/Al	3.27	3.16	2.82	2.48	3.41	3.61
A/CNK	1.09	1.12	1.00	1.10	0.83	0.79
FeOt/(FeOt+MgO)	0.88	0.77	0.84	0.83	0.91	0.83

* total iron expressed as Fe_2O_3. n.d.: not detected

† elements measured by instrumental neutron activation (INA) analysis noted in italics; all other elements measured by X-ray fluorescence.

Table 4. Geochemical data for basement rocks from the field trip area.—Continued

Stop	15	20	20	20
Map Unit	Ylg2	Ylgg	Yfqj	Yfqj
Sample	SNP-03-199	SNP-99-90	SNP-99-91	SNP-99-92
SiO_2	75.67	74.26	62.57	58.59
TiO_2	0.14	0.20	1.58	1.78
Al_2O_3	12.65	13.93	13.87	15.44
Fe_2O_3*	0.85	1.94	9.45	10.79
MnO	0.02	0.02	0.12	0.17
MgO	0.01	0.22	0.85	2.99
CaO	0.61	0.79	3.26	2.16
Na_2O	3.02	3.15	2.35	3.40
K_2O	6.73	6.16	4.82	3.26
P_2O_5	0.02	0.04	0.60	0.85
Total	99.71	100.71	99.47	99.45
Rb	237.1	161.5	144.0	89.6
Ba	126	1009	2132	978
Sr	60	157	351	92
Pb	46	28	31	8
Th†	34.64	33.4	1.75	3.1
U	13	1.2	1.1	0.2
Zr	75	169	1676	1157
Hf	4.53	6.8	45.0	34.7
Nb	3.9	6.7	24.2	32.7
Ta	0.16	0.72	1.45	2.2
Ni	1	4	2	1
Zn	20	18	286	420
Cr	19	30	13	13
Ga	17	22	28	22
V	1	5	42	50
La	81.7	94	91.1	123.7
Ce	144.4	190	193	273
Nd	58.7	64	105	142
Sm	11.25	8.35	22.4	20.8
Eu	0.52	1.65	4.95	5.01
Tb	0.96	0.62	1.54	1.53
Yb	1.22	1.38	6.4	6.8
Lu	0.15	0.2	1.10	1.0
Y	10.6	8.1	69.7	83.1
Sc	3.19	3.75	18.71	20.35
Ga/Al	2.54	2.98	3.81	2.69
A/CNK	0.95	1.05	0.92	1.18
FeOt/(FeOt+MgO)	0.98	0.89	0.91	0.76

* total iron expressed as Fe_2O_3.

† elements measured by instrumental neutron activation (INA) analysis noted in italics; all other elements measured by X-ray fluorescence.

Table 5. Geochemical data for mafic dike rocks from the field trip area.

Stop	1	5	5	--	--	18	18	18	18
Sample	SNP-01-159	SNP-01-144	SNP-01-145	SNPD-99-1	SNPD-99-3	SNPD-99-7	SNPD-99-8	SNPD-99-9	SNPD-99-6
SiO_2	51.64	50.98	47.48	51.14	49.43	53.67	51.80	53.59	49.68
TiO_2	2.92	2.75	1.90	2.98	2.82	1.26	1.23	1.07	2.66
Al_2O_3	13.03	13.05	16.41	12.97	12.92	15.07	15.06	15.14	13.05
Fe_2O_3*	15.32	15.26	12.12	15.75	16.22	11.49	12.43	10.70	15.66
MnO	0.22	0.21	0.18	0.23	0.23	0.15	0.17	0.15	0.22
MgO	4.18	4.65	7.58	4.52	4.69	6.74	6.91	7.48	5.72
CaO	8.66	7.19	8.62	9.02	9.88	7.87	7.76	7.84	9.93
Na_2O	2.77	4.32	4.00	2.77	2.16	3.14	3.23	3.01	2.02
K_2O	0.97	0.81	0.66	0.97	1.06	0.72	0.77	0.64	0.81
P_2O_5	0.49	0.43	0.47	0.44	0.37	0.16	0.15	0.13	0.30
Total	100.22	99.66	99.43	100.79	99.79	100.27	99.50	99.75	100.04
Rb	20.4	40.6	40.1	32.2	25.3	18.3	20	16.5	18.8
Ba	353	338	201	373	326	197	249	246	313
Sr	340	168	279	282	263	369	299	358	227
Pb	5	5	12	3	2	4	5	4	2
Th†				1.74	1.86	0.64	1.00	0.89	1.34
U	n.d	n.d	n.d	0.4	0.4	0.2	0.0	0.2	0.4
Zr	267	297	151	270	229	78	100	106	197
Hf				7.1	6.5	2.2	3.0	3.1	5.4
Nb	17.0	19.9	18.7	20.1	22	4.6	5.4	6.5	17.1
Ta				1.17	1.44	0.29	0.38	0.43	1.14
Ni	9	25	122	26	36	130	108	104	48
Zn	160	170	129	158	136	97	115	114	140
Cr	20	52	276	54	107	385	278	249	124
Ga	23	21	19	22	21	19	20	20	20
V	316	321	125	329	303	115	132	130	291
La	25	22	14	26	21	10	13	10	17
Ce				54.2	49.5	17.7	23.9	24.3	40.0
Nd				30	30	10	14	14	21
Sm				7.12	6.92	2.76	3.45	3.74	6.37
Eu				2.41	2.40	1.06	1.23	1.35	1.98
Tb				1.52	1.40	0.49	0.58	0.70	1.24
Yb				3.7	3.2	1.0	1.4	1.3	3.0
Lu				0.48	0.47	0.15	0.22	0.18	0.40
Y	38.5	39.4	19.0	41.5	36.7	12.2	16.5	16.2	34
Sc				31.45	33.44	16.91	18.79	18.20	34.95

* total iron expressed as Fe_2O_3. n.d.: not detected

† elements measured by instrumental neutron activation (INA) analysis noted in italics; all other elements measured by X-ray fluorescence.

deformation include both leucocratic granitoids ranging from alkali feldspar granite to syenogranite and low-silica charnockite that is likely unrelated to the contemporaneous leucocratic rocks. Results from U-Pb isotopic analysis of zircons indicate that mineralogically similar leucocratic granitoids were emplaced during each of the three magmatic intervals presently identified within the Blue Ridge study area. The ~1,180-Ma leucocratic granitoid and megacrystic leucocratic granite gneiss (Ylg), which also includes abundant leucogranite pegmatite, constitutes an intrusive complex characterized by multiple generations of igneous activity and represents the oldest dated rock in the region. Pervasively deformed screens and xenoliths of leucogranite gneiss (Ylgg) of ~1,080-Ma age occur within low-silica charnockite and represent the youngest intrusive unit presently recognized to predate regional Grenvillian deformation. Following deformation, magmatic activity continued to produce leucocratic granitoids represented by the garnetiferous syenogranite (Ygg), Old Rag magmatic suite (Ygr), and two small bodies of coarse-grained alkali feldspar granite (Yaf) exposed in the Madison quadrangle (fig. 3) which may be correlative with the larger Old Rag magmatic suite.

Geologic mapping and related studies throughout five contiguous 7.5-minute quadrangles in the north-central Blue Ridge (fig. 3) indicate that Mesoproterozic basement rocks define three groups based on age and field characteristics: (1) foliated rocks of about 1,180- to 1,160-Ma age, (2) foliated rocks of 1,115- to 1,080-Ma age, and (3) largely nonfoliated rocks of ≤1,060-Ma age. Each group is characterized by the following features.

Foliated rocks of 1,180- to 1,160-Ma age: This group comprises a compositionally diverse assemblage of lithologies, including leucocratic granitoids and granitoid gneisses, layered gneiss, and foliated charnockite. All rocks display evidence of pervasive, typically ductile deformation that is interpreted as Grenvillian in origin. Within the mapped quadrangles, this group includes the following lithologic units: (1) leucocratic granitoid and megacrystic leucocratic granite gneiss (Ylg); (2) high-silica charnockite (Ycf, *charnockite and farsundite*); (3) garnetiferous granite gneiss (Yg); and (4) garnetiferous gneiss (Ygn). Charnockitic layered granodiorite gneiss (Ylgn) may also belong to this group.

Foliated rocks of 1,115- to 1,080-Ma age: Rocks within this group also predate the major deformational event believed to be responsible for developing pervasive, high-temperature fabrics in many of the basement units. Two dated lithologic units are placed within this group: (1) foliated pyroxene granite (*farsundite*, Yfpg) and (2) leucogranite gneiss (Ylgg). Similar to the older high-silica charnockite (Ycf), the foliated pyroxene granite (Yfpg) contains abundant orthopyroxene of likely magmatic origin and is likewise also charnockitic.

Nonfoliated rocks of ≤1,060-Ma age: Nonfoliated lithologic units are interpreted as postorogenic with respect to the main period of Grenvillian deformation in the Blue Ridge. All rocks in this group within the field trip area are broadly granitic and include the following: (1) garnetiferous syenogranite (Ygg); (2) the Old Rag magmatic suite (Hackley, 1999), which includes pyroxene-bearing leucogranites of varying grain size and mineralogical composition (Ygr); (3) alkali feldspar granite (Yaf); and (4) low-silica charnockite (Yfqj, *farsundite and quartz jotunite*). The compositionally similar granitic units (including Ygg, Ygr, and Yaf) are distinctive leucocratic rocks with high potassium feldspar to plagioclase ratios and likely constitute a regional suite.

In summary, results from recent field, petrologic, and geochronological studies indicate that basement rocks of the northern Blue Ridge preserve evidence of tectonomagmatic events that spanned over 160 m.y. of Grenvillian orogenesis (Aleinikoff and others, 2000; Tollo and others, in press a). Presently, ages derived from high-precision U-Pb isotopic analyses of zircons indicate that an early interval of magmatic activity occurred at about 1,180 to 1,140 Ma and involved granitoids (now gneisses and deformed megacrystic leucogranites) of considerable compositional diversity. This episode was followed at about 1,110 Ma by a second period of magmatism presently defined by two compositionally dissimilar plutons within the northern Blue Ridge. Following another hiatus, plutonism resumed at about 1,080 Ma and was rapidly followed by a significant period of deformation that occurred within the interval 1,080 to 1,060 Ma. Most of the ductile fabrics developed in many of the older plutonic rocks were likely formed during this episode. Following deformation, plutonism continued to about 1,050 Ma, producing granitoids of considerable compositional diversity, including charnockite of A-type affinity. Isotopic evidence further indicates that thermal disturbances occurred throughout the region at 1,020 to 980 Ma. This temporal framework is similar to the sequence of Grenvillian events documented in the Adirondacks and Canadian Grenville province (McLelland and others, 1996; Rivers, 1997), suggesting the possibility of tectonic correlations between the Blue Ridge and these Laurentian terranes.

Geochemical characteristics

Geochemical data indicate that basement rocks within the field trip area are characterized by diverse chemical compositions and a range in silica content of nearly 30 weight percent (figs. 5A–F). Most lithologic units are felsic, containing ≥65 weight percent SiO_2, a compositional characteristic that is reflected in the abundance of granitoids throughout the field area (figs. 3, 4). Mafic to intermediate rock types are represented only by the low-silica charnockite (Yfqj) and foliated pyroxene quartz diorite (Ypqd), which form a large pluton and small inlier, respectively (fig. 3). Although variation for the region as a whole is extensive, most individual lithologic units are characterized by relatively modest chemical diversity, suggesting that significant differentiation did not occur at or near the emplacement level of most individual

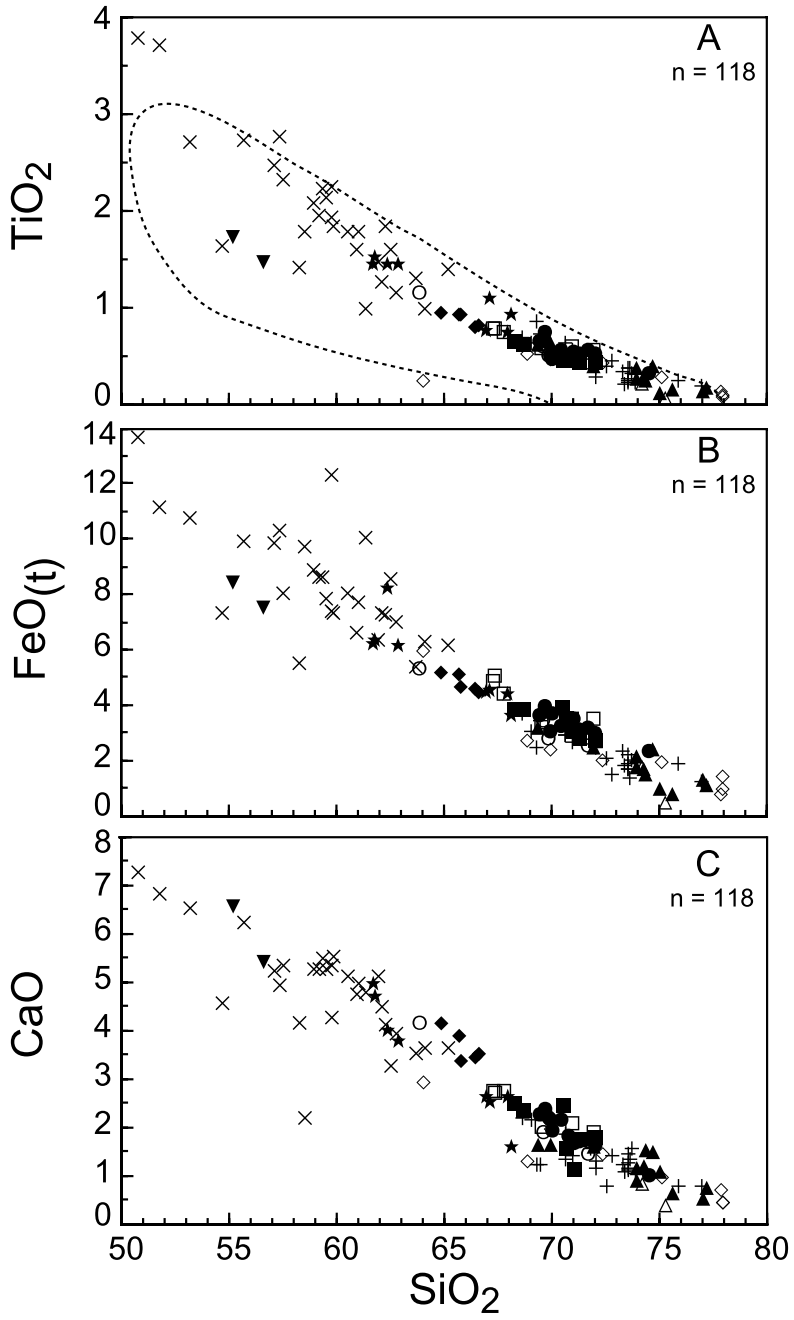

Figure 5. Plots of SiO_2 versus (A) TiO_2, (B) FeO_t (total iron expressed as FeO), (C) CaO, (D) aluminum saturation index (A/CNK=molar $Al_2O_3/(CaO+Na_2O+K_2O)$, (E) Na_2O+K_2O, and (F) FeO_t/MgO for basement rocks from the field trip area. Dashed line in A encloses field of igneous charnockites from Kilpatrick and Ellis (1992). Dashed line separating alkaline and subalkaline fields in E is from Irvine and Baragar (1971). Dashed line separating tholeiitic and calc-alkaline fields in F is from Miyashiro (1974). All data are expressed in weight percent. Symbols are the same as in figure 4.

plutons. In contrast to most lithologic units, the low-silica charnockite (Yfqj) and biotite granitoid gneiss (Ybg) exhibit trends in compositional and normative variation that are both considerable and petrologically distinctive. The internally differentiated low-silica charnockite, which includes abundant compositionally related dikes and fractionated pegmatite (Tollo and others, in press a), ranges in silica content from 50 to 65 weight percent, defining about half of the variation documented to date in the study area (fig. 5). Chemical variations in the biotite granitoid gneiss are bimodal, with compositions clustering at about 62 and 67 weight percent SiO_2 (fig. 5). This compositional diversity corresponds to normative compositions ranging from syenogranite to quartz monzonite (fig. 4), and is likely a reflection of compositional layering that

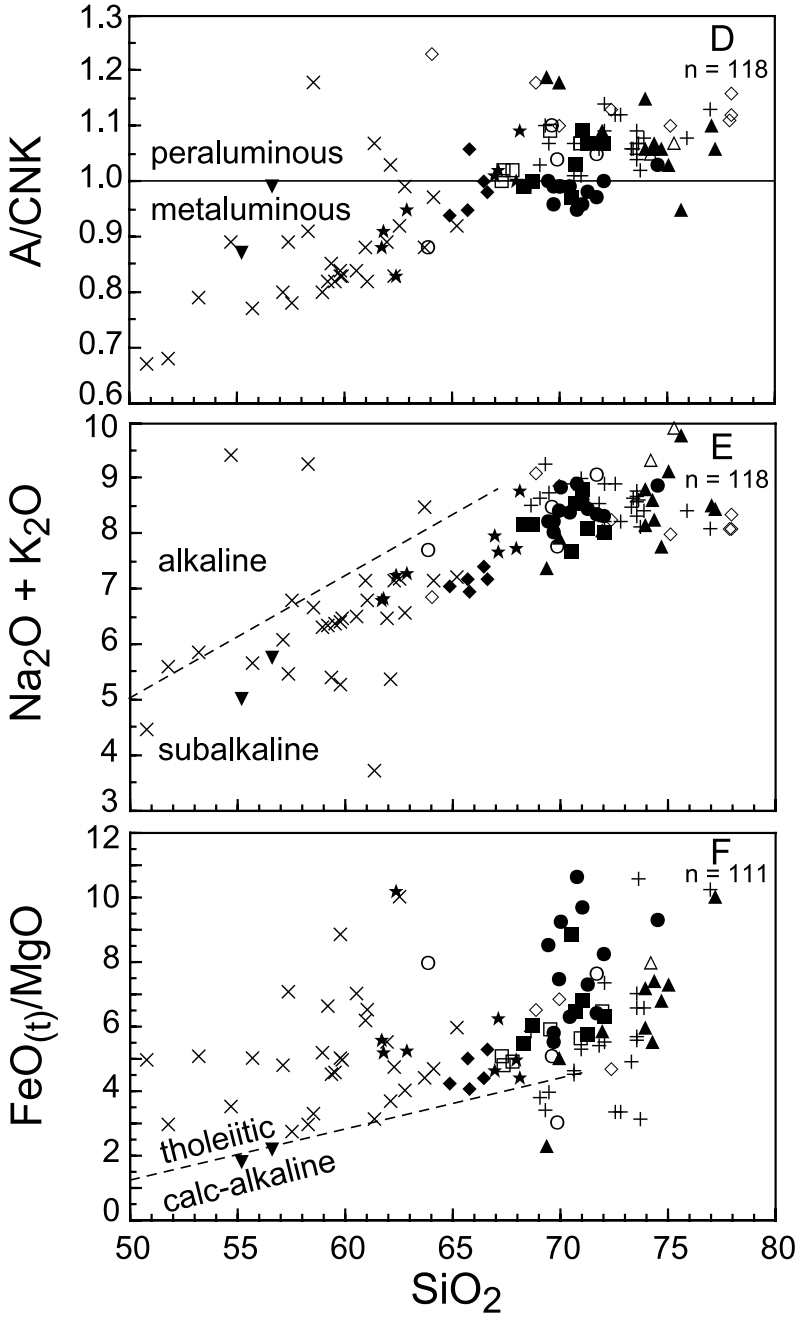

Figure 5. Continued

characterizes this lithologic unit in the field (Bailey and others, 2003; Hackley, 1999).

Most lithologic units are transitional metaluminous to peraluminous in composition, consistent with the typical pyroxene±amphibole mineral assemblages (fig. 5D); however, all leucogranitic rocks are characteristically peraluminous, as reflected in their locally biotite- and garnet-bearing compositions. Collectively, basement rocks within the field trip area are subalkaline and tholeiitic (figs. 5E and F, respectively), and thus share many compositional features with granitoids and charnockites of the classic anorthosite-mangerite-charnockite-granite (AMCG) suites documented in the Adirondacks and other Precambrian massifs that include abundant intrusive rocks (McLelland and Whitney, 1990; Frost and Frost, 1997). Trace-element concentrations of most of the Blue Ridge granitoids plot in a region of the source-sensitive Nb+Y versus Rb diagram of Pearce and others (1984) (fig. 6) that is characteristic of granitoids emplaced in broadly defined post-orogenic geologic settings. Such compositional characteristics suggest that magmas were derived from mixed sources that included both crustal and arc-related components (Sylvester, 1989; Förster and others, 1997). As noted by previous studies

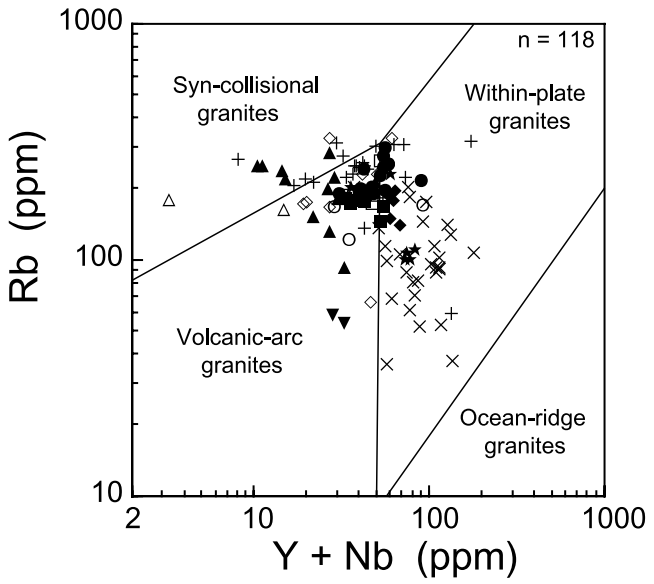

Figure 6. Plot of Y+Nb versus Rb for basement rocks from the field trip area. Symbols are the same as in figure 4. Diagram modified after Pearce and others (1984).

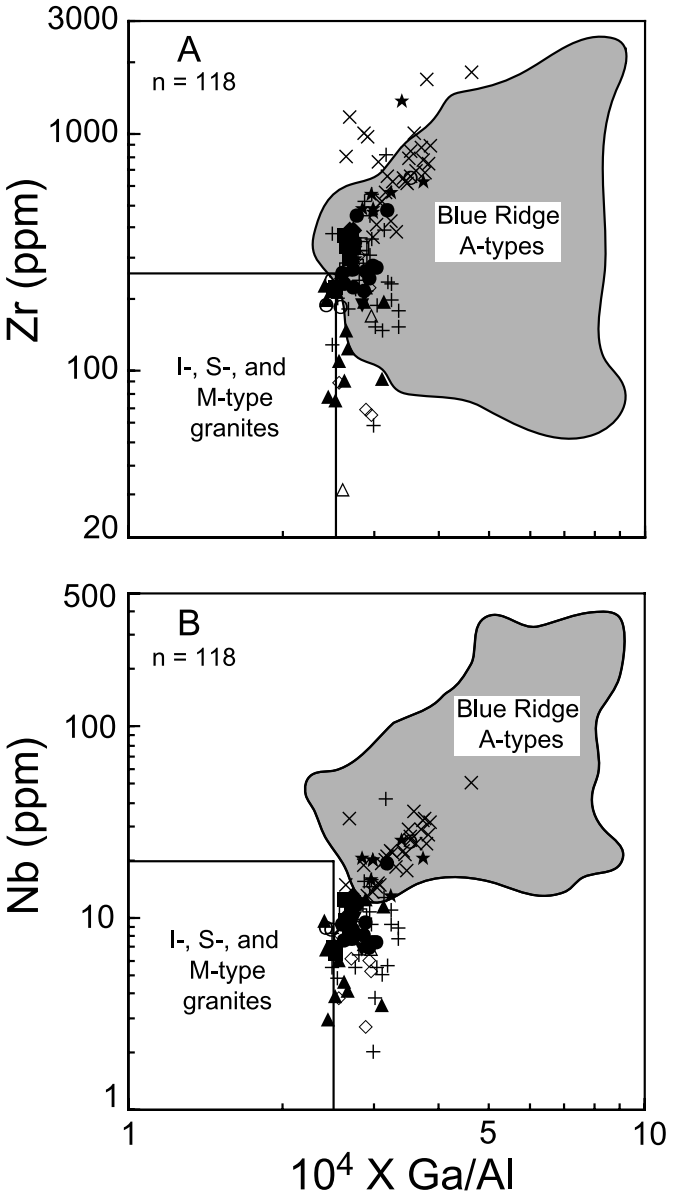

Figure 7. Plot of (A) Zr and (B) Nb versus $10^4 \times$ Ga/Al for basement rocks from the field trip area, compared to Neoproterozoic A-type granitoids from the central Appalachians (shaded field, 150 analyses from Tollo and Aleinikoff, 1996; Tollo and others, in press a). Diagrams modified after Whalen and others (1987). Symbols are the same as in figure 4.

(Pearce and others, 1984; Sylvester, 1989; Maniar and Piccoli, 1989; Eby, 1990, 1992; Förster and others, 1997), granites associated with postorogenic processes and (or) within-plate tectonic environments include both anorogenic and postorogenic types. Such suites typically include A-type granitoids characterized by broad compositional variation that reflects derivation from sources of mixed origin (Sylvester, 1989; Eby, 1990, 1992; Förster and others, 1997). Geochemical data indicate that the low-silica charnockite (Yfqj) displays considerable similarity to A-type granitoids, whereas most other rocks within the study area exhibit compositional features that are transitional between I- and A-types (fig. 7) (Tollo and others, in press a). The contemporaneous low-silica charnockite and leucogranitoids (Ygr, Ygg, and Yaf) display compositional characteristics, such as comparable FeO_t/MgO (fig. 5F) and similar Eu/Eu* (not shown), which suggest that these contrasting rock types are unlikely to define a continuous liquid line of descent. The occurrence of A-type and relatively evolved I-type granitoids that are closely related in both space and time is not unusual in orogenic belts worldwide, as illustrated by examples from Australia (Landenberger and Collins, 1996).

The Blue Ridge rocks thus appear to have been derived through melting of mixed sources present in the evolving Grenvillian orogenic belt. Compositionally transitional intermediate and felsic rocks, including peraluminous leucogranites, were emplaced episodically over a 100-m.y. time span that largely predated local orogenesis at 1,080 to 1,060 Ma. Peraluminous leucogranitoids and low-silica charnockite,

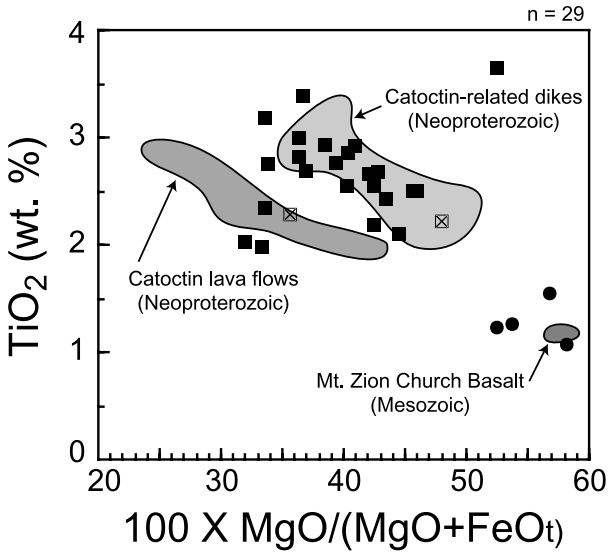

Figure 8. Plot of $100(MgO/MgO+FeO_t)$ versus TiO_2 for mafic (metabasalt, metadiabase, and diabase) dikes of inferred late Neoproterozoic (25 samples, filled squares) and Early Jurassic (4 samples, filled circles) age that intrude basement rocks within the field trip area. Data for samples of two greenstone dikes (squares with diagonal crosses) that intrude basement are also plotted. Data from Hackley (1999), Wilson and Tollo (2001), and Tollo and others (in press b). Compositional fields for (a) relatively unaltered lava flows from the Neoproterozoic Catoctin Formation (10 samples; Badger, 1989), (b) mafic dikes associated with and assumed to be contemporaneous with the Catoctin Formation (20 samples; Badger, 1989), and (c) Early Jurassic Mount Zion Church Basalt from the nearby Culpeper basin (18 samples; Tollo and others, 1988) are plotted for comparison.

which geochemical data suggest were derived from separate sources, postdated orogenesis and marked the termination of local magmatic activity.

Structural Relations

Mesoproterozoic

The older Mesoproterozoic units (>1,060 Ma) commonly display foliations and compositional layers that developed under high-grade metamorphic conditions during Grenvillian orogenesis. Foliation is defined by aligned feldspars and quartz aggregates, and individual grains have a very weak grain-shape preferred orientation with straight grain boundaries. Microstructures and certain mineral assemblages that define this foliation, such as orthopyroxene+garnet, are consistent with high-temperature (>600°C) upper amphibolite- to granulite-facies conditions (Passchier and Trouw, 1996). Regionally, this foliation generally strikes approximately east-west and dips steeply to both the north and south. Folded foliation is only rarely observed, but at some outcrops it is axial planar to folds developed in competent layers such as coarse-grained leucogranitic dikes. The kinematics of this high-grade deformation are unclear; however, based on foliation and fold orientations, the Blue Ridge basement experienced significant ~north-south (in present-day geometry) shortening during this event. The high-temperature fabric is best preserved in units with crystallization ages of >1,080 Ma (Yg, Ygn, Ylg, and Yfpg) and generally absent in units ~1,060 Ma. Grenvillian fabrics are cut and overprinted by a lower temperature foliation defined by greenschist-facies metamorphic minerals and microstructures of probable Paleozoic age. Such low-grade fabrics are present in numerous mafic dikes of late Neoproterozoic age that locally intrude basement but are absent in mafic dikes of probable Mesozoic age. Such dikes are also compositionally distinguishable on the basis of TiO_2 content (fig. 8).

Paleozoic

The identification and interpretation of structural elements of Paleozoic age has evolved greatly during the past three decades, leading to recent recognition of the important role of high-strain zones in the structural development of the Blue Ridge. Indeed, recent discoveries regarding Paleozoic structures have called into question some longstanding ideas regarding the structural genesis of the terrane and have served as the basis for new developmental models of the Blue Ridge. Nevertheless, because of the complex, multi-stage structural evolution of the Blue Ridge, precise determination of timing relations characterizing such structural features remains in its infancy.

A younger fabric of probable Paleozoic age, defined by aligned phyllosilicates, elongate quartz, and fractured feldspars, is common in many Mesoproterozoic units. The foliation generally strikes to the northeast and dips moderately toward the southeast, and is commonly associated with a downdip mineral lineation. The microstructures and minerals that define this fabric are indicative of deformation that occurred at greenschist-facies conditions. In the northern Virginia Blue Ridge, Burton and others (1992) obtained late Paleozoic (~300 Ma) $^{40}Ar/^{39}Ar$ cooling ages on similar fabrics, whereas Furcron (1969) reported early Paleozoic (~450 Ma) K-Ar ages for metamorphic minerals in the Mechum River Formation in central Virginia.

Mitra (1977, 1979) was among the first to demonstrate the kinematic and mechanical significance of high-strain zones (ductile deformation zones) in the northern Virginia Blue Ridge. In central Virginia, Bartholomew and others (1981) named the Rockfish Valley fault zone and suggested that it forms a major tectonic boundary that separates Mesoproterozoic basement massifs (Pedlar and Lovingston) of distinctly different character. Bartholomew and others (1981) and Bartholomew and Lewis (1984) extended the Rockfish Valley fault zone northward from central Virginia to northern Virginia and linked it southward with the Fries fault

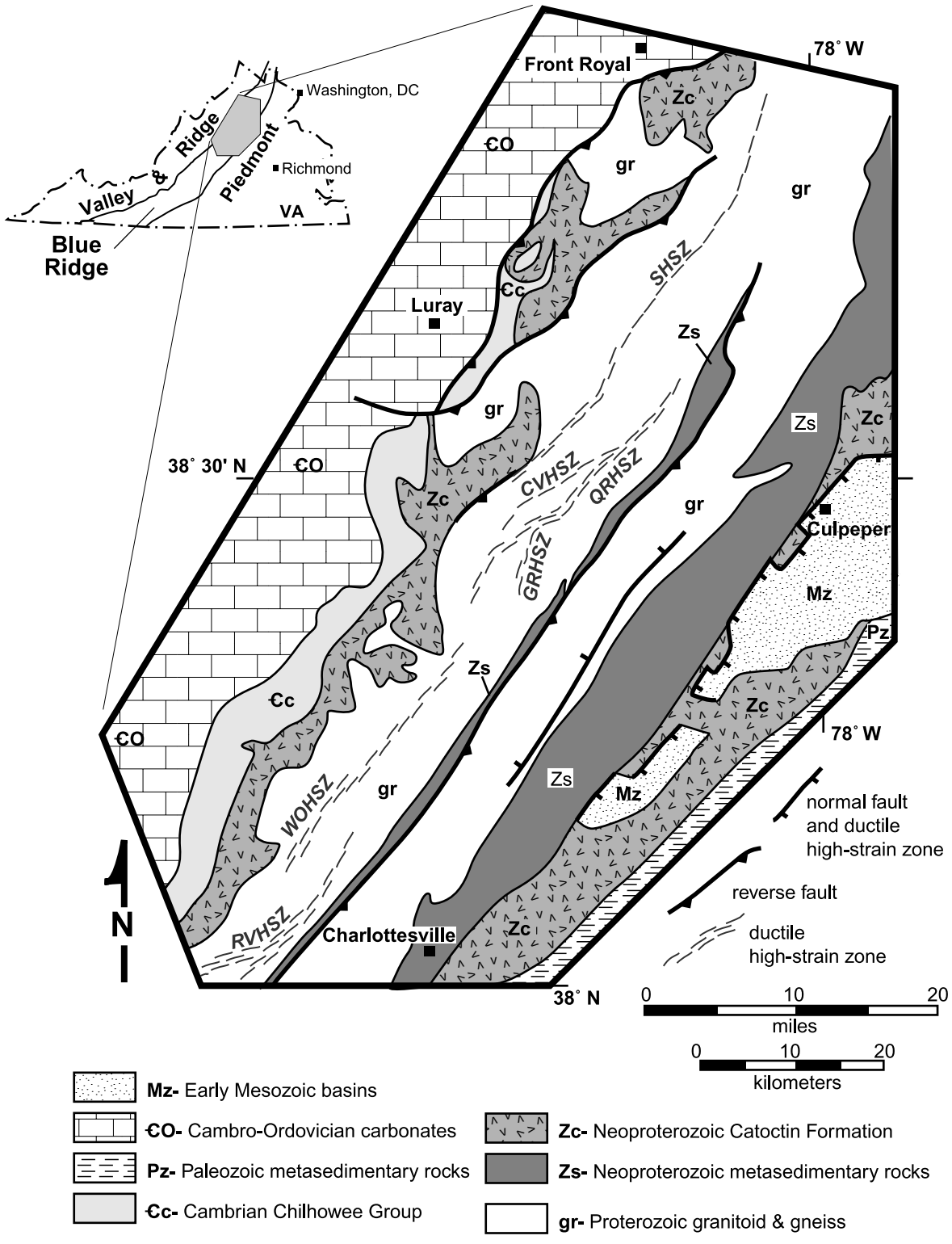

Figure 9. Generalized geologic map of the north-central Virginia Blue Ridge illustrating the location of major Paleozoic high-strain zones, including (from south to north) RVHSZ, Rockfish Valley high-strain zone; WOHSZ, White Oak high-strain zone; GRHSZ, Garth Run high-strain zone; QRHSZ, Quaker Run high-strain zone; CVHSZ, Champlain Valley high-strain zone; and SHSZ, Sperryville high-strain zone. Geology based, in part, on Virginia Division of Mineral Resources (1993); high-strain zones based on 1:24,000- and 1:100,000-scale mapping by authors.

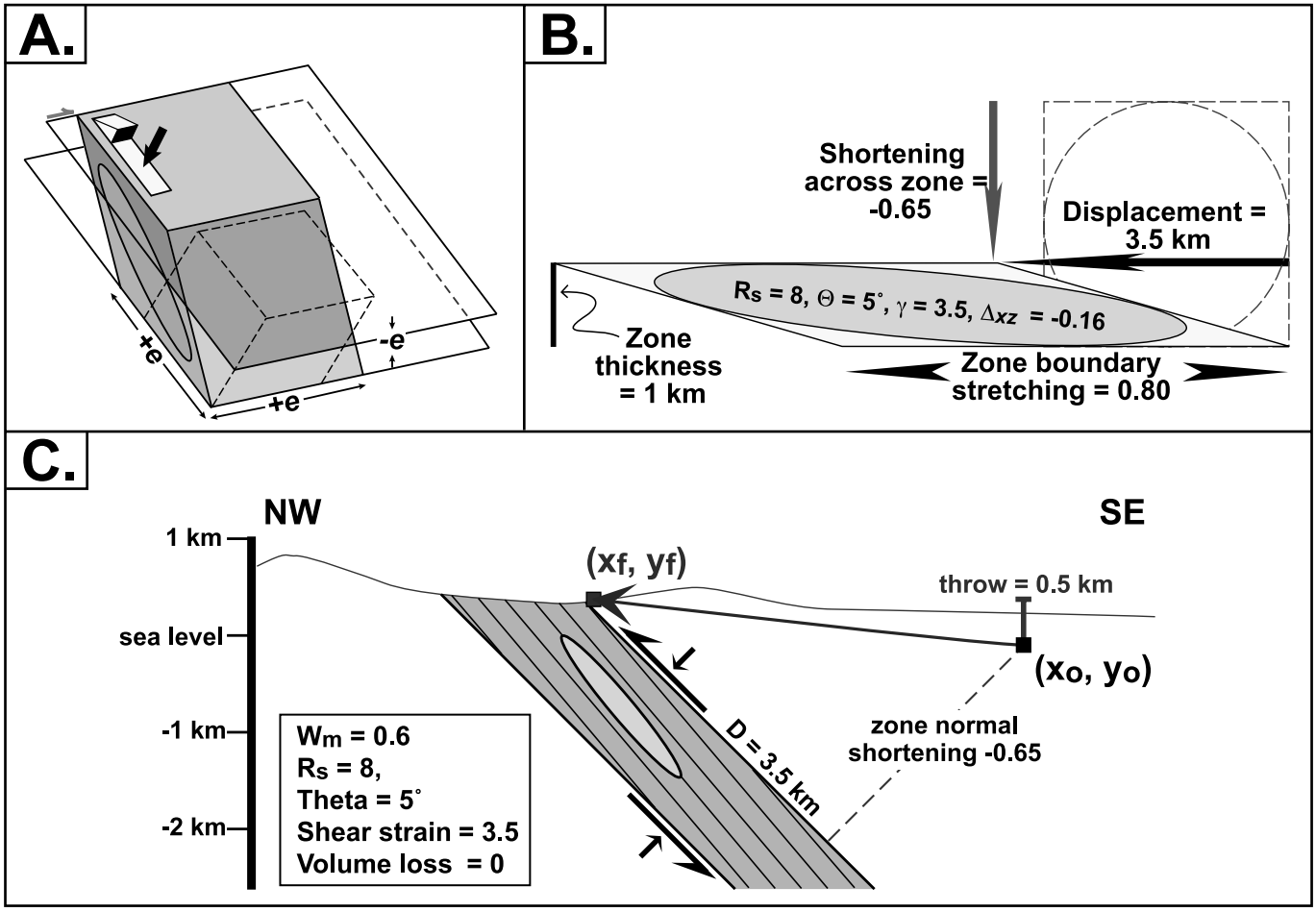

Figure 10. A, Idealized finite deformation for Blue Ridge high-strain zones characterized by a weak triclinic symmetry, general shear, and flattening strain (elongation in two directions, shortening in one). Ellipse represents *XZ* section of the three-dimensional finite strain ellipsoid. B, Kinematic model for deformation in the Quaker Run high-strain zone. The box and circle represent basement in undeformed state that is transformed into parallelogram and ellipse during homogeneous deformation. The model assumes a monoclinic deformation symmetry, general shear (W_m= 0.6), flattening strain (K=0.6), and no volume loss (delta=0). The zone is ~1 km (0.6 mi) thick, the mean *XZ* strain ratio (R_{XZ}) is 8:1 (based on strain estimates from quartz grain shapes), shear strain (gamma) is 3.5, and the orientation between the foliation and high-strain zone boundary (theta) is 5°. There is a sectional area loss ($delta_{XZ}$ =-0.16) because of flattening strain with no volume change. Displacement across the zone is 3.5 km (2.2 mi) and is accompanied by 80 percent stretching parallel to the zone boundary and 65 percent shortening across the zone. C, Displacement, shortening, and tectonic throw across the Quaker Run high-strain zone viewed in cross section, based on deformation parameters illustrated in figure 10B. Rock exposed at (X_f,Y_f) originated at (X_o,Y_o) prior to deformation.

zone in the southern Virginia Blue Ridge. The temporal, kinematic, and tectonic significance of the Rockfish Valley zone has been discussed by a number of workers (Bartholomew and others, 1981; Conley, 1989; Simpson and Kalaghan, 1989; Bailey and Simpson, 1993; Burton and Southworth, in press). Different workers have variously interpreted the Rockfish Valley fault zone to be a reverse, normal, and strike-slip structure.

Recent mapping in the central and northern Virginia Blue Ridge (at both 1:24,000 and 1:100,000 scale) indicates that basement rocks are cut by a series of anastomosing high-strain fault zones (fig. 9) rather than by a single fault zone (for example, the Rockfish Valley fault zone). Individual high-strain zones form northeast-southwest-striking belts of mylonitic rock, 0.5 to 3 km (0.3–1.9 mi) thick, that dip moderately to the southeast. Mineral elongation lineations plunge directly downdip to obliquely downdip. Deformation is heterogeneous and associated penetrative fabrics diminish away from the high-strain zones. From north to south, these zones include the Sperryville, Champlain Valley, Quaker Run, White Oak, and Rockfish Valley zones (fig. 9). Collectively, these zones display an en-echelon map pattern. Individual zones extend 30 to 100 km (19–60 mi) and pinch out along strike. Mylonitic rocks are characterized by microstructures

consistent with deformation occurring at greenschist-facies (~350–400°C) conditions with abundant fluids (Bailey and others, 1994).

Blue Ridge high-strain zones are characterized by both monoclinic and triclinic deformation symmetries (fig. 10) (Bailey and others, in press; Bailey, 2003). Triclinic symmetries are revealed by the geometry of fabric elements with respect to high-strain zone boundaries and fabric asymmetries on planes both parallel and normal to elongation lineations. Elongation lineations plunge to the southeast and kinematic indicators on *XZ* sections record a northwest-directed (reverse) sense of shear. Mylonitic rocks with a triclinic symmetry also record a component of strike-parallel sinistral shear. Strain ratios, measured with quartz grain shapes and boudinaged feldspars, range from 4 to 20 in *XZ* sections. Three-dimensional strains are moderately to strongly oblate (K=0.8–0.0). Vorticity analysis indicates that these high-strain zones experienced bulk general shear deformation (W_m=0.6–0.9).

The total displacement across individual high-strain zones, estimated by integrating shear strains over zone thickness, range from 1 to 4 km (0.6–2.5 mi) (fig. 10). Total displacement estimates are in accord with field relations demonstrating that, at many locations, the same basement unit occurs in both the footwall and hanging wall of the high-strain zone. These modest offsets are incompatible with tectonic models that suggest Blue Ridge high-strain zones separate distinctly different Grenvillian massifs. The kinematic significance of Blue Ridge high-strain zones indicates that (1) these zones accommodated significant crustal shortening, (2) displacement on these zones is on the order of a few kilometers, and (3) widespread flattening strains require significant strike-parallel (orogen-parallel) material movement (fig. 10).

The absolute age of movement on Blue Ridge high-strain zones is not precisely known. Field relations from the central Virginia Blue Ridge indicate that mylonitic high-strain zones are cut by brittle thrusts of Alleghanian (~320–280 Ma) age (Bailey and Simpson, 1993). Polvi (2003) reported an $^{40}Ar/^{39}Ar$ plateau age of 355±3 Ma for muscovite from a greenschist-facies contractional high-strain zone in Nelson County, located approximately 100 km (60 mi) southwest of the field trip area. This cooling age is incompatible with an Alleghanian age for ductile deformation, but could reflect cooling from either a Taconian (Ordovician) or Devonian event possibly synchronous with the Acadian orogeny in New England.

Summary and Regional Implications

The new mapping and supporting investigations of basement in the study area illustrate the lithologic complexity and protracted geologic evolution of rocks associated with Mesoproterozoic orogenesis. The structural studies indicate the importance of multiple high-strain zones in accommodating the effects of Paleozoic deformation within the Blue Ridge core, and suggest that the role of the Rockfish Valley fault zone was not as significant as previously suggested. This finding necessitates a re-evaluation of models for Paleozoic structural development of the Blue Ridge that involve the Rockfish Valley fault zone as the dominant internal tectonic element responsible for the present distribution of major rock types in the anticlinorium. The lithologic variation documented in Blue Ridge basement rocks by these studies refines previous models of the province that were based largely on reconnaissance-scale mapping by demonstrating the complex juxtaposition of rocks of different composition, age, and tectonic significance. The dominance of granitic rocks in the study area is similar to the compositional characteristics documented elsewhere in the Appalachian massifs (for example, Rankin and others, 1989b; Carrigan and others, 2003). However, the lack of rocks generally associated with orogeny is noteworthy and contrasts with the presence of lithologies of calc-alkaline affinity in the Adirondacks (McLelland and others, 1996) and New Jersey Highlands (Volkert, in press). Results from geochronologic studies completed to date indicate that the northern Blue Ridge also differs from the well-documented Adirondacks in lacking rocks of >1,200-Ma age. Correspondingly, there is at present no evidence of Elzevirian orogenic processes in the Blue Ridge of Virginia, suggesting either that the province did not undergo this earlier pulse of Grenvillian orogenic activity that is otherwise well documented in the Adirondacks and some parts of the southeastern Canadian Grenville province (Rivers, 1997; Wasteneys and others, 1999; Gower and Krogh, 2002), or that the lithologic signature of this event was destroyed by subsequent Mesoproterozoic orogenesis. Nevertheless, trace-element geochemical characteristics of many of the Mesoproterozic granitic rocks of the northern Virginia Blue Ridge indicate the presence of components of calc-alkaline affinity in the magmatic sources, suggesting that pre-existing Laurentian crust contains evidence of pre-1,200-Ma tectonic processes (Tollo and others, in press a). The geochronology of basement rocks from the northern Blue Ridge indicates that the province shares many temporal characteristics with other Appalachian massifs (Aleinikoff and others, 1990; Carrigan and others, 2003; Hatcher and others, in press) and supports definition of the Appalachian outliers as outposts of Laurentian crust affected by Grenvillian orogenic processes (Rankin and others, 1989b). Nevertheless, the petrologic and compositional heterogeneity and substantial range in emplacement ages that characterize Blue Ridge basement rocks suggest that detailed correlation of events and processes recorded within individual massifs will depend on continued scientific advances.

References Cited

Aleinikoff, J.N., Burton, W.C., Lyttle, P.T., Nelson, A.E., and Southworth, C.S., 2000, U-Pb geochronology of zircon and monazite from Mesoproterozoic granitic gneisses of the northern Blue Ridge, Virginia and Maryland, USA:

Precambrian Research, v. 99, p. 113–146.

Aleinikoff, J.N., Ratcliffe, N.M., Burton, W.C., and Karabinos, P.A., 1990, U-Pb ages of Middle Proterozoic igneous and metamorphic events, Green Mountains, Vermont [abs.]: Geological Society of America Abstracts with Programs, v. 22, no. 2, p. 1.

Aleinikoff, J.N., Zartman, R.E., Walter, M., Rankin, D.W., Lyttle, P.T., and Burton, W.C., 1995, U-Pb ages of metarhyolites of the Catoctin and Mount Rogers Formations, central and southern Appalachians; Evidence for two pulses of Iapetan rifting: American Journal of Science, v. 295, p. 428–454.

Allen, R.M., 1963, Geology and mineral resources of Greene and Madison Counties, Virginia: Virginia Division of Mineral Resources Bulletin 78, 102 p.

Andersen, D.J., Lindsley, D.H., and Davidson, P.M., 1993, QUILF; A Pascal program to assess equilibria among Fe-Mg-Mn-Ti oxides, pyroxenes, olivine, and quartz: Computers and Geosciences, v. 19, no. 9, p. 1333–1350.

Badger, R.L., 1989, Geochemistry and petrogenesis of the Catoctin volcanic province, central Appalachians: Blacksburg, Virginia Polytechnic Institute, Ph.D thesis, 337 p.

Badger, R.L., 1999, Geology along Skyline Drive: Helena, Mont., Falcon Publishing, Inc., 100 p.

Badger, R.L., and Sinha, A.K., 1988, Age and Sr isotopic signature of the Catoctin volcanic province; Implications for subcrustal mantle evolution: Geology, v. 16, p. 692–695.

Bailey, C.M., 2003, Kinematic significance of monoclinic and triclinic high-strain zones in the Virginia Blue Ridge province [abs.]: Geological Society of America Abstracts with Programs, v. 35, no. 1, p. 21.

Bailey, C.M., and Peters, S.E., 1998, Glaciogenic sedimentation in the Late Neoproterozoic Mechum River Formation, Virginia: Geology, v. 26, p. 623–626.

Bailey, C.M., and Simpson, C., 1993, Extensional and contractional deformation in the Blue Ridge province, Virginia: Geological Society of America Bulletin, v. 105, p. 411–422.

Bailey, C.M., and Tollo, R.P., 1998, Late Neoproterozoic extension-related magma emplacement in the central Appalachians; An example from the Polly Wright Cove pluton: Journal of Geology, v. 106, p. 347–359.

Bailey, C.M., Berquist, P.J., Mager, S.M., Knight, B.D., Shotwell, N.L., and Gilmer, A.K., 2003, Bedrock geology of the Madison quadrangle, Virginia: Virginia Division of Mineral Resources Publication 157.

Bailey, C.M., Mager, S.M., Gilmer, A.G., and Marquis, M.N., in press, Monoclinic and triclinic high-strain zones; Examples from the Blue Ridge province, central Appalachians: Journal of Structural Geology.

Bailey, C.M., Simpson, C., and De Paor, D.G., 1994, Volume loss and tectonic flattening strain in granitic mylonites from the Blue Ridge province, central Appalachians: Journal of Structural Geology, v. 16, p. 1403–1416.

Bartholomew, M.J., and Lewis, S.E., 1984, Evolution of Grenville massifs in the Blue Ridge geologic province, southern and central Appalachians, *in* Bartholomew, M.J., Force, E.R., Sinha, A.K., and Herz, N., eds., The Grenville event in the Appalachians and related topics: Geological Society of America Special Paper 194, p. 229–254.

Bartholomew, M.J., and Lewis, S.E., 1988, Peregrination of Middle Proterozoic massifs and terranes within the Appalachian orogen, eastern U.S.A.: Trabajos de Geología, Universidad de Oviedo, v. 17, p. 155–165.

Bartholomew, M.J., Gathright, T.M., II, and Henika, W.S., 1981, A tectonic model for the Blue Ridge in central Virginia: American Journal of Science, v. 281, p. 1164–1183.

Berquist, P.J., and Bailey, C.M., 2000, Displacement across Paleozoic high-strain zones in the Blue Ridge province, Madison County, Virginia; The Pedlar and Lovingston massifs reconsidered [abs.]: Geological Society of America Abstracts with Programs, v. 32, no. 2, p. 4.

Bloomer, R.O., and Werner, H.J., 1955, Geology of the Blue Ridge in central Virginia: Geological Society of America Bulletin, v. 66, p. 579-606.

Burton, W.C., and Southworth, Scott, in press, Tectonic evolution of the northern Blue Ridge massif, Virginia and Maryland, *in* Tollo, R.P., Corriveau, L., McLelland, J., and Bartholomew, M.J., eds., Proterozoic tectonic evolution of the Grenville orogen in North America: Geological Society of America Memoir 197.

Burton, W.C., Froelich, A.J., Pomeroy, J.S., and Lee, K.Y., 1995, Geology of the Waterford quadrangle, Virginia and Maryland, and the Virginia part of the Point of Rocks quadrangle: U.S. Geological Survey Bulletin 2095, 30 p., scale 1:24,000.

Burton, W.C., Kunk, M.J., and Lyttle, P.T., 1992, Age constraints on the timing of regional cleavage formation in the Blue Ridge anticlinorium, northernmost Virginia [abs.]: Geological Society of America Abstracts with Programs, v. 24, no. 2, p. 5.

Carrigan, C.W., Miller, C.F., Fullagar, P.D., Bream, B.R., Hatcher, R.D., Jr., and Coath, C.D., 2003, Ion microprobe age and geochemistry of southern Appalachian basement, with implications for Proterozoic and Paleozoic reconstructions: Precambrian Research, v. 120, p. 1–36.

Clarke, J.W., 1984, The core of the Blue Ridge anticlinorium in northern Virginia, *in* Bartholomew, M.J., Force, E.R., Sinha, A.K., and Herz, N., eds., The Grenville event in the Appalachians and related topics: Geological Society of America Special Paper 194, p. 155–160.

Conley, J.F., 1989, Stratigraphy and structure across the Blue Ridge and Inner Piedmont in central Virginia: International Geological Congress Field trip guidebook T207, American Geophysical Union, 23 p.

Dalziel, I.W.D., Mosher, S., and Gahagan, L.M., 2000, Laurentia-Kalahari collision and the assembly of Rodinia: Journal of Geology, v. 108, p. 499–513.

Deer, W.A., Howie, R.A., and Zussman, J., 1992, An introduction to the rock-forming minerals: Essex, Addison Wesley Longman Limited, 696 p.

Duchesne, J.C., and Wilmart, E., 1997, Igneous charnockites and related rocks from the Bjerkreim-Sokndal layered intrusion (southwest Norway); A jotunite (hypersthene monzodiorite)-derived A-type granitoid suite: Journal of Petrology, v. 38, p. 337–369.

Eaton, L.S., Morgan, B.A., Kochel, R.C., and Howard, A.D., 2003, Role of debris flows in long term landscape denudation in the central Appalachians of Virginia: Geology, v. 31, no. 4, p. 339–342.

Eby, G.N., 1990, The A-type granitoids; A review of their occurrence and chemical characteristics and speculations on their petrogenesis: Lithos, v. 26, p. 115–134.

Eby, G.N., 1992, Chemical subdivision of the A-type granitoids; Petrogenetic and tectonic implications: Geology, v. 20, p. 641–644.

Evans, N.H., 1991, Latest Precambrian to Ordovician metamorphism in the Virginia Blue Ridge; Origin of the contrasting Lovingston and Pedlar basement massifs: American Journal of Science, v. 291, p. 425–452.

Fenneman, N.M., 1938, Physiography of eastern United States: New York, McGraw-Hill, 714 p.

Fetter, A.H., and Goldberg, S.A., 1995, Age and geochemical characteristics of bimodal magmatism in the Neoproterozoic Grandfather Mountain rift basin: Journal of Geology, v. 103, p. 313–326.

Förster, H.-J., Tischendorf, G., and Trumbull, R.B., 1997, An evaluation of the Rb vs. (Y+Nb) discrimination diagram to infer tectonic setting of silicic igneous rocks: Lithos, v. 40, p. 261–293.

Froelich, A.J., and Gottfried, D., 1988, An overview of early Mesozoic intrusive rocks in the Culpeper basin, Virginia and Maryland, *in* Froelich, A.J., and Robinson, G.R., Jr., eds., Studies of early Mesozoic basins of eastern North America: U.S. Geological Survey Bulletin 1776, p. 151–165.

Frost, C.D., and Frost, B.R., 1997, Reduced rapakivi-type granites; The tholeiitic connection: Geology, v. 25, p. 647–650.

Frost, B.R., Frost, C.D., Hulsebosch, T.P., and Swapp, S.M., 2000, Origin of the charnockites of the Louis Lake batholith, Wind River Range, Wyoming: Journal of Petrology, v. 41, p. 1759–1776.

Furcron, A.S., 1969, Late Precambrian and Early Paleozoic erosional and depositional sequences of northern and central Virginia: Georgia Geological Survey Bulletin, v. 101, p. 339–354.

Gathright, T.M., II, 1976, Geology of the Shenandoah National Park in Virginia: Virginia Division of Mineral Resources Bulletin 86, 93 p.

Gower, C.F., and Krogh, T.E., 2002, A U-Pb geochronological review of the Proterozoic history of the eastern Grenville province: Canadian Journal of Earth Sciences v. 39, p. 795–829.

Hackley, P.H., 1999, Petrology, geochemistry, and field relations of the Old Rag Granite and associated charnockitic rocks, Old Rag Mountain 7.5-minute quadrangle, Madison and Rappahannock Counties, Virginia: Washington, D.C., The George Washington University, M.S. thesis, 244 p.

Hackley, P.H., and Tollo, R.P., in press, Geology of basement rocks in a portion of the Old Rag Mountain quadrangle, Virginia: Virginia Division of Mineral Resources Publication 170, Part C, scale 1:24,000.

Hamilton, M., McLelland, J., and Selleck, B., in press, SHRIMP U-Pb zircon geochronology of the anorthosite-mangerite-charnockite-granite (AMCG) suite, Adirondack Mountains, New York; Ages of emplacement and metamorphism, *in* Tollo, R.P., Corriveau, L., McLelland, J., and Bartholomew, M.J., eds., Proterozoic tectonic evolution of the Grenville orogen in North America: Geological Society of America Memoir 197.

Hanchar, J.M., and Miller, C.F., 1993, Zircon zonation patterns as revealed by cathodoluminescence and backscattered electron images; Implications for the interpretation of complex crustal histories: Chemical Geology, v. 110, no. 1–3, p. 1013.

Hanchar, J.M., and Rudnick, R.L., 1995, Revealing hidden structures; The application of cathodoluminescence and back-scattered electron images to dating zircons from lower crustal xenoliths: Lithos, v. 36, no. 3–4, p. 289–303.

Hatcher, R.D., Jr., Bream, B.R., Miller, C.F., Eckert, J.O., Jr., Fullagar, P.D., and Carrigan, C.W., in press, Paleozoic structure of internal basement massifs, southern Appalachian Blue Ridge, incorporating new geochronologic, Nd and Sr isotopic, and geochemical data, *in* Tollo, R.P., Corriveau, L., McLelland, J., and Bartholomew, M.J., eds., Proterozoic tectonic evolution of the Grenville orogen in North America: Geological Society of America Memoir 197.

Hughes, S.S., Lewis, S.E., Bartholomew, M.J., Sinha, A.K., and Herz, N., in press, Geology and geochemistry of granitic and charnockitic rocks in the central Lovingston massif of the Grenvillian Blue Ridge terrane, U.S.A., *in* Tollo, R.P., Corriveau, L., McLelland, J., and Bartholomew, M.J., eds., Proterozoic tectonic evolution of the Grenville orogen in North America: Geological Society of America

Memoir 197.

Irvine, T.N., and Baragar, W.R.A., 1971, A guide to the chemical classification of the common volcanic rocks: Canadian Journal of Earth Sciences, v. 8, p. 523–548.

Jonas, A.I., ed., 1928, Geologic map of Virginia: Charlottesville, Virginia Division of Mineral Resources, scale 1:500,000.

Kilpatrick, J.A., and Ellis, D.J., 1992, C-type magmas; Igneous charnockites and their extrusive equivalents, *in* Brown, P.E., and Chappell, B.W., eds., The Second Hutton Symposium on the origin of granites and related rocks: Geological Society of America Special Paper 272, p. 155–164.

Kretz, R., 1983, Symbols for rock-forming minerals: American Mineralogist, v. 68, p. 277–279.

Kunk, M.J., and Burton, W.C., 1999, $^{40}Ar/^{39}Ar$ age-spectrum data for amphibole, muscovite, biotite, and K-feldspar samples from metamorphic rocks in the Blue Ridge anticlinorium, northern Virginia: U.S. Geological Survey Open-File Report OF–99–0552, 110 p.

Landenberger, B., and Collins, W.J., 1996, Derivation of A-type granites from a dehydrated charnockitic lower crust; Evidence from the Chaelundi Complex, eastern Australia: Journal of Petrology, v. 37, p. 145–170.

Leake, B.E., Woolley, A.R., Arps, C.E.S., Birch, W.D., Gilbert, M.C., Grice, J.D., Hawthorne, F.C., Kato, A., Kisch, H.J., Krivovichev, V.G., Linthout, K., Laird, J., Mandarino, J.A., Maresch, W.V., Nickel, E.H., Rock, N.M.S., Schumacher, J.C., Smith, D.C., Stephenson, N.C.N., Ungaretti, L., Whittaker, E.J.W., and Youzhi, G., 1997, Nomenclature of amphiboles; Report of the Subcommittee on Amphiboles of the International Mineralogical Association, Commission on New Minerals and Mineral Names: American Mineralogist, v. 82, p. 1019–1037.

Le Maitre, R.W., Bateman, P., Dudek, A., Keller, J., Lameyre, J., Le Bas, M.J., Sabine, P.A., Schmid, R., Sørensen, H., Streckeisen, A., Woolley, A.R., and Zanettin, B., 1989, A classification of igneous rocks and glossary of terms; Recommendations of the International Union of Geological Sciences Subcommission on the Systematics of Igneous Rocks: Oxford, United Kingdom, Blackwell Scientific Publications, 193 p.

Lindsley, D.H., 1983, Pyroxene thermometry: American Mineralogist, v. 68, p. 477–493.

Malm, O.A., and Ormaasen, D.E., 1978, Mangerite-charnockite intrusives in the Lofoten-Vesterålen area, north Norway; Petrography, chemistry, and petrology: Norges Geologiske Undersokelse, v. 338, p. 38–114.

Maniar, P.D., and Piccoli, P.M., 1989, Tectonic discrimination of granitoids: Geological Society of America Bulletin, v. 101, p. 635–643.

McLelland, J., and Whitney, P., 1990, Anorogenic, bimodal emplacement of anorthositic, charnockitic, and related rocks in the Adirondack Mountains, New York, *in* Stein, H.J., and Hannah, J.L., eds., Ore-bearing granite systems; Petrogenesis and mineralizing processes: Geological Society of America Special Paper 246, p. 301–315.

McLelland, J., Daly, J.S., and McLelland, J.M., 1996, The Grenville orogenic cycle (ca. 1350–1000 Ma); An Adirondack perspective: Tectonophysics, v. 256, p. 1–28.

McLelland, J., Hamilton, M., Selleck, B., McLelland, J.M., Walker, D., and Orrell, S., 2001, Zircon U-Pb geochronology of the Ottawan orogeny, Adirondack Highlands, New York; Regional and tectonic implications: Precambrian Research, v. 109, p. 39–72.

Mitra, G., 1977, The mechanical processes of deformation of granitic basement and the role of ductile deformation zones in the deformation of Blue Ridge basement in northern Virginia: Baltimore, Md., Johns Hopkins University, unpublished Ph.D. dissertation, 219 p.

Mitra, G., 1979, Ductile deformation zones in Blue Ridge basement and estimation of finite strains: Geological Society of America Bulletin, v. 90, p. 935–951.

Mitra, G., and Lukert, M.T., 1982, Geology of the Catoctin-Blue Ridge anticlinorium in northern Virginia, *in* Lyttle, P.T., Central Appalachian geology, Field trip guidebook for the joint meeting of the Northeastern and Southeastern Sections of the Geological Society of America, Washington, D.C., 1982: Falls Church, Va., American Geological Institute, p. 83–108.

Miyashiro, A., 1974, Volcanic rock series in island arcs and active continental margins: American Journal of Science, v. 274, p. 321–355.

Morgan, B.A., Wieczorek, G.F., and Campbell, R.H., 1999, Map of rainfall, debris flows, and flood effects of the June 27, 1995, storm in Madison County, Virginia: U.S. Geological Survey Geologic Investigations Series Map I–2623–A, scale 1:24,000.

Morimoto, N., 1988, Nomenclature of pyroxenes: Mineralogical Magazine, v. 52, p. 535–550.

Passchier, C.W., and Trouw, R.A.J., 1996, Microtectonics: New York, Springer Verlag, 283 p.

Pearce, J.A., Harris, N.B.W., and Tindle, A.G., 1984, Trace element discrimination diagrams for the tectonic interpretation of granitic rocks: Journal of Petrology, v. 25, p. 956–983.

Polvi, L.E., 2003, Structural and geochronological analysis of the Lawhorne Mill high-strain zone, central Virginia Blue Ridge province: Williamsburg, Va., College of William and Mary, unpublished B.S. thesis, 51 p.

Rankin, D.W., Drake, A.A., Jr., and Ratcliffe, N.M., 1989a, Geologic map of the U.S. Appalachians showing the

Laurentian margin and Taconic orogen, *in* Hatcher, R.D., Jr., Thomas, W.A., and Viele, G.W., eds., The Appalachian-Ouachita orogen in the United States, v. F–2 *of* The geology of North America: Boulder, Colo., Geological Society of America, plate 2.

Rankin, D.W., Drake, A.A., Jr., Glover, L., III, Goldsmith, R., Hall, L.M., Murray, D.P., Ratcliffe, N.M., Read, J.F., Secor, D.T., Jr., and Stanley, R.S., 1989b, Pre-orogenic terranes, *in* Hatcher, R.D., Jr., Thomas, W.A., and Viele, G.W., eds., The Appalachian-Ouachita orogen in the United States, v. F–2 *of* The geology of North America: Boulder, Colo., Geological Society of America, p. 7–100.

Rivers, T., 1997, Lithotectonic elements of the Grenville province; Review and tectonic implications: Precambrian Research, v. 86, p. 117–154.

Sheraton, J.W., Black, L.P., and Tindle, A.G., 1992, Petrogenesis of plutonic rocks in a Proterozoic granulite-facies terrane—The Bunger Hills, East Antarctica: Chemical Geology, v. 97, p. 163–198.

Simpson, C., and De Paor, D.G., 1993, Strain and kinematic analysis in general shear zones: Journal of Structural Geology, v. 15, p. 1–20.

Simpson, C., and Kalaghan, T., 1989, Late Precambrian crustal extension preserved in Fries fault zone mylonites, southern Appalachians: Geology, v. 17, p. 148–151.

Simpson, E.L., and Eriksson, K.A., 1989, Sedimentology of the Unicoi Formation in southern and central Virginia; Evidence for Late Proterozoic to Early Cambrian rift-to-drift passive margin transition: Geological Society of America Bulletin, v. 101, p. 42–54.

Sinha, A.K., and Bartholomew, M.J., 1984, Evolution of the Grenville terrane in the central Virginia Appalachians, *in* Bartholomew, M.J., Force, E.R., Sinha, A.K., and Herz, N., eds., The Grenville event in the Appalachians and related topics: Geological Society of America Special Paper 194, p. 175–186.

Southworth, Scott, 1994, Geologic map of the Bluemont quadrangle, Loudoun and Clarke Counties, Virginia: U.S. Geological Survey Geologic Quadrangle Map GQ–1739, scale 1:24,000.

Southworth, Scott, 1995, Geologic map of the Purcellville quadrangle, Loudoun County, Virginia: U.S. Geological Survey Geologic Quadrangle Map GQ–1755, scale 1:24,000.

Southworth, Scott, and Brezinski, D.K., 1996, Geology of the Harpers Ferry quadrangle, Virginia, Maryland, and West Virginia: U.S. Geological Survey Bulletin 2123, 33 p., scale 1:24,000.

Spear, F.S., 1993, Metamorphic phase equilibria and pressure-temperature-time paths: Mineralogical Society of America Monograph 1, 799 p.

Streckeisen, A.J., and Le Maitre, R.W., 1979, A chemical approximation to the modal QAPF classification of the igneous rocks: Neues Jahrbuch für Mineralogie, Abhandlungen, v. 136, p. 169–206.

Su, Q., Goldberg, S.A., and Fullagar, P.D., 1994, Precise U-Pb zircon ages of Neoproterozoic plutons in the southern Appalachian Blue Ridge and their implications for the initial rifting of Laurentia: Precambrian Research, v. 68, p. 81–95.

Sylvester, P.J., 1989, Post-collisional alkaline granites: Journal of Geology, v. 97, p. 261–280.

Tollo, R.P., and Aleinikoff, J.N., 1996, Petrology and U-Pb geochronology of the Robertson River igneous suite, Blue Ridge province, Virginia; Evidence for multistage magmatism associated with an early episode of Laurentian rifting: American Journal of Science, v. 296, p. 1045–1090.

Tollo, R.P., and Hutson, F.E., 1996, 700 Ma age for the Mechum River Formation, Blue Ridge province, Virginia; A unique time constraint on pre-Iapetan rifting of Laurentia: Geology, v. 24, p. 59–62.

Tollo, R.P., Aleinikoff, J.N., Bartholomew, M.J., and Rankin, D.W., 2004, Neoproterozoic A-type granitoids of the central and southern Appalachians; Intraplate magmatism associated with episodic rifting of the Rodinian supercontinent: Precambrian Research, v. 128, p. 3–38.

Tollo, R.P., Aleinikoff, J.N., Borduas, E.A., and Hackley, P.C., in press a, Petrologic and geochronologic evolution of the Grenville orogen, northern Blue Ridge province, Virginia, *in* Tollo, R.P., Corriveau, L., McLelland, J., and Bartholomew, M.J., eds., Proterozoic tectonic evolution of the Grenville orogen in North America: Geological Society of America Memoir 197.

Tollo, R.P., Borduas, E.A., and Hackley, P.C., in press b, Geology of basement rocks in the Thornton Gap, Old Rag Mountain, and Fletcher quadrangles, Virginia: Virginia Division of Mineral Resources Publication 170.

Tollo, R.P., Gottfried, D., and Froelich, A.J., 1988, Field guide to the igneous rocks of the southern Culpeper basin, Virginia, *in* Froelich, A.J., and Robinson, G.R., Jr., eds., Studies of early Mesozoic basins of eastern North America: U.S. Geological Survey Bulletin 1776, p. 391–403.

Virginia Division of Mineral Resources, 1993, Geologic map of Virginia: [Richmond], Virginia Division of Mineral Resources, scale 1:500,000.

Volkert, R.A., in press, Mesoproterozoic rocks of the New Jersey Highlands, north-central Appalachians; Petrogenesis and tectonic history, *in* Tollo, R.P., Corriveau, L., McLelland, J., and Bartholomew, M.J., eds., Proterozoic tectonic evolution of the Grenville orogen in North America: Geological Society of America Memoir 197.

Wadman, H.M., Owens, B.E., and Bailey, C.M., 1998, Petrological analysis of the White Oak Dam exposure, Blue Ridge province, Virginia [abs.]: Geological Society of

America Abstracts with Programs, v. 30, no. 4, p. 64.

Wasteneys, H., McLelland, J., and Lumbers, S., 1999, Precise zircon geochronology in the Adirondack Lowlands and implications for revising plate-tectonic models of the Central Metasedimentary Belt and Adirondack Mountains, Grenville province, Ontario and New York: Canadian Journal of Earth Sciences, v. 36, p. 967–984.

Wehr, F.L., II, 1988, Transition from alluvial to deep-water sedimentation in the lower Lynchburg (Upper Proterozoic), Virginia, *in* Bartholomew, M.J., Hyndman, D.W., Mogk, D.W., and Mason, R., eds., Characterization and comparison of ancient and Mesozoic continental margins; Proceedings of the 8th International Conference on Basement Tectonics: Dordrecht, The Netherlands, Kluwer Academic Publishers, p. 407–423.

Whalen, J.B., Currie, K.L., and Chappell, B.W., 1987, A-type granites; Geochemical characteristics, discrimination and petrogenesis: Contributions to Mineralogy and Petrology, v. 95, p. 407–419.

Wieczorek, G.F., Morgan, B.A., and Campbell, R.H., 2000, Debris-flow hazards in the Blue Ridge of central Virginia: Environmental and Engineering Geoscience, v. VI, no. 1, p. 3–23.

Wilson, E.W., and Tollo, R.P., 2001, Geochemical distinction and tectonic significance of Mesozoic and Late Neoproterozoic dikes, Blue Ridge province, Virginia [abs.]: Geological Society of America Abstracts with Programs, v. 33, no. 2, p. 70.

ROAD LOG AND STOP DESCRIPTIONS FOLLOW

Road Log and Stop Descriptions

The field trip begins at the McDonald's restaurant on U.S. 522/U.S. 340 directly south of Exit 6 off I-66 in Front Royal, Va.

NOTE: Throughout the road log, numbers in the left-hand column indicate cumulative mileage for the entire field trip; numbers in the right-hand column indicate cumulative mileage within each stop-to-stop segment of the trip.

Mileage

Trip Cumulative	Stop-to-Stop Cumulative	
	0.0	Proceed south on U.S. 522/U.S. 340.
0.5	0.5	Cross the North Fork of the Shenandoah River. *Relatively undeveloped flood plain is visible on both sides of the highway.*
0.8	0.8	Proceed straight at intersection with Va. 55 toward Front Royal.
1.0	1.0	Cross the South Fork of the Shenandoah River. *Residential development bordering the flood plain is visible on the left.* Remain in left lane.
1.6	1.6	Turn left at traffic light to remain on U.S. 522/U.S. 340/Va. 55. Remain in right lane.
2.2	2.2	Proceed straight through traffic light to remain on U.S. 340 S/ Va. 55 E. Proceed straight through Front Royal on U.S. 340 S (Royal Avenue).
3.0	3.0	Pass United Methodist Church. *The church is constructed largely of limestone of the type commonly obtained from carbonate valleys of the central Appalachians.*
3.5	3.5	Proceed straight through traffic light to remain on U.S. 340 S. Merge into left lane.
4.0	4.0	Pass entrance to Shenandoah National Park on the left.
4.2	4.2	Turn left onto Va. 649 S (Browntown Road).
8.2	8.2	*Roadcut on left side exposes very fresh, medium- to coarse-grained, garnet+biotite leucogranite that contains locally abundant, disseminated graphite.*
8.4	8.4	Stop 1. Turn right onto Gooney Falls Lane. Follow Trip Leaders PRIVATE PROPERTY

Stop 1. Garnetiferous alkali feldspar granite to syenogranite (Ygg).

This outcrop is part of a series of exposures along Gooney Run located near the northern end of the garnetiferous alkali feldspar granite to syenogranite (Ygg) pluton, which extends south to the vicinity of Gravel Springs Gap Road where it is cut, but not truncated, by a northeast-southwest-striking fault (fig. 3). This lithologic unit is typically garnet-bearing, leucocratic, and characterized by alkali feldspar-to-plagioclase ratios >1. The rock at this outcrop is syenitic, and may represent a feldspar cumulate. The syenitic composition is in contrast to that of other exposures in the area which are generally granitic, especially in the southern part of the pluton. The foliation visible in this outcrop (strike 355°, dip 65° E.) is likely to have developed during regional Paleozoic orogenesis due to the absence of high-temperature textural and mineralogical characteristics. This lithologic unit is inferred to intrude the orthopyroxene+amphibole quartz diorite (Ypqd), on the basis of field relations observed at Boyd's Mill (Stop 3). The granitoid is intruded by north-south-striking metadiabase dikes at this outcrop, one of which is about 20 m (66 ft) wide. The chemical

composition of a sample collected from the largest dike is presented in table 5 (sample SNP-01-159), and the significance of these data is discussed in the text devoted to Stop 6). Such dikes are very common throughout the Blue Ridge, but are especially abundant in the northern Blue Ridge (Burton and others, 1995).

Throughout the field trip area, the Ygg unit includes white, medium- to very coarse-grained, inequigranular, weakly to strongly foliated syenogranite and white, medium-grained, equigranular, weakly foliated alkali feldspar granite to syenogranite composed of 35 to 40 percent orthoclase, 15 to 25 percent plagioclase, and 20 to 25 percent quartz with 2 to 10 percent garnet, 2 to 5 percent biotite, and 2 to 5 percent pseudomorphs after orthopyroxene. Accessory minerals include apatite, zircon, and ilmenite. Locally strong foliation within medium- to very coarse-grained syenogranite is defined by alignment of tabular feldspar megacrysts and elongate, polygranular garnet in garnet+biotite-rich domains. Weak foliation in the medium-grained, equigranular alkali feldspar granite to syenogranite is defined by alignment of polygranular garnet-rich domains. Meter- to decimeter-scale dikes of medium-grained, equigranular alkali feldspar granite to syenogranite locally intrude medium- to very coarse-grained syenogranite. Rare pegmatitic dikes, typically <10 cm (4 in) in width, locally intrude all lithologic phases of this unit. This lithologic unit is mineralogically and geochemically similar to medium- to very coarse-grained, inequigranular, massive to weakly foliated granite and medium-grained, equigranular to inequigranular, massive to weakly foliated leucocratic granite (Ygr) that occurs in the Old Rag Mountain 7.5-minute quadrangle (Hackley and Tollo, in press) and adjacent areas (fig. 3). However, these units can be distinguished in the field on the basis of quartz color: quartz is typically gray to white in garnet-bearing alkali feldspar granite to syenogranite (Ygg); whereas coarse-grained Old Rag Granite (Yor of Hackley and Tollo, in press) and associated medium-grained leucogranite (Ygr of Hackley and Tollo, in press) typically contains blue quartz.

Rocks within this lithologic unit typically have silica contents in excess of 69 weight percent and are mildly to moderately peraluminous (fig. 5). These leucocratic granitoids have high concentrations of Na_2O+K_2O, a compositional feature that is reflected in the characteristic modal abundance of alkali feldspar relative to plagioclase (fig. 4). K_2O/Na_2O molar ratios are characteristically high and similar to those of other leucocratic rocks in the field trip area. The high-silica, alkali-rich compositions are a distinctive geochemical characteristic of the post-tectonic leucocratic granitoids in the field trip area (fig. 5E). The low-silica concentration characterizing the granitoid at this exposure (table 4, sample SNP-03-197) is compositionally atypical of the Ygg unit in the field trip area and appears to be representative of a relatively minor lithologic variant. For this reason, the composition of a more chemically typical sample of the pluton collected 0.67 km (0.42 mi) northwest of the field trip stop along Gooney Run is also included in table 4 (sample SNP-01-164).

Ygg is part of a group of leucocratic granitoids that were emplaced following the main episode of local Grenvillian orogenesis that occurred at 1,080 to 1,060 Ma (Tollo and others, in press a). In addition to Ygg, these postorogenic rocks in the field trip area include the typically garnet- and (or) biotite-bearing leucocratic granitoids of the Old Rag magmatic suite (Ygr) (Hackley, 1999), which is associated with the pluton at Old Rag Mountain (fig. 3), and alkali feldspar granite (Yaf) that occurs as two small bodies near Madison (Bailey and others, 2003) (fig. 3). Southworth (1994, 1995) and Southworth and Brezinski (1996) mapped possibly correlative, nonfoliated to weakly foliated, leucocratic rocks in the northern Blue Ridge of northernmost Virginia and Maryland as garnet monzogranite (unit Ygt on the geologic map of Virginia (Virginia Division of Mineral Resources, 1993)).

Detailed SHRIMP analysis indicates that zircons from this locality are compositionally and isotopically complex. SHRIMP data suggest that crystallization occurred at 1,064±7 Ma (table 3, sample SNP-02-197). This age is similar to isotopic data obtained by conventional isotope-dilution thermal ionization mass spectrometry (ID-TIMS) techniques obtained by Aleinikoff and others (2000) for possibly related garnetiferous metagranite (Ygt) and white leucocratic metagranite (Yg) from the northern Blue Ridge dated at 1,077±4 Ma and 1,060±2 Ma, respectively.

Mileage

Trip Cumulative	Stop-to-Stop Cumulative	
	0.0	Proceed to intersection of Gooney Falls Lane and Va. 649.
8.7	0.3	Turn right (south) onto Va. 649.
		Buck Mountain, visible on the right, is underlain by typically coarse-grained leucocratic granitoid of the Ygg lithologic unit.
9.1	0.7	*Prominent roadcut on the left exposes relatively fresh foliated pyroxene+biotite quartz diorite (Ypqd).*
9.8	1.4	Stop 2.
		Outcrop on left (east) side of Va. 649.

Stop 2. Pyroxene+biotite quartz diorite (Ypqd).

This fresh outcrop of pyroxene+biotite quartz diorite (Ypqd) is typical of roadcuts along Va. 649. The unit is mapped as a small, elongate body that is intruded by and enclosed within garnetiferous alkali feldspar granite to syenogranite (Ygg). The body is interpreted to form an inlier within the larger leucocratic Ygg pluton. Gneissic layering defined by alternating feldspar- and pyroxene+biotite-rich domains is characteristic of this unit, and is best seen on weathered surfaces. Isoclinal folds developed locally within the compositional layering exhibit considerable thickening of the layers in the hinge zones, and are interpreted to have formed under ductile conditions during Grenvillian orogenesis.

Samples of this lithologic unit are typically dark-gray, medium-grained, equigranular, moderately to strongly foliated quartz diorite to quartz monzodiorite (fig. 4) composed of 20 to 25 percent orthoclase, 60 to 65 percent plagioclase, and 12 to 15 percent quartz with 5 to 7 percent orthopyroxene and 2 to 4 percent biotite. Accessory minerals include apatite, zircon, and Fe-Ti oxide. Alignment of biotite and orthopyroxene grains typically defines foliation that is parallel to centimeter-scale gneissic layering.

The Ypqd lithologic unit is one of the most chemically distinctive lithologic units documented within the field trip area. Two samples have similar low-silica compositions (fig. 5), with SiO_2 contents ranging from 55 to 57 weight percent. These compositions rank among the most chemically primitive observed within the field trip area. Although major-element abundances are similar to the most silica-poor variants of the low-silica charnockite (Yfqj), trace-element concentrations differ significantly, indicating likely separate petrologic lineages. Lower concentrations of high-field-strength elements in the Ypqd samples suggest an origin involving sources with a significant volcanic-arc component, in contrast to the more typical crustal-type sources from which the low-silica charnockite was likely derived. Compositionally, the Ypqd unit corresponds closely to typical I-type granites, whereas the low-silica charnockite (Yfqj), with high Nb+Y concentrations and elevated $10^4 \times Ga/Al$ and FeO_t/MgO ratios, exhibits close chemical affinity to A-type granitoids (fig. 7).

Field relations observed at Boyd's Mill (Stop 3) indicate that the Ypqd unit is older than, and likely intruded by, the surrounding Ygg leucogranitoids, suggesting that the former is older than 1,062 Ma. The available field and petrologic data are insufficient to suggest correlation between the Ypqd lithologic unit and older, similarly charnockitic units of known age that occur to the south.

Mileage

Trip Cumulative	Stop-to-Stop Cumulative	
	0.0	Proceed south on Va. 649.
10.2	0.4	Stop 3.
		Intersection of Va. 622 and Va. 649 at Boyd's Mill.

Outcrop on left side of Va. 649.
Park on right side beyond intersection.

Stop 3. Garnetiferous alkali feldspar granite to syenogranite (Ygg) intruding pyroxene+biotite quartz diorite (Ypqd).

Field relations observed at this roadcut indicate intrusion of the Ygg leucocratic granitoid into medium-grained, equigranular, charnockitic rocks of the Ypqd inlier. Coarse-grained, garnet+biotite-bearing leucocratic granite is interlayered on a scale ranging from decimeters to meters with medium- to dark-gray, medium- to coarse-grained, foliated pyroxene-bearing gneissic granitoid that locally contains garnet. Geologically, this roadcut is located along the mapped north-south-trending contact separating leucocratic granitoid rocks of the Ygg pluton from the western border of the Ypqd inlier (fig. 3), and thus the exposure is interpreted as part of the contact zone formed by intrusion of leucogranitoid into the melanocratic gneissic rocks. The leucocratic granitoid in this roadcut is composed of abundant perthitic orthoclase+plagioclase+quartz+garnet+biotite+Fe-Ti oxide+chlorite. Plagioclase is typically altered to sericite; primary garnet is partly replaced by chlorite+minor titanite. Garnet in the melanocratic granitoid occurs in proximity to leucocratic granite and is interpreted as metamorphic in origin.

Geochemical data for a sample of leucocratic granitoid from this roadcut (table 4, sample SNP-01-174) indicate a high-silica, peraluminous composition with high K_2O/Na_2O molar ratio, corresponding closely to the average composition of rocks constituting the Ygg pluton. The composition of a representative sample of the melanocratic granitoid (table 4, sample SNP-01-155) bears close chemical similarity to rocks collected elsewhere from the inlier except for distinctly higher silica contents, lower concentrations of CaO, K_2O, and Na_2O, and correspondingly high values of aluminum saturation index (molar $Al_2O_3/(Na_2O+K_2O+CaO)$. Such differences in composition are interpreted to reflect chemical exchange that occurred as a result of metamorphic reactions induced by intrusion of the leucogranite.

Mileage

Trip Cumulative	Stop-to-Stop Cumulative	
	0.0	Turn around and proceed north on Va. 649.
15.9	5.7	Turn right (northeast) onto U.S. 340.
16.1	5.9	Turn right into the entrance to Shenandoah National Park and Skyline Drive South.
16.7	6.5	Pass through entrance station to Shenandoah National Park.
18.9	8.7	Shenandoah Valley Overlook. *The view from the overlook on the right includes the abandoned former Avtek factory located along the Shenandoah River in Front Royal. This factory and the surrounding environmentally sensitive area constitute a designated Superfund site slated for remediation.*
20.8	10.6	Dickey Ridge Visitor Center.
21.9	11.7	Signal Knob Overlook. *On a day with high visibility, the view from this overlook provides a rich perspective on the geology of the central Appalachians. The double-topped linear ridges in the middle distance define Massanutten Mountain, a complex syncline whose topographic expression is defined by resistant Silurian sandstone. Most of the floor of the surrounding Shenandoah Valley is underlain by the Ordovician Martinsburg Formation and Cambrian and Ordovician carbonate rocks exposed in the footwall block beneath the Blue Ridge thrust that runs*

		along the base of the foothills in the foreground. North Mountain, which forms the long linear ridge on the horizon, is capped by Devonian sandstone and is a typical landform of the Appalachian Valley and Ridge province.
		The roadcut on the east side of Skyline Drive exposes two lava flows of the Neoproterozoic Catoctin Formation separated by a 1- to 1.5-m (3.3–4.9 ft)-thick stratum of terrestrial sedimentary deposits. Jasper veins developed in the metasedimentary layer are typical of the contact zone beneath and between lava flows in this area.
23.1	12.9	Gooney Run Overlook.
		View to the west overlooks areas of the Chester Gap 7.5-minute quadrangle visited in Stops 1–3. Buck Mountain, underlain by leucocratic granitoids of the Ygg pluton, is located directly west of the overlook. Stop 1 is located at the northern end of the mountain; Stops 2 and 3 are located along the road extending along its eastern flank.
25.6	15.4	Stop 4.
		Outcrop on left (east) side of Skyline Drive.

Stop 4. Orthopyroxene+amphibole layered granodiorite gneiss (Ylgn).

The large roadcut at Lands Run Gap on Skyline Drive exhibits characteristics typical of the orthopyroxene+amphibole layered granodiorite gneiss (Ylgn) and is designated as the lithologic type locality for this unit (Tollo and others, in press b). This stop is located about 0.5 km (0.3 mi) east of an unnamed fault that juxtaposes basement units and greenstone against basement (fig. 3). The Ylgn lithologic unit underlies a large area in the central part of the Chester Gap quadrangle where it is both overlain by and in fault contact with greenstones of the Catoctin Formation. Compton Peak, visible to the south, represents an isolated erosional remnant of the cover sequence that preserves a succession of rocks of the Swift Run and Catoctin Formations nonconformably overlying basement (Gathright, 1976) (fig. 3).

The Ylgn lithologic unit consists of dark-gray, medium- to coarse-grained, inequigranular, strongly foliated granodioritic (*opdalite*) gneiss composed of 35 to 40 percent alkali feldspar (microcline or orthoclase), 30 to 40 percent plagioclase, and 20 percent quartz with 3 to 5 percent amphibole and 3 to 5 percent orthopyroxene. Accessory minerals include apatite, zircon, and ilmenite. Characteristic gneissosity is defined by alternating centimeter-scale quartz+feldspar-rich (light) and pyroxene+amphibole-rich (dark) layers that form intrafolial folds within a foliation plane defined by discontinuous polygranular domains of amphibole and orthopyroxene. Interlayered and crosscutting, decimeter-scale sheets of light-gray to white, medium- to coarse-grained, inequigranular, massive leucogranite composed mostly of white feldspar and gray quartz are characteristic, and likely represent dikes of younger granitoid that may be related to the circa-1,060-Ma postorogenic type that includes the Old Rag magmatic suite and other similar rocks. The development of gneissosity, leucogranitoid boudins, and isoclinal intrafolial folds are interpreted to reflect deformation of probable Grenvillian age.

Geochemical data indicate that the Ylgn lithologic unit is mildly metaluminous and intermediate in composition with SiO_2 contents of 64 to 67 weight percent (fig. 5D). The overall chemical correspondence of this unit to typical granodioritic compositions is interpreted as evidence for an igneous protolith. Ylgn is the least chemically evolved of the orthopyroxene-bearing granitic units characterized by silica contents >60 weight percent in the field area. Like the other charnockites, Ylgn exhibits compositional features that are transitional between I- and A-type granitoids (fig. 7) and was likely derived from sources of mixed composition, including both volcanic-arc and crustal components (fig. 6).

The characteristic gneissic fabric of this lithologic unit indicates that Ylgn is part of the older group of deformed rocks in the area. This group includes a compositionally diverse array of charnockitic and non-charnockitic granitoids that display mineralogic and

textural evidence of deformation that occurred at high-grade conditions. Dated rocks within this group, which include the Ycf (1,147±16 Ma) and Ylg (1,183±11 Ma) lithologic units, represent the oldest recognized lithologies in the field area. Two tabular bodies of dark-colored, foliated to massive, fine-grained, biotite-rich granitoid, both <1.3 m (4.3 ft) in width, occur at a slight angle to foliation and gneissosity in a nearby roadcut, and are interpreted to be dikes cutting the Ylgn lithologic unit. Mineralogic and geochemical similarity of these dike rocks (table 4, sample SNP-01-149) to the pyroxene quartz diorite (Ypqd) lithologic unit (table 4, sample SNP-01-175) suggest that Ypqd is younger than Ylgn.

Mileage

Trip Cumulative	Stop-to-Stop Cumulative	
	0.0	Proceed south on Skyline Drive.
26.9	1.3	Indian Run Overlook.
		Rocks exposed in the long roadcut display one of the finest examples of columnar jointing in metabasalt of the Catoctin Formation within Shenandoah National Park. Such columns, which are common throughout the Catoctin Formation on the west limb of the Blue Ridge anticlinorium, are evidence of the subaerial eruptive origin of the lava flows.
28.5	2.9	Jenkins Gap Overlook.
33.7	8.1	Gravel Springs Gap.
35.1	9.5	Mount Marshall Overlook.
36.1	10.5	Stop 5.
		Little Devil Stairs Overlook. Outcrop on west side of road.

Stop 5. Orthopyroxene+amphibole syeno- and monzogranite (Ycf).

The large roadcut at Little Devil Stairs Overlook is located about 200 ft (61 m) north of the unconformable contact separating basement from the overlying Catoctin Formation, exposed in the hillslope to the south (Gathright, 1976). This stop is located about 1.1 km (0.7 mi) west of a fault that intersects the Stanley fault near Keyser Mountain to the southeast (Gathright, 1976). Despite their appearance in the roadcut, basement rocks at this locality are intensely weathered and preserve only partial evidence of the primary ferromagnesian mineral assemblage. Throughout the exposure, fine-grained charnockite forms meter-scale dikes cutting coarser grained charnockite. The rocks exhibit weak to moderately developed, steeply dipping foliation striking 075° to 090°. The predominantly east-west strike of the foliation is unusual in an area that is otherwise dominated by northeast-southwest fabrics associated with Paleozoic orogenesis (Mitra and Lukert, 1982), and is likely to have been developed during the Grenvillian orogeny. Both the fine- and coarse-grained varieties of charnockite are composed of alkali feldspar microperthite (dominantly microcline in the coarse-grained variety, mostly orthoclase in the fine-grained variety), plagioclase and quartz, with rare amphibole and abundant pseudomorphs that likely formed after orthopyroxene. This primary mineral assemblage is also characteristic of the foliated pyroxene granite (Yfpg) (table 2, fig. 3).

Chemical compositions of samples of both fine- and coarse-grained charnockite collected from this outcrop (table 4, samples SNP-01-142 and SNP-01-143, respectively) display geochemical similarities to samples of both the high-silica charnockite (Ycf) and foliated pyroxene granite (Yfpg) (table 4, samples SNP-96-10 and SNP-02-177, respectively). The Ycf unit and the foliated pyroxene granite (Yfpg), which have crystallization ages that differ by 45 m.y., are both foliated, amphibole+orthopyroxene-bearing, siliceous charnockites, and thus the mineral assemblage and chemical composition of the rocks at this roadcut do not represent sufficient evidence on which to establish lithodemic correlation. However, the more homogeneous (albeit foliated) fabric and more disseminated nature of the

orthopyroxene in Ycf are features that are similar to the rocks at this exposure, contrasting with the characteristically very coarse and clustered nature of orthopyroxene in Yfpg. Thus, on the basis of this fabric, the rocks at Little Devil Stairs Overlook are considered part of the Ycf lithologic unit, pending detailed mapping of basement lithologies in the Bentonville 7.5-minute quadrangle.

The charnockite is cut by five large metabasalt (greenstone) dikes of meter-scale thickness at the northern end of the exposure. Numerous fine- to medium-grained mafic dikes intrude basement rocks throughout the field trip area and across the Shenandoah massif. Such dikes exhibit diverse textures, metamorphic grade, and mineralogic compositions ranging from basalt to diabase to greenstone. Although largely undated by modern isotopic techniques, most mafic dikes have been mapped as either Mesozoic or Neoproterozoic in age on the basis of crosscutting relations, mineralogic composition, and the presence or absence of metamorphic fabrics (for example, Burton and others, 1995; Southworth, 1995; Southworth and Brezinski, 1996; Bailey and others, 2003). In general, dikes of late Neoproterozoic age contain mineralogic evidence of recrystallization at greenschist-facies metamorphic conditions, including development of assemblages containing actinolite+biotite+serpentine, which are commonly absent in Mesozoic dikes (Wilson and Tollo, 2001). Many Neoproterozoic dikes display tectonic cleavage as a result of deformation and retrograde metamorphic recrystallization; such cleavage is absent in Mesozoic dikes. Samples of the dikes cutting basement at this stop contain abundant chlorite+epidote±serpentine, and are typical of the most abundant type documented by studies within the Blue Ridge which generally have weakly quartz-normative, tholeiitic compositions. Nevertheless, dikes throughout the area show major- and trace-element characteristics that are largely bimodal and may be indicative of two ages of emplacement. As illustrated in figure 8, the bimodal major-element compositions of Blue Ridge dikes correspond closely to either the Mesozoic Mt. Zion Church Basalt in the nearby Culpeper basin or relatively unaltered lava flows and associated dikes of likely Neoproterozoic age (Badger, 1989). Chemical analyses of two of the dikes at this locality (table 5, samples SNP-01-144 and SNP-01-145) indicate high TiO_2 contents and low values of $100(MgO/(MgO+FeO_t)$ (fig. 8), suggesting close compositional affinity to dikes and lava flows associated with the Catoctin Formation (Badger, 1989). Such dikes may have served as conduits for magma moving toward the surface during eruption, an interpretation that is consistent with the physical proximity of these dikes to the overlying Catoctin greenstones. The usefulness of the chemical discriminants plotted in figure 8 is underscored by the similarity in compositions of two samples of thoroughly retrograded greenstone (squares with diagonal crosses) to those of less retrograded metabasalt and metadiabase (filled squares), indicating that, in many cases, Paleozoic greenschist-facies metamorphism did not result in mass transfer of chemical components. Dikes formed during Mesozoic rifting are apparently much less abundant in the Blue Ridge, and can be distinguished chemically from dikes of inferred Neoproterozoic age on the basis of lower TiO_2 contents and higher $100(MgO/(MgO+FeO_t)$ ratios (Wilson and Tollo, 2001) (fig. 8). Mesozoic dikes also contain higher SiO_2 contents, are relatively enriched in compatible elements such as Ni and Cr, and show lower concentrations of high-field-strength elements, including Zr, Nb, and Y (Wilson and Tollo, 2001). In figure 8, only 4 dikes (from the total population of 29 dikes sampled as part of this study) correspond closely in composition to the tholeiitic Mount Zion Church Basalt, which is the oldest and most primitive basalt type in the nearby early Mesozoic Culpeper basin (fig. 2). This composition also corresponds to the most common type of diabase sheets that intruded sedimentary strata within the basin, and is the only Mesozoic diabase magma type that is comparable to any of the dikes in the Blue Ridge (Froelich and Gottfried, 1988).

Mileage

Trip Cumulative	Stop-to-Stop Cumulative	
	0.0	Proceed south on Skyline Drive.
40.0	3.9	Pass Elkwallow Store.
47.3	11.2	Pass intersection with U.S. 211 at Thornton Gap.
47.4	11.3	Pass Panorama on right of Skyline Drive.
48.0	11.9	North portal of Mary's Rock Tunnel.
		A large, northeast-striking mafic dike displaying prominent columnar jointing cuts high-silica charnockite (Ycf) on the west side of the tunnel portal. The fine-grained diabase contains microphenocrysts of clinopyroxene+pigeonite+plagioclase and shows relatively little evidence of retrograde metamorphism. Nevertheless, the chemical composition of the dike (table 5, sample SNPD-99-1) indicates high-TiO_2 content and trace-element characteristics that are typical of dikes of Neoproterozoic age (Wilson and Tollo, 2001). The overall lack of development of retrograde mineral assemblage and tectonic cleavage in the dike is a likely consequence of its occurrence within the rigid, relatively anhydrous charnockite pluton.
48.2	12.1	South portal of Mary's Rock Tunnel.
		Stop 6.
		Parking on left (east) side of Skyline Drive.

Stop 6. Orthopyroxene+amphibole syeno- and monzogranite (Ycf).

The view toward the east from the tunnel parking lot provides an informative perspective on the physiographic Piedmont province of the central Appalachians and geological framework of the Blue Ridge anticlinorium. The Blue Ridge foothills located in the foreground directly to the east are underlain mostly by Mesoproterozoic basement rocks, including some lithologic units that also occur along Skyline Drive. These foothills give way eastward to the typical low topography of the core of the Blue Ridge anticlinorium, most of which is included in the Piedmont physiographic province (Fenneman, 1938). The core of the anticlinorium is underlain primarily by Mesoproterozoic basement rocks and, locally, by igneous and metasedimentary rocks formed during Neoproterozoic rifting. The two symmetric hills in the middle distance (Little Battle Mountain and Battle Mountain, north and south peaks, respectively) are underlain by the Battle Mountain volcanic complex that includes both volcanic and subvolcanic felsic rocks associated with the extension-related, 730- to 702-Ma Robertson River batholith (Tollo and Aleinikoff, 1996; Tollo and Hutson, 1996). The elongate batholith continues both north and south of these hills, ultimately stretching nearly 110 km (70 mi) across the anticlinorium from the west limb in the north to the east limb in the south (fig. 2); however, the intrusion only locally underlies steep topography. The flat-topped ridge of the Bull Run Mountains occupies the horizon and is underlain by resistant quartzite of the upper Neoproterozic to Lower Cambrian Weverton Formation, which is stratigraphically underlain by the Catoctin Formation for much of the length of the ridge. These rocks constitute part of the Blue Ridge cover-rock sequence, thus locally defining the eastern limb of the Blue Ridge anticlinorium.

This stop is located in the central part of a pluton consisting of moderately to strongly foliated, coarse- to very coarse-grained, orthopyroxene±amphibole-bearing syeno- and monzogranite (*charnockite* and *farsundite*, Ycf). This lithologic unit occurs across most of the Thornton Gap quadrangle (fig. 3) and is a member of the oldest group of plutonic rocks in the region. In this area, the Ycf pluton includes map-scale inliers of coarse-grained, orthopyroxene+garnet granite gneiss (*farsundite* gneiss, Yg), which constitute probable screens of older rocks. Mapping also indicates that Ycf is intruded by elongate bodies of

massive to weakly foliated granite of the Old Rag magmatic suite (Ygr) and massive to weakly foliated, low-silica charnockite (Yfqj) (fig. 3). Collectively, charnockitic rocks of the Ycf, Yg, and much younger Yfqj lithologic units constitute part of the classic orthopyroxene-bearing Pedlar Formation that was mapped throughout much of this part of the Blue Ridge (Gathright, 1976) before the advent of modern analytical methods made geochemical and age-based differentiation of mineralogically similar units possible.

The rocks near the tunnel expose strongly foliated, coarse- to very coarse-grained, orthopyroxene±amphibole, inequigranular to megacrystic syeno- and monzogranite (*charnockite* and *farsundite*) that is typical of the Ycf pluton. The rock is composed of 22 to 57 percent alkali feldspar microperthite (chiefly microcline), 10 to 37 percent plagioclase, and 11 to 49 percent quartz with <1 to 14 percent orthopyroxene, 0 to 11 percent amphibole, and rare clinopyroxene. Accessory minerals include apatite, ilmenite, magnetite, zircon, epidote, and actinolite. Locally prominent gneissic layering is defined by interlayered quartz+feldspar- and ferromagnesian mineral-rich domains ranging from less than 1 cm (0.4 in) to greater than 13 cm (5 in) and is especially visible on weathered surfaces. Foliation is defined locally by planar alignment of ferromagnesian minerals and is parallel to gneissic layering. Subhedral to euhedral, monocrystalline alkali feldspar megacrysts range up to 13 cm (5 in) in length and are best observed on weathered surfaces. The strongly developed fabric is characteristic of the older group of plutonic rocks in the field trip area.

Electron microprobe analyses indicate that pyroxenes in the Ycf lithologic unit display strong Quad (Ca-Fe-Mg) compositional features, according to the criteria of Morimoto (1988). Pyroxene compositions show very little variation both within individual grains and between grains in single thin sections. Clinopyroxenes in the Ycf charnockite are relatively Fe-rich (average $Wo_{43}En_{22}Fs_{35}$); however, application of the charge-balance criteria of Lindsley (1983) indicate that ferric iron contents are negligible. Orthopyroxenes in Ycf are very Ca-poor and Fe-rich (average $Wo_2En_{27}Fs_{71}$). Visible exsolution is rare in either pyroxene type. Compositions of coexisting pyroxenes in Ycf indicate equilibration temperatures of less than 500°C, as calculated by the QUILF program of Andersen and others (1993) for pressures consistent with observed granulite-facies mineral assemblages. Because such temperatures fall hundreds of degrees below likely crystallization temperatures for igneous charnockites (Kilpatrick and Ellis, 1992), and because the pyroxenes exhibit evidence of thorough compositional homogenization, the rocks are inferred to have undergone an extended interval of subsolidus re-equilibration at temperatures that remained elevated but below peak granulite-facies conditions.

Amphiboles are typically brown and closely associated with orthopyroxene, locally separated by a narrow optical transition zone. Compositions of the amphiboles correspond to hornblende (*sensu lato*) according to the criteria of Deer and others (1992) and to the calcic group of Leake and others (1997). Data from electron microprobe traverses of individual grains indicate little evidence of compositional zoning, and repeated analyses of multiple grains within single samples indicate restricted compositional variation. Amphiboles in Ycf (and Yfqj) display compositional similarities to amphiboles observed in charnockites from the calc-alkaline Louis Lake batholith in the Wind River Range of Wyoming, which were interpreted by Frost and others (2000) to represent primary phases that crystallized from igneous melts. Amphiboles of likely igneous origin occur in charnockitic rocks of tholeiitic affinity from many other locations (Malm and Ormaasen, 1978; Duchesne and Wilmart, 1997; Sheraton and others, 1992), suggesting that the occurrence of igneous amphiboles in charnockitic rocks is not uncommon. For this reason, and because of their association with pyroxene that displays textural features consistent with original igneous crystallization, the Blue Ridge charnockitic amphiboles are also interpreted as primary magmatic minerals.

Chemical analyses indicate that Ycf rocks show only restricted compositional variation thoughout the field trip area. The granitoids are mildly metaluminous, with SiO_2 contents in the range of 68 to 72 weight percent (table 4; fig. 5). The high-silica Ycf pluton is one of several siliceous rocks of charnockitic affinity in the northern part of the study area.

Others include the garnetiferous granite gneiss (Yg), foliated pyroxene granite (Yfpg) (both units shown on fig. 3) and a small, typically medium-grained, equigranular charnockitic pluton documented by recent mapping in the Big Meadows quadrangle (not shown in fig. 3). However, of these four orthopyroxene-bearing units, only the charnockite from Big Meadows and the distinctive Ycf unit are characterized on fresh surfaces by the dark-greenish-gray appearance that is typical of charnockites worldwide. Trace-element analyses of Ycf rocks suggest derivation from mixed sources of possible volcanic-arc and crustal affinity (fig. 6) and indicate that the pluton displays chemical characteristics that are transitional between I- and A-type granitoids (fig. 7).

U-Pb isotopic analyses obtained using SHRIMP techniques indicate that zircons in the Ycf lithologic unit are compositionally complex. Two populations are present, based on crystal morphology: (1) euhedral, elongate prisms displaying dipyramidal terminations and (2) smaller, nearly equant grains (Tollo and others, in press a). Examination of the prismatic zircons in cathodoluminescence (CL) indicates the presence of cores characterized by concentric oscillatory zoning surrounded by narrow unzoned rims. Multiple analyses indicate a weighted average $^{206}Pb/^{238}U$ age of 1,159±14 Ma for the zoned cores, which is interpreted as the time of igneous crystallization. Analyses of the equant grains and overgrowths on the prismatic grains indicate a composite age of 1,052±14 Ma, which likely corresponds to a period of regional thermal activity. Results from ID-TIMS dating by Aleinikoff and others (2000) indicate that meta-igneous rocks of similar age, possibly including a charnockite, occur in the Blue Ridge north of the field trip area.

Mileage

Trip Cumulative	Stop-to-Stop Cumulative	
	0.0	Proceed south on Skyline Drive.
48.7	0.5	Stop 7. Buck Hollow Overlook. Parking on left (east) side of Skyline Drive.

Stop 7. Orthopyroxene+garnet granite gneiss (Yg) and orthopyroxene+amphibole syeno- and monzogranite (Ycf).

The roadcut opposite the overlook exposes one of the freshest examples of orthopyroxene+garnet granite gneiss in Shenandoah National Park. Field relations indicate that this exposure is part of a large screen of garnetiferous gneiss mapped as lithologic unit Yg that is enclosed within high-silica charnockite (Ycf) (fig. 3), suggesting that the latter pluton intruded and enveloped the former (Tollo and others, in press a,b). Direct crosscutting relations have not been observed in outcrop, however. This field relation and the ubiquitous, strongly developed fabric of the granitic gneiss, which is characteristic of rocks that predate the main episode of Grenvillian orogenesis in the area, suggest that Yg predates the high-silica charnockite (Ycf) and therefore is older than 1,159 Ma. The curved contacts of the screen and adjacent rocks of the Old Rag magmatic suite suggest the presence of map-scale folds developed in the basement rocks (fig. 3). The locally parallel alignment of gneissic layering defined by primary minerals and the trend of the folded contacts further suggest that such deformation may be Grenvillian in age.

Rocks at this locality include light-gray to gray, medium- to coarse-grained, inequigranular, strongly foliated syeno- to monzogranite gneiss (*farsundite* gneiss) composed of 28 to 49 percent alkali feldspar microperthite (chiefly microcline), 14 to 30 percent plagioclase, and 28 to 35 percent quartz with 4 to 6 percent orthopyroxene, <1 to 7 percent garnet, <1 to 3 percent biotite, and rare clinopyroxene. Accessory minerals include apatite, ilmenite, magnetite, zircon, and chlorite. Typically prominent gneissic layering is defined by interlayered quartz+feldspar- and ferromagnesian mineral-rich domains ranging

from less than 1 cm (0.4 in) to greater than 70 cm (28 in) in thickness. Foliation is defined locally by planar alignment of ferromagnesian minerals and is parallel to gneissic layering. A locally well-developed mineral lineation is defined by elongate domains of garnet and biotite located within the foliation plane.

Clinopyroxene in the garnetiferous granite gneiss (Yg) is generally too altered for meaningful chemical analysis. However, orthopyroxene ($Wo_1En_{28}Fs_{71}$) is similar in composition to orthopyroxene in the high-silica charnockite (Ycf), but consistently indicates slightly lower temperatures of equilibration. Like orthopyroxene, garnet exhibits very little compositional variation both within individual grains and among multiple grains. Garnet in Yg is Fe-rich (Grs: 9.3, Alm: 79.5, Prp: 11.2), reflecting the elevated FeO_t/MgO whole-rock ratio (fig. 5F).

Samples of the Yg lithologic unit are borderline metaluminous to moderately peraluminous with SiO_2 contents of 70 to 75 weight percent (fig. 5D). The Yg rocks display overall compositional features that are similar to other siliceous charnockites in the region, including relatively low TiO_2, FeO_t, and CaO contents (table 4). Compositionally, Yg differs from the Ycf unit that encloses it in having generally higher SiO_2 contents, higher FeO_t/MgO ratios, and distinctly peraluminous bulk compositions (table 4; fig. 5D, F). These geochemical characteristics and normative compositions of granitic affinity suggest that Yg is meta-igneous in origin.

Map relations and the characteristic deformed fabric of the garnetiferous granite gneiss suggest that the lithologic unit is one of the oldest rocks in the area. Like the leucogranite gneiss (Ylgg) lithologic unit that occurs in the Fletcher 7.5-minute quadrangle (fig. 3), Yg rocks occur only as inliers that are isolated within igneous plutons of likely younger age. These field relations suggest that the present erosion surface in the Blue Ridge coincides with a paleodepth interval at which Grenvillian plutons were successively emplaced. This zone of emplacement is dominated by plutons and is characterized by an apparent paucity of preexisting country rocks. Whether the missing country rock was removed by subsequent erosion of higher levels or remains as roof pendants concealed at depth is not presently known.

Large outcrops and roadcuts of medium-grained, gray-green, orthopyroxene+amphibole syeno- and monzogranite (Ycf) occur nearby, adjacent to Skyline Drive about 200 ft (61 m) north of the Buck Hollow Overlook exposure. The contact separating Ycf from the Yg inlier is not exposed, but likely is located in the east-trending stream valley that crosses Skyline Drive south of Skinner Ridge. The atypical finer grain size of the Ycf rocks in this area is interpreted to result from contact-related cooling against the Yg screen during magmatic emplacement.

Mileage

Trip Cumulative	Stop-to-Stop Cumulative	
	0.0	Proceed south along Skyline Drive.
49.3	0.6	Meadow Springs Overlook and Parking Area. *Exposures of low-silica charnockite (Yfqj) along the west side of Skyline Drive opposite the overlook are part of a small dike that intruded along the contact separating high-silica orthopyroxene+amphibole syeno- and monzogranite (charnockite+farsundite,Ycf) from garnetiferous granite gneiss (farsundite gneiss, Yg) (fig. 3). Sample SNP-96-17 (table 4) was collected from the roadcut and is mineralogically and geochemically typical of the Yfqj pluton, but generally finer grained.*
52.3	3.6	Jewel Hollow Overlook. *The view to the west includes the Massanutten Mountain synclinorium in the middle distance and North Mountain on the horizon. Outcrops at the overlook expose high-silica charnockite of the Ycf lithologic unit.*

53.5	4.8	*A large northeast-striking mafic dike cuts garnetiferous granite gneiss (Yg) in the roadcut on the west side of Skyline Drive. The chemical composition of the dike (table 5, sample SNPD-99-3) is typical of Catoctin-related mafic rocks in the area. This geochemical affinity and close spatial association with extrusive metabasalt of the Catoctin Formation occurring to the south suggest that the dike is part of the feeder complex that provided magma to the rift-related basalt flows.*
54.4	5.7	*Stony Man Mountain, a well-known landmark in Shenandoah National Park, is visible directly to the south. The mountain is underlain by metavolcanic and metasedimentary rocks of the Catoctin Formation (Gathright, 1976) that define five major eruptive flow units and at least two layers of intercalated metasedimentary rocks and volcanic breccia, all of which dip gently toward the southeast (Badger, 1999). The view to the west includes a broad expanse of the eastern Shenandoah Valley. The South Fork of the Shenandoah River is visible east of Massanutten Mountain, where it has a low-gradient path characterized by numerous meanders.*
55.1	6.4	*Skyline Drive ascends uphill through roadcuts of Catoctin Formation greenstone.*
57.5	8.8	*Entrance to Skyland on the right, highest point on Skyline Drive at 3,680 ft (1,122 m). Like the eastern part of Skyland, most of the higher elevations in the Park are underlain by greenstones of the Catoctin Formation. Examples include Hawksbill Mountain at 4,050 ft (1,234 m), Stony Man Mountain at 4,011 ft (1,223 m), and Hazeltop Mountain at 3,812 ft (1,162 m).*
59.0	10.3	Stop 8. Timber Hollow Overlook.

Stop 8. Unakite developed in nonfoliated low-silica amphibole-bearing charnockite (Yfqj).

This overlook provides views to the west of the eastern Shenandoah Valley and Massanutten Mountain in the middle distance. On a clear day, talus slopes composed of variably sized blocks of white Silurian quartz arenite of the Massanutten Formation can be observed on the flanks of the ridges. Such talus deposits are a characteristic feature of the hillslopes, which are typically capped by resistant quartz-rich sandstone. New Market Gap, where U.S. 211 crosses Massanutten Mountain, can also be observed west of Luray. The north-striking Stanley fault, part of the thrust that transported Blue Ridge basement rocks northwestward over lower Paleozoic sedimentary strata during late Paleozoic Alleghanian orogenesis, is located about 4.0 km (2.5 mi) west of the overlook in the valley below.

Timber Hollow Overlook is underlain by low-silica charnockite that is correlated mineralogically and geochemically with a larger pluton composed of amphibole-bearing *farsundite* and *quartz jotunite* (Yfqj) mapped to the south (fig. 3). Gathright (1976) mapped stratified rocks of the Catoctin Formation (dominantly greenstones) and underlying Swift Run Formation (dominantly phyllites) as unconformably overlying charnockite in this area, with a contact located about 1,000 ft (305 m) to the east of the overlook. As a result of the low dip of this contact, charnockite outcrops located below the overlook display abundant mineralogic evidence of contact metamorphism related to thermal effects caused by extrusion of overlying lava flows. The normally dark-greenish-gray charnockite is typically bleached light gray due to retrograde recrystallization of abundant primary plagioclase and lesser alkali feldspar. Ferromagnesian minerals are completely pseudomorphed by hydrous, low-temperature assemblages. Parts of the charnockite located adjacent to major joints are locally converted to unakite, in which plagioclase is mostly replaced by green epidote-group minerals, alkali feldspar is replaced largely by a pink hematite-bearing assemblage, and small amounts of originally blue quartz remain relatively unaltered. The localization of

well-developed unakite adjacent to fractures is a likely consequence of hydrothermal fluid migration induced by heat from the overlying lavas during Neoproterozoic extension. The effects of thermal metamorphism decrease rapidly downhill away from the contact. Unakite is a visually distinctive, but rare, rock type that is typically developed in Blue Ridge basement rocks through retrograde recrystallization associated with (1) extrusion of the overlying Catoctin Formation, (2) enhanced fluid flow associated with fault zones, or (3) local effects of regional Paleozoic metamorphism (Tollo and others, in press b; Wadman and others, 1998).

Mileage

Trip Cumulative	Stop-to-Stop Cumulative	
	0.0	Proceed south along Skyline Drive.
63.5	4.5	Stop 9. Fisher's Gap. Proceed to Dark Hollow Falls.

Stop 9. Erosional window exposing coarse-grained, inequigranular, amphibole-bearing charnockite (Yfqj).

Fisher's Gap and the surrounding area are located within the thrust sheet that carried basement and overlying rocks northwest over Paleozoic strata during Alleghanian orogenesis. Drainage from the nearby Big Meadows area flows northeast along Hogcamp Branch, which is partly responsible for developing an erosional window through cover rocks north of the falls (Gathright, 1976). Dark Hollow Falls is located within stratified rocks of the Catoctin Formation, which locally include massive and phyllitic greenstone, amygdaloidal greenstone, and metaconglomerate containing cobble-sized clasts of basement rocks (Badger, 1999). The Catoctin Formation nonconformably overlies basement rocks throughout the area, but has been removed by erosion in the vicinity of Hogcamp Branch, leading to exposure of the underlying basement rocks. The contact separating greenstone from charnockite is located in the stream valley below the intersection of the access road and Hogcamp Branch (Gathright, 1976). Charnockite is well exposed in ledges located within and adjacent to the stream, from an elevation of about 2,600 ft (790 m) down to near the intersection of Hogcamp Branch and the small stream that descends from Rose River Falls. The basement rocks are composed of massive to weakly foliated, coarse-grained, inequigranular, amphibole-bearing charnockite that is correlated with the large Yfqj pluton located about 3.2 km (2 mi) to the southeast (fig. 3). This low-silica charnockite is distinguished in the field by typically massive to weakly foliated fabric, relatively low quartz content, abundance of pyroxene, and local presence of magnetite. This widespread lithologic unit underlies a significant part of the Big Meadows 7.5-minute quadrangle (geology not shown in fig. 3), as well as most of the Fletcher 7.5-minute quadrangle (fig. 3).

Mileage

Trip Cumulative	Stop-to-Stop Cumulative	
	0.0	Proceed north along Skyline Drive.
68.0	4.5	Timber Hollow Overlook.
78.3	14.8	Buck Hollow Overlook.
78.8	15.3	Mary's Rock Tunnel.
79.8	16.3	Turn right off Skyline Drive toward U.S. 211.
79.9	16.4	Turn left onto U.S. 211 and proceed east.
80.6	17.1	*Earth flows are continually developed in loose soils underlying*

		the steep slope adjacent to the road on the left.
81.3	17.8	*A small quarry in greenstone of the Catoctin Formation is located on the left.*
81.7	18.2	*Outcrops located along the road expose garnetiferous granite gneiss (Yg) near the northern end of a large screen within foliated amphibole-bearing high-silica charnockite (Ycf) of 1,159-Ma age.*
85.4	21.9	Stop 10. Outcrop on left side of U.S. 211.

Stop 10. Old Rag magmatic suite (Ygr).

This outcrop is located near the eastern border of a map-scale dike of garnet-bearing leucogranite that cuts foliated amphibole-bearing high-silica charnockite (Ycf). The large dike is part of the Old Rag magmatic suite and is composed of both medium- and coarse-grained leucogranites that, in this area, cannot be mapped separately at a scale of 1:24,000. The lithologically similar, large pluton that underlies Old Rag Mountain and vicinity is the most likely source of this magma but may be separated from the dike by the Sperryville high-strain zone (SHSZ, fig. 3) originally mapped by Gathright (1976).

Rocks of the Old Rag magmatic suite include massive to moderately foliated, fine- to coarse-grained, inequigranular granite and leucogranite that locally contains biotite+orthopyroxene+garnet (Hackley, 1999). This composite unit was mapped as Old Rag Granite by previous workers (Allen, 1963; Gathright, 1976). In this study, Old Rag Granite is defined only in the vicinity of Old Rag Mountain, where it forms a triangular-shaped plutonic body composed of homogeneous, massive to weakly foliated, coarse- to very coarse-grained, inequigranular, garnet+orthopyroxene granite and leucogranite. Using mineralogic, geochemical, and field criteria, Hackley (1999) demonstrated that the fine- to locally coarse-grained, inequigranular granite and leucogranite that is the dominant lithology of the map-scale dike (and other smaller bodies) and the coarse- to very coarse-grained granite at Old Rag Mountain are petrologically consanguineous, and considered both lithologic varieties to constitute the Old Rag magmatic suite. All granitoids within the suite are composed of variable amounts of alkali feldspar+plagioclase+quartz (typically blue). Orthopyroxene, biotite, and garnet occur nonsystematically as primary ferromagnesian phases. The rocks are typically massive to weakly foliated; alignment of ductilely deformed quartz locally defines a crude lineation.

Rocks of the Old Rag magmatic suite are characterized by high SiO_2 contents (table 4) and peraluminous compositions (fig. 5D). The suite includes some of the most chemically evolved rocks in the area; however, similar FeO_t/MgO ratios suggest that the Old Rag rocks are not petrologic derivatives of the penecontemporaneous low-silica Yfqj charnockite (fig. 5F). Two representative chemical analyses of rocks of the suite are included in table 4: OR-97-35, coarse-grained garnetiferous leucogranite; and OR-97-51, fine-grained biotite leucogranite. Both samples were collected from Old Rag Mountain; zircons from OR-97-35 were analyzed isotopically for U-Pb geochronology, as described below. These leucogranites display trace-element features that suggest derivation from sources of mixed composition and are typical of post-tectonic granitoids (Förster and others, 1997) (fig. 6). As such, rocks of the Old Rag magmatic suite display geochemical characteristcs that are transitional between I- and A-type granitoids (fig. 7).

Mineralogically and geochemically similar, massive to weakly foliated, leucocratic granitoids constitute a significant lithologic component of Blue Ridge Mesoproterozoic basement, including the Old Rag magmatic suite, garnetiferous alkali feldspar and syenogranite (Ygg), and alkali feldspar granite (Yaf). Gathright (1976) was among the first to recognize that the nonfoliated to weakly foliated fabric and crosscutting field relations of the Old Rag granitoids indicated a relatively late emplacement age among basement rocks. Results from high-precision SHRIMP analyses of zircons from a sample of coarse-grained Old Rag Granite collected from Old Rag Mountain demonstrate a complex geochronological history for this unit. CL imaging indicates that nearly all of the zircons have oscillatory

zoned cores and dark overgrowths. Thirteen analyses of the oscillatory zoned portions of zircons from the Old Rag Granite yield a weighted average of the $^{207}Pb/^{206}Pb$ ages of 1,060±5 Ma, which we interpret as the time of emplacement of the Old Rag Granite and, by extension, the Old Rag magmatic suite. Ages of overgrowths indicate two episodes of post-magmatic crystallization occurring at 1,019±15 Ma and 979±11 Ma, which we interpret as indicating times of thermal disturbance. Monazite from the Old Rag Granite was also dated by SHRIMP methods. Five analyses yield an age of 1,059±8 Ma, identical within uncertainty to the emplacement age interpreted from zircon. Six other monazite analyses yield an age of 1,027±9 Ma and one grain is 953±30 Ma, both within uncertainty of the zircon overgrowth ages of 1,019±15 and 979±11 Ma, respectively. Thus, these data appear to indicate that a significant episode of post-tectonic igneous activity occurred at about 1,060 Ma, following a period of deformation that must have begun after 1,080 Ma (Tollo and others, in press a). This magmatism was, in turn, followed by one or two periods of regional thermal disturbance.

Mileage

Trip Cumulative	Stop-to-Stop Cumulative	
	0.0	Proceed east on U.S. 211.
91.5	6.1	Turn left onto U.S. Bus. 211 and proceed north toward Washington, Va.
92.7	7.3	Continue straight on Main Street at intersection with Va. 622. Va. 622 branches left from Va. 628; continue straight on Va. 628.
95.2	9.8	Stop 11. Turn right onto Horseshoe Hollow Lane. Follow Trip Leaders PRIVATE PROPERTY

Stop 11. Foliated pyroxene granite (Yfpg).

Foliated pyroxene granite (Yfpg) defines a circular pluton that appears to cut Flint Hill Gneiss in the southeastern part of the Chester Gap 7.5-minute quadrangle (fig. 3). The northwest border of the body is truncated by the Stanley fault, which juxtaposes Yfpg charnockite against greenstone of the Catoctin Formation. This meta-igneous intrusive body is part of a subset of charnockitic rocks characterized by high to moderately high silica contents, but its emplacement age is different from any other charnockites presently dated within the field trip area. The ages of silica-rich charnockitic rocks already dated and field characteristics of a recently discovered high-silica charnockite in the Big Meadows 7.5-minute quadrangle suggest that silica-rich charnockitic magmas were emplaced during each of the three main episodes of magmatic activity in the northern Blue Ridge.

The Yfpg pluton is composed of light-gray, medium- to coarse-grained, inequigranular, strongly foliated monzogranite (*farsundite*) composed of 30 to 40 percent microcline, 30 to 40 percent plagioclase, and 15 to 20 percent quartz with 5 to 7 percent orthopyroxene, 0 to 2 percent amphibole, 0 to 5 percent biotite, and rare garnet. Accessory minerals include apatite, zircon, and ilmenite. Foliation is defined by discontinuous, centimeter-scale domains composed of ferromagnesian minerals. Dikes composed of coarse-grained, nonfoliated alkali feldspar+blue quartz, that range up to 1 m (3.3 ft) in width, and coarse-grained, nonfoliated garnet-bearing leucogranite, that range up to 1.5 m (4.9 ft) in width, locally intrude monzogranite and are typically oriented parallel to foliation. The strong foliation defined by discontinuous clusters of minerals sets this lithologic unit apart from all other charnockites in the area. Overall grain size is greatly reduced, and mineralogic segregation becomes less pronounced where the pluton is affected by deformation along the Stanley fault.

Rocks analyzed from the Yfpg pluton exhibit a range in SiO_2 content of 67 to 72 weight percent and are weakly peraluminous to borderline metaluminous (fig. 5D). The

composition of a sample collected from this outcrop for U-Pb geochronologic analysis is included in table 4 (sample SNP-02-177). The Yfpg rocks are geochemically similar to other, older high-silica charnockites, including the garnetiferous gneiss (Yg) and amphibole-bearing *charnockite* and *farsundite* (Ycf) (fig. 5). Trace-element data indicate that, like these rocks, Yfpg was probably derived from sources of mixed composition.

Zircons analyzed from a sample collected from this outcrop are isotopically complex and provide considerable insight into the regional geologic history. Analyses of zircon cores provide a weighted average age of 1,178±14 Ma, which we interpret as indicative of inheritance. Analyses of zoned mantles indicate a likely crystallization age of 1,115±13 Ma, which is interpreted as the time of pluton emplacement. Analyses of rim overgrowths indicate ages of 1,050±13 Ma and ~1,010 Ma. The 1,115-Ma emplacement age indicates that the Yfpg pluton intruded nearly contemporaneously with the 1,111-Ma Marshall Metagranite, a lithologically complex noncharnockitic granitoid that occurs in the Blue Ridge approximately 32 km (20 mi) to the northeast, and which was dated by Aleinikoff and others (2000) using ID-TIMS techniques. The local significance of this magmatic episode is not yet understood; however, McLelland and others (1996) suggested that magmatism of similar age in the Adirondacks resulted from far-field effects of activity associated with development of the Midcontinent Rift. The 1,178-Ma inherited age of the Yfpg pluton corresponds closely to the age of megacrystic leucocratic granite gneiss (Ylg) that occurs in the southern part of the field trip area and suggests that crust produced during the earlier magmatic episode was partly recycled during subsequent magma genesis. Finally, the overgrowth ages of 1,050 and 1,010 Ma are each considered to preserve evidence of thermal disturbance. The former age corresponds to the timing of the final magmatic episode in the Blue Ridge, during which rocks such as the Old Rag magmatic suite (Ygr) and low-silica charnockite (Yfqj) were emplaced, and the 1,010-Ma date falls within the range of a possible heating event for which evidence is preserved as overgrowths on zircons from other basement rocks in the Blue Ridge (table 3) (Tollo and others, in press a).

Mileage

Trip Cumulative	Stop-to-Stop Cumulative	
	0.0	Proceed north on Va. 628.
96.6	1.4	Turn left to continue on Va. 628 at intersection with Va. 606.
97.4	2.2	Turn right onto Va. 628 at (poorly marked) four-way intersection.
99.3	4.1	Turn left onto Va. 630, which becomes unpaved.
101.2	6.0	Stop 12.
		Outcrop on left side of Va. 630 before bridge.

Stop 12. Flint Hill Gneiss (Yfh).

The Flint Hill Gneiss constitutes a distinct lithologic unit that underlies a large, elongate area of the Blue Ridge basement core east of the Sperryville high-strain zone in northern Virginia (Virginia Division of Mineral Resources, 1993). The rock is characterized by a strongly developed gneissic fabric and abundance of typically blue quartz. The unit has not been dated by modern isotopic techniques, but the strongly deformed fabric suggests that it is likely part of the oldest group of basement rocks in the region.

The Yfh lithologic unit includes dark-gray, medium- to coarse-grained, inequigranular, strongly foliated syeno- to monzogranitic gneiss composed of 35 percent microcline, 20 percent plagioclase, and 20 percent quartz with 2 percent biotite and 5 percent chlorite. Accessory and secondary minerals include apatite, leucoxene, zircon, and ilmenite. Gneissic layering is defined by alternating quartz+feldspar-rich and biotite+chlorite-rich domains that are typically 1 to 10 cm (0.4–4 in) in thickness. Foliation is defined by planar alignment of biotite and is parallel to gneissic layering. Granular quartz ranges from dark gray to blue; locally abundant quartz veins are typically blue. The characteristic composi-

tional banding in the gneiss is commonly contorted and kinked (Clarke, 1984), preserving visible evidence of the high degree of deformation that has affected this unit. Veins composed primarily of blue quartz and dikes composed of fine- to medium-grained leucocratic granite are common within the Flint Hill Gneiss. Clarke (1984) reported that the widespread blue quartz veins are generally conformable to gneissic layering, whereas dikes typically crosscut banding.

The Flint Hill Gneiss is characterized by SiO_2 contents that are generally in the range of 69 to 72 weight percent (table 4; fig. 5). Limited sampling of Flint Hill rocks suggests that a lower silica variant with SiO_2 contents about 64 weight percent is present in nearby quadrangles. The rocks are generally mildly peraluminous, consistent with the ubiquitous presence of biotite. Normative compositions and trace-element characteristics and occurrence of this lithologic unit within a terrane that is otherwise dominated by rocks of intrusive magmatic origin suggest that the Flint Hill Gneiss is meta-igneous in origin. Results from previous geochronologic investigations involving U-Pb isotopic analysis of zircons from the Flint Hill Gneiss are considered unreliable due to the isotopic complexities that have been documented in zircons from other Grenvillian rocks in the area (Aleinikoff and others, 2000; Tollo and others, in press a).

Mileage

Trip Cumulative	Stop-to-Stop Cumulative	
	0.0	Turn around and proceed east on Va. 630.
103.1	1.9	Turn left to continue on Va. 630.
103.9	2.7	Turn right onto U.S. 522 and proceed south through the town of Flint Hill.
108.7	7.5	Turn right onto U.S. 522/U.S. 211 and proceed west.
116.7	15.5	Turn left onto U.S. 522/Va. 231 in Sperryville and proceed south. Cross bridge over the Thornton River.
116.8	15.6	Turn left to remain on U.S. 522 and proceed southeast.
117.4	16.2	Turn right onto Va. 231 and proceed south.
126.6	25.4	*Old Rag Mountain is visible to the west (right). The mountain, formerly called "Old Raggedy," is characterized by steep rocky slopes and is a popular local recreational destination. The mountain is underlain by typically coarse-grained, locally garnet-bearing leucogranite of the Old Rag magmatic suite, defining a fault-bounded pluton.*
132.5	31.3	Turn right onto Va. 670 and proceed west. *View toward the west (straight ahead) of Double Top Mountain, which is underlain primarily by amphibole-bearing low-silica charnockite (Yfqj).*
133.3	32.1	Stop 13. Follow Trip Leaders. PRIVATE PROPERTY

Stop 13. Biotite Granitoid Gneiss (Ybg) containing xenoliths of medium-grained foliated leucocratic granitoid (Ylg).

Medium- to coarse-grained biotite granitoid gneiss and layered granitoid gneiss, mapped together within a single lithologic unit (Ybg), underlie a large area east of the Quaker Run fault zone in the northern part of the Madison 7.5-minute quadrangle (fig. 3). This mineralogically distinctive unit, and other similarly biotite-rich rocks mapped east of the Rockfish Valley fault zone in areas of the Blue Ridge province located to the south (Hughes and others, in press), contrast sharply with the more typical granites, leucogranites, and charnockitic rocks that underlie much of the area. Pegmatites associated with the Old Rag Granite pluton appear to cut biotite granitoid gneiss along the southeastern margin of the body southeast of Old Rag Mountain (Hackley, 1999), indicating that the peraluminous leucogranitoids of the Old Rag magmatic suite are likely younger than the Ybg rocks. Dikes of probable Ybg affinity intrude leucogranite gneiss (Ylg) at Stop 15 and elsewhere

Figure 11. Photograph of xenolith of medium- to coarse-grained foliated leucocratic granitoid (Ylg) within foliated medium-grained biotite granitoid gneiss (Ybg) at Stop 13. Hammer handle, oriented parallel to foliation in the gneiss, is 82 cm (32 in) long.

in the Madison area, indicating that Ybg is younger than the Ylg lithologic complex.

The Ybg unit includes gray to grayish-black, medium- to coarse-grained, massive to foliated, biotite granitoid containing a dominant mineral assemblage of alkali feldspar+plagioclase+quartz+biotite. The unit also contains medium- to coarse-grained, layered granitic gneiss with 1- to 3-cm (0.4–1.2-in)-thick felsic domains composed of plagioclase+alkali feldspar+quartz separated by weakly developed layers of biotite+epidote+quartz (Bailey and others, 2003). Biotite typically constitutes 15 to 25 percent of the rock. This outcrop exposes protomylonitic biotite granitoid gneiss containing porphyroclasts of white feldspar and elongate quartz lenses. Abundant biotite+epidote bands define a foliation that strikes 020° and dips steeply to the east. The mineralogic assemblage defining this foliation is indicative of formation at greenschist-facies conditions and suggests that the fabric was developed during Paleozoic orogenesis.

Geochemical data indicate that the Ybg lithologic unit is characterized by a bimodal range in silica contents, with compositions corresponding to SiO_2 values of 61 to 63 and 67 to 68 weight percent (fig. 5). The rocks are metaluminous to mildly peraluminous (fig. 5D), and display trace-element characteristics such as high concentrations of high-field-strength elements and modestly high Ga/Al ratios that suggest affinity to A-type granites (figs. 6, 7). These compositional characteristics and the overall tholeiitic and subalkaline nature of the rocks suggest that Ybg rocks were likely igneous in origin.

Xenoliths of foliated medium- to coarse-grained leucocratic granitoid, interpreted to be derived from the Ylg lithologic unit, occur within the foliated biotite granitoid gneiss at this locality (fig. 11). Foliation defined by alignment of feldspar megacrysts and discontinuous compositional banding involving recrystallized quartz within the xenoliths is oriented at an angle to foliation in the surrounding biotite granitoid gneiss. This relation, and the likely higher-temperature ductile origin of foliation within the xenoliths, suggests that the fabric in the leucogranite formed during Grenvillian orogenesis. This field relation is consistent with the presence of dikes of Ybg affinity that cut Ylg rocks elsewhere in the vicini-

ty, and thus provides a maximum age constraint of 1,183±11 Ma (age of emplacement for part of the Ylg lithologic complex) for emplacement of protolith magmas for the Ybg rocks.

Mileage

Trip Cumulative	Stop-to-Stop Cumulative	
	0.0	Continue west on Va. 670 through Criglersville.
134.1	0.8	*Outcrops within and adjacent to the riverbed on the left expose contact relations between the Ylg and Ybg lithologic units (Bailey and others, 2003).*
134.3	1.0	Turn left onto Va. 649 (Double Top Road.)
136.8	3.5	Becomes dirt road.
137.3	4.0	Stop 14. Pull over to the right at hairpin turn.

Stop 14. Low-silica charnockite (Yfqj) and mylonite in the Quaker Run high-strain zone.

Amphibole-bearing low-silica charnockite (Yfqj) ranging from monzogranite (*farsundite*) to quartz monzodiorite (*quartz jotunite*) in normative composition (fig. 4) is widespread throughout the field trip area, constituting a large pluton located east of the crest of the Blue Ridge. Similar rocks also occur as dikes and small plutons in areas located to the north. The characteristic nonfoliated to weakly foliated fabric of this rock unit indicates that it is part of the youngest group of Grenvillian plutonic rocks in this part of the Blue Ridge.

The outcrop at the sharp bend in the road is an outstanding example of a fresh, massive, coarse-grained charnockite. This lithologic unit is composed of dark-gray to dark-gray-green, medium- to very coarse-grained, equigranular to inequigranular, massive to weakly foliated monzogranite, granodiorite, and quartz monzodiorite (*farsundite*, *opdalite*, and *quartz jotunite*) composed of 9 to 30 percent alkali feldspar microperthite (chiefly microcline), 30 to 49 percent plagioclase, and 14 to 26 percent quartz with 10 to 17 percent orthopyroxene, 0 to 7 percent amphibole, and rare clinopyroxene. Accessory minerals include apatite, ilmenite, magnetite, zircon, epidote, and actinolite. Rare, typically weakly developed foliation is defined locally by planar alignment of ferromagnesian minerals. Lenticular, magnetite-rich enclaves, which range in length to 0.5 m (20 in), occur locally and are aligned parallel to foliation. Subhedral to euhedral, monocrystalline alkali feldspar megacrysts range up to 10 cm (4 in) in length and are best observed on weathered surfaces. The rock typically weathers to form a distinct orange rind and similarly colored, clay-rich soils that are useful in mapping. This outcrop is located within the Quaker Run high-strain zone (fig. 3) (Bailey and others, 2003), as indicated by fabric observed in other exposures along the road where undeformed charnockite grades into mylonite with multigranular feldspar porphyroclasts and elongate quartz ribbons. The occurrence of undeformed rock within highly strained rocks illustrates the heterogeneous nature of strain within the Quaker Run high-strain zone. The northwestern boundary of the high-strain zone is clearly defined by massive charnockite; however, the southeastern boundary is more difficult to define due to the abundance of phyllosilicates and the foliated nature of the biotite granitoid gneiss (Ybg).

The compositionally diverse Yfqj lithologic unit is characterized by relatively low silica contents (51 to 65 weight percent SiO_2) that distinguish the unit from most of the other, typically high-silica Grenvillian rocks in the area (fig. 5). The rocks are generally metaluminous and exhibit subalkaline tholeiitic characteristics (fig. 5D–F). The Yfqj rocks are also distinguished compositionally by relatively high Ga/Al ratios and concentrations of high-field-strength elements, including Y, Nb, and Zr (figs. 6, 7). These features, especially the high concentrations of both Zr and Nb, distinguish this unit from nearly all other rocks studied in the area, and suggest geochemical affinity to A-type granitoids (Eby, 1990;

Whalen and others, 1987) and within-plate granitoids (Pearce and others, 1984). These features suggest that Yfqj magmas were derived from dominantly crustal sources (Landenberger and Collins, 1996), in contrast to the typically mixed heritage that characterizes most other units in the region (Tollo and others, in press a).

Yfqj charnockite is locally cut by dikes of coarse-grained leucogranite that are likely related to the 1,060±5-Ma Old Rag Granite (Tollo and others, in press a,b). The characteristic unfoliated to weakly foliated fabric of both units indicates that the rocks were emplaced after the major episode of deformation that affected the 1,078±9-Ma leucogranite gneiss (Ylgg) unit. Analysis of a sample of the Yfqj pluton collected from the Fletcher 7.5-minute quadrangle indicates that the euhedral to subhedral prismatic zircons contain (1) cores distinguished by oscillatory zoning that likely reflects compositional variation resulting from igneous crystallization and (2) unzoned rims that typically contain higher U concentrations than the cores (Tollo and others, in press a). Tollo and others (in press a) reported results from 18 analyses of cores that yielded a weighted average of the $^{207}Pb/^{206}Pb$ ages of 1,050±8 Ma, which they interpreted as the time of igneous crystallization of the charnockite. Five analyses of the overgrowths indicated a subsequent episode of thermal flux related to metamorphism at 1,018±14 Ma. The 1,060±5-Ma emplacement age of the Old Rag Granite overlaps the emplacement age of the charnockite and, considering the crosscutting field relations documented in the area, suggests that the magmatic protoliths of these rocks intruded over possibly extended, penecontemporaneous intervals.

Mileage

Trip Cumulative	Stop-to-Stop Cumulative	
	0.0	Turn around and proceed downhill along Va. 649.
140.1	2.8	Turn right onto Va. 670 and proceed southeast.
141.4	4.1	*Outcrops in river are biotite granitoid gneiss (Ybg).*
142.0	4.7	Turn right onto Va. 231 and proceed southeast.
142.5	5.2	Intersection with Va. 609. Bridge across the Robinson River.
142.7	5.4	*Outcrop to the south exposes the eastern contact of the Mechum River Formation and Ylg lithologic unit.*
143.0	5.7	Turn right onto Va. 651 (Aylor Road). *Outcrops in the field to the left expose biotite granitoid gneiss (Ybg) near the intrusive contact with alkali feldspar syenite of the Neoproterozoic Robertson River batholith (Bailey and others, 2003).*
145.9	8.6	Bear right to remain on Va. 651.
146.5	9.2	Stop 15. Follow Trip Leaders PRIVATE PROPERTY

Stop 15. Ylg basement complex exposed in debris-flow scar.

The dominant rock types in this exposure constitute a composite felsic pluton composed of multiple lithologies including (from oldest to youngest): (1) foliated, coarse-grained to megacrystic leucocratic granite (Ylg1), (2) medium-grained, equigranular, weakly to moderately foliated leucogranite (Ylg2), and (3) coarse-grained to very coarse-grained, inequigranular, nonfoliated to weakly foliated leucogranite pegmatite (Ylg3). Because of similarities in mineral assemblage and geochemical composition, these distinctive rocks are collectively mapped as the Ylg lithologic unit in the southern part of the field trip area (Bailey and others, 2003; Tollo and others, in press b).

Although dominantly leucogranitoids, constituent lithologic units of the Ylg plutonic complex exhibit minor differences in mineral assemblage. The strongly foliated, megacrystic leucocratic granite is composed of alkali feldspar mesoperthite (both microcline and orthoclase), plagioclase, quartz, and intergrown biotite+chlorite, whereas the medium-

Figure 12. Photograph of folded medium-grained leucocratic granite dike within coarse-grained to megacrystic leucocratic granitoid at Stop 15. Pen (top center), oriented parallel to foliation in the megacrystic granitoid and parallel to the trace of the axial plane in the folded dike, is 14 cm (5.5 in) long. Development of small lens of pegmatite within the dike on the left limb of the fold suggests that pegmatite was derived through differentiation of the medium-grained granitoid magma.

grained, equigranular, weakly to moderately foliated leucogranite is composed of alkali feldspar (chiefly microcline), plagioclase, and quartz with minor secondary biotite; and the nonfoliated to weakly foliated leucogranite pegmatite is composed of alkali feldspar (microcline), minor plagioclase, and quartz. These mineralogic differences, especially the progressive decrease in biotite content, reflect a weak trend toward more evolved chemical compositions.

This large exposure illustrates crosscutting relations among several Blue Ridge basement units. Field relations indicate that the foliated coarse-grained to megacrystic leucocratic granite is the oldest rock at this outcrop. Dikes exposed in some of the steep ledges indicate that the megacrystic granite was intruded by medium-grained leucogranite that was subsequently folded with axial planes that are nearly parallel to foliation in the coarse-grained megacrystic granitoid (fig. 12). Very coarse-grained leucogranite pegmatite occurs as locally boudinaged dikes cutting both the coarse-grained leucocratic granitoid (Ylg1) and medium-grained equigranular leucogranite (Ylg2). Local development of leucogranitic pegmatite within medium-grained leucogranite (fig. 12) further suggests that the pegmatite was derived through differentiation of medium-grained leucogranite magma. A 30- to 50-cm (12–20-in)-wide dike of fine- to medium-grained biotite granodiorite intrudes all of the leucocratic granitoid units in ledges located near the base of the exposure. This dike, which contains a mineral assemblage that is similar to biotite granitoid gneiss (Ybg), clearly post-dates the deformation recorded in the leucocratic rocks, and suggests that Ybg is younger than Ylg, a relation that is consistent with field relations observed at Stop 14.

At the base of the outcrop a ~15-cm (6-in)-thick dike of coarse-grained pegmatite cuts medium-grained leucogranite and is deformed into a series of tight folds with rounded hinges (fig. 13). The medium-grained leucogranite displays weak foliation that strikes ~070°, dips steeply to the northwest, and is axial planar to the folds in the leucogranite dike. Line-length restoration of the dike indicates ~70 percent shortening in a north-north-

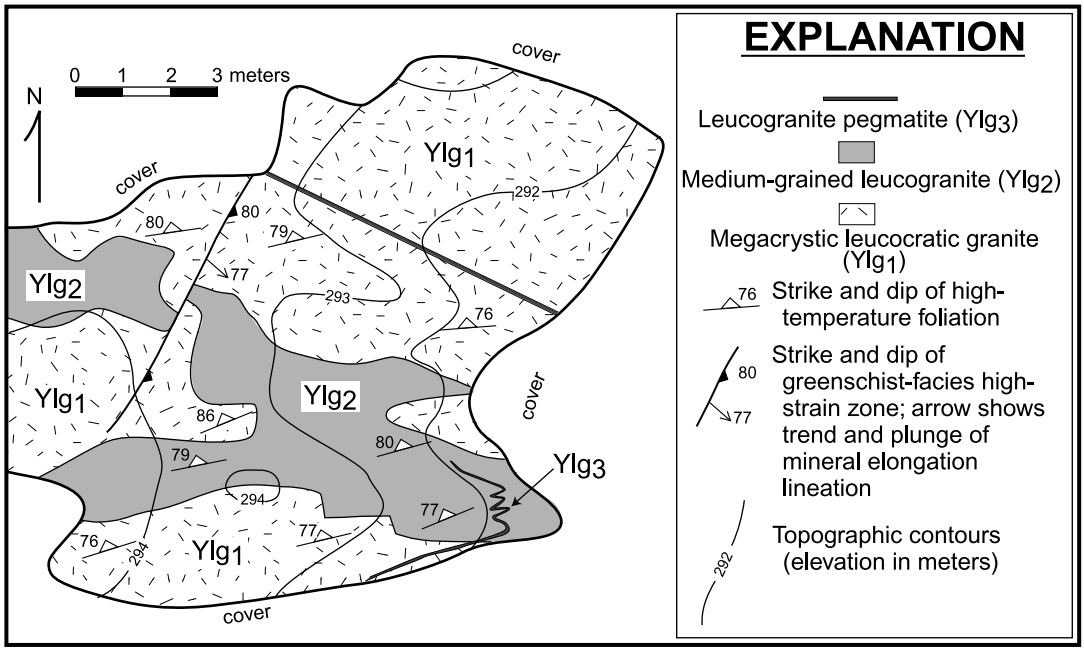

Figure 13. Detailed geologic map of outcrop exposed at the base of debris-flow scar at Stop 15.

west–south-southeast direction, but the fabric in the enclosing leucogranite is barely visible. We interpret the medium-grained leucogranite to have statically recrystallized at high temperatures after deformation, and thus it does not faithfully record the total strain history. The high-temperature deformation recorded in the pegmatite is interpreted to be Mesoproterozoic in age and is commonly overprinted by a foliation defined by aligned micas. Crosscutting relations observed throughout the exposure are interpreted to indicate multiple episodes of magmatic injection occurring throughout an extended interval of time.

Basement units are cut by a northeast-striking, ~5-m (16-ft)-wide dike of porphyritic hornblende metagabbro. The metagabbro is composed of hornblende, extensively altered plagioclase, epidote, and chlorite. The dike is part of a suite of mafic to ultramafic igneous rocks that intrude Blue Ridge basement and Neoproterozoic metasedimentary units and which are interpreted to be associated with an early, pre-Catoctin pulse of Neoproterozoic rifting (Bailey and others, 2003).

A set of discrete high-strain zones cuts all basement units in this exposure. These zones range from a few centimeters in thickness to millimeter-scale. Where discernible, mineral elongation lineations plunge obliquely downdip. The apparent offset, as illustrated on the subhorizontal outcrop surface, is dextral. However, there clearly was out-of-section movement as well. The mineralogy and microstructures in the high-strain zones are consistent with formation at greenschist-facies conditions and are interpreted to result from Paleozoic contraction.

U-Pb isotopic analysis of zircons from foliated megacrystic granitoid collected from this exposure indicate igneous crystallization at 1,183±11 Ma, followed by metamorphic recrystallization at 1,043±16 Ma and ~1,110 Ma (table 3, sample SNP-02-189). These data indicate that Ylg is currently the oldest lithologic unit recognized in the area. Chemical analyses of samples collected from both the medium-grained and megacrystic leucocratic granitoids indicate that the rocks are characterized by SiO_2 contents of 69 to 77 weight percent, with most compositions in the range of 74 to 76 weight percent (table 4, fig. 5). Such chemically evolved compositions are similar to those of the much younger, ~1,060-Ma leucocratic granitoids of the Old Rag magmatic suite (Ygr) and garnetiferous alkali feldspar granite (Ygg), and thus suggest that production of leucogranite magmas was cyclic. Compositions of Ylg samples differ from the younger leucocratic rocks in having lower concentrations of Y+Nb (fig. 6), a characteristic that suggests derivation from different sources.

Mileage

Trip Cumulative	Stop-to-Stop Cumulative	
	0.0	Turn around and return east along Va. 651.
147.0	0.5	Turn right onto Va. 652 (Gaar Mountain Road).
149.3	2.8	Turn right onto Va. 656 (Ruth Road).
149.7	3.2	First intersection (Ruth Road and Courtney Hollow Lane).
150.0	3.5	Stop 16.
		Follow Trip Leaders
		PRIVATE PROPERTY

Stop 16. Nonfoliated coarse-grained alkali feldspar granite (Yaf).

Nonfoliated, coarse-grained alkali feldspar granite (Yaf) defines two small (< 1 km^2; 0.4 mi^2) plutons located within foliated biotite granitoid gneiss (Ybg) east of the Mechum River Formation in the southern part of the Madison 7.5-minute quadrangle (fig. 3). This lithologic unit includes gray-white, coarse-grained, equigranular to porphyritic alkali feldspar granite composed of 1- to 5-cm (0.5–2.0-in) white alkali feldspar+blue-gray quartz with minor plagioclase, biotite, titanite, and Fe-Ti oxide minerals (Bailey and others, 2003).

Anastomosing high-strain zones (up to 30 cm (12 in) thick) composed of well-foliated, mica-rich mylonite and ultramylonite locally cut the coarse-grained leucogranite. Detailed kinematic, fabric, and chemical analysis of the largest high-strain zone suggests bulk isochemical (isovolumetric?) behavior, modest flattening strains, and a general shear deformation with monoclinic symmetry (Bailey and others, in press).

The nonfoliated fabric and abundant alkali feldspar+quartz mineral assemblage of the Yaf unit indicates that these bodies are likely correlative with the group of postorogenic leucocratic granitoids documented to the north that includes the Old Rag magmatic suite (Ygr) and garnetiferous syenogranite (Ygg), which have emplacement ages of 1,060±5 Ma and 1,064±7 Ma, respectively (table 3). Consistent with this correlation, alkali feldspar granite dikes of Yaf affinity that range in width from 0.1 to 3 m (0.3–10 ft) cut both the leucocratic granitoid complex (Ylg) and the biotite granitoid gneiss (Ybg) (Bailey and others, 2003).

Mileage

Trip Cumulative	Stop-to-Stop Cumulative	
	0.0	Turn around and proceed east on Va. 656.
		Continue straight at intersection with Va. 652.
154.0	4.0	Turn right onto Main Street.
154.1	4.1	Intersection with Va. 634 (Washington Street); continue straight.
155.1	5.1	Merge onto U.S. 29 (Seminole Trail) and proceed south.
157.0	7.0	Turn right onto Va. 230 (Wolftown-Hood Road) and proceed west.
160.6	10.6	Turn right onto Va. 622 (Graves Mill Road).
162.1	12.1	Turn left onto Va. 665 (Garth Run Road).
162.9	12.9	Turn right to remain on Va. 665.
		Kirtley Mountain, visible to the west, was the site of numerous debris flows in the 1995 storm that affected this area. The large exposures of bedrock in the denuded channels visible from the highway are composed dominantly of amphibole-bearing low-silica charnockite (Yfqj) (Tollo and others, in press b).

164.3	14.3	Stop 17. Pull over south of the bridge over Garth Run. Proceed to exposures in stream valley.

Stop 17. Mylonitic rocks of the Garth Run high-strain zone.

The Garth Run high-strain zone is well exposed in a 200-m (650-ft)-long outcrop scoured out along the channel of Garth Run during the June 1995 storm. This exposure has proven to be seminal to our understanding of ductile deformation in the Blue Ridge. The high-strain zone strikes north-northwest to north-northeast and joins the 1- to 2-km (0.6–1.2-mi)-wide Quaker Run high-strain zone to the north and tips out to the south (Berquist and Bailey, 2000). Although the high-strain-zone boundary is not exposed, outcrop data indicate the zone is approximately 125 m (410 ft) thick). The zone is bounded to the west by medium- to coarse-grained, equigranular to porphyritic charnockite (Yfqj), and to the east by rocks of the leucogranite complex (Ylg). Medium-grained layered granitic gneiss is the dominant rock type east of the Garth Run high-strain zone. The gneiss is intruded by a series of fine- to coarse-grained leucogranite dikes ranging from 0.3 to 5 m (1–16 ft) in thickness.

Rocks exposed in the Garth Run high-strain zone are dominantly porphyroclast-bearing protomylonites and mylonites. Finely-layered mylonitic leucogneiss, leucogranite, and well-foliated fine-grained metabasalt occur as tabular to lenticular bodies that are 0.2 to 2 m (0.6–6.5 ft) thick throughout the high-strain zone. These tabular bodies are both subparallel and slightly discordant to the foliation. Foliation, defined by mica-rich surfaces, elongate quartz grains, and fractured feldspars, strikes 345° to 010° and dips 30 to 50° to the east. A mineral elongation lineation plunges downdip or obliquely to the east-northeast; however, mineral elongation lineations are not present everywhere.

Sheath folds occur in the finely-layered mylonitic leucogneiss and sheath axes plunge moderately to the east, parallel to the mineral elongation lineation. Coarse-grained leucogranitic bodies display pinch-and-swell structures, and are commonly isolated as lozenge-shaped boudins surrounded by porphyroclastic mylonites. Leucogranitic boudins record elongation both parallel and normal to the east-northeast-plunging elongation lineation, indicating bulk extension in both the *Y* and *X* directions. Leucogranites have a weak foliation and are cut by numerous transgranular fractures. Slightly discordant, tabular, boudinaged leucogranitic dikes are locally folded. At a few locations, the mylonitic foliation is kinked into narrow bands that are 2 to 5 cm (0.8–2.0 in) wide.

Asymmetric structures such as sigma and delta porphyroclasts, shear bands, and asymmetric boudins are common in the Garth Run high-strain zone. Asymmetric structures, both parallel (reverse sense of shear) and perpendicular (sinistral sense of shear) to the mineral elongation lineation, are consistent with triclinic deformation symmetry. Sectional strains estimated from discrete quartz lenses and ribbons range from 3:1 to 23:1. Three-dimensional strains record apparent flattening. The kinematic vorticity number was estimated using the porphyroclast hyperbolic distribution method of Simpson and De Paor (1993) on ultramylonite thin sections and joint faces with well-exposed porphyroclasts. W_n-values range from 0.6 to 0.4, indicating general shear deformation. Shear strain is conservatively estimated at 4 and integrates to a total displacement of ~500 m (1,640 ft) across the Garth Run high-strain zone. Discrete brittle faults with displacements of 0.2 to 2 m (8–79 in) cut the mylonitic fabrics.

Folded leucogranite boudins may offer a clue about the progressive deformation history of the Garth Run high-strain zone. These structures formed when competent leucogranite dikes were first elongated and then shortened. During progressive steady-state deformation, material rotated from the field of shortening into the field of extension, a progression that did not fold boudins. Folded boudins are generally interpreted to develop by polyphase deformation, such that material elongated during the first deformation is shortened by a second deformation having a different orientation. However, a change in the incremental vorticity will cause some material that was originally deformed in the field of extension to

move into the field of shortening. There are no crosscutting ductile fabrics in the Garth Run high-strain zone. Bailey and others (in press) proposed a model in which the dominant mechanism of deformation changed from simple shear to pure shear over time.

Mileage

Trip Cumulative	Stop-to-Stop Cumulative	
	0.0	Turn around and proceed south on Va. 665.
165.7	1.4	Turn left to remain on Va. 665.
166.4	2.1	Turn left onto Va. 622 (Graves Mill Road) and proceed north.
167.4	3.1	*View of debris-slide scars to the east on German Mountain.*
170.2	5.9	Graves Mill.
		Continue straight onto Va. 615 (Bluff Mountain Road).
171.4	7.1	Stops 18 and 19.
		Pull into parking area on right side of Va. 615.

Stop 18. Kinsey Run, west branch: low-silica amphibole-bearing charnockite (Yfqj) and associated pegmatite; mylonite, and protomylonite.

Stops 18 and 19 are located about 2 km (1.2 mi) uphill from the road and can be reached by hiking along a logging trail to the upper reaches of Kinsey Run. The stops include the denuded channels caused by mass-wasting processes resulting from the intense rainfall that affected the area in June 1995. The stops are located on two branches of Kinsey Run that were significantly widened by the debris flows. Stop 19 can be reached from the logging trail by hiking eastward from the west branch over the drainage divide to the east branch.

Both stops are located within medium- to very coarse-grained, equigranular to inequigranular, massive to weakly foliated, amphibole-bearing low-silica charnockite (Yfqj) that defines a large pluton in the southern part of the field trip area (fig. 3). The generally nonfoliated fabric of the charnockite indicates postorogenic emplacement and is consistent with the 1,050±8-Ma age determined by U-Pb isotopic analysis (Tollo and others, in press a; table 3). Microstructural characteristics also indicate emplacement within a post-deformation environment. Quartz grains (2–7 mm), which compose 15 to 25 modal percent of the rock, are bleb-like and display no grain-shape preferred orientation, attesting to the relatively undeformed nature of the charnockite. Orthopyroxene exhibits partial alteration to a mixture of fine-grained uralitic amphibole+secondary biotite that is localized along grain boundaries and most likely indicative of Paleozoic retrograde metamorphism.

The Yfqj charnockite in the main area of exposure contains several decimeter- to meter-size pods of coarse-grained amphibole+magnetite-bearing pegmatite that generally grades into the surrounding medium- to coarse-grained charnockite. The mineral assemblage within these pegmatite pods is similar to the surrounding charnockite. Moreover, amphiboles in these pegmatites are characterized by edenitic (nomenclature after Leake and others, 1997) compositions that are similar to amphiboles within the surrounding charnockite, indicating that the pegmatites are most likely derived from the charnockitic magmas through local fluid saturation and differentiation.

Three subvertical mafic dikes, striking ~350°, are exposed intruding the charnockite (fig. 14). Contacts are well exposed and display both chilled margins and fragments of country rocks that indicate emplacement under brittle conditions. The dikes are composed of clinopyroxene+plagioclase±pigeonite, with minor amounts of magnetite, chlorite, actinolite, biotite, and quartz. The presence of pigeonite is especially characteristic of dikes of Mesozoic age (Wilson and Tollo, 2001), and is consistent with the whole-rock chemical compositions that indicate high SiO_2 and relatively low TiO_2 contents (table 5, samples SNP-99-7, -8, and -9) compared to metabasalt of the Neoproterozoic Catoctin Formation.

Figure 14. Photograph of three mafic dikes (darker colored rocks) of probable Mesozoic age cutting low-silica charnockite at Stop 18. Middle dike is about 2 m (80 in) wide.

These dikes are part of a widespread suite of Jurassic (~200 Ma) igneous bodies that intruded Blue Ridge, Piedmont, and Valley and Ridge country rocks during early Mesozoic rifting. In contrast, an east-west-striking greenstone dike that occurs in outcrops located below the main bedrock exposure contains highly altered orthopyroxene phenocrysts and abundant retrograde chlorite+epidote+actinolite. The low SiO_2 and high TiO_2 content of this dike (sample SNP-99-6 in table 5) is similar to the composition of Catoctin greenstones and suggests a Neoproterozoic age.

An approximately 30-m (98-ft)-wide high-strain zone is exposed in the channel above the diabase dikes. This zone strikes ~080° and dips steeply to the northwest (fig. 15). The zone is bounded by charnockite that passes into protomylonite and mylonite within the high-strain zone. Two deformed metabasalt dikes occur within the zone and strike subparallel to the zone boundary (fig. 15). Foliation internal to the high-strain zone dips steeply to both the northwest and southeast, and a downdip mineral elongation lineation occurs at a few locations. Asymmetric kinematic indicators generally display a reverse sense of shear on foliation normal and lineation parallel sections. Protomylonite and mylonite developed within the charnockite are composed of 30 to 50 percent quartz, 10 to 25 percent fine-grained muscovite, 10 to 20 percent alkali feldspar, 10 to 15 percent epidote, and 10 percent biotite. Feldspars are extensively fractured with quartz-filled cracks and muscovite mantles along grain boundaries. Quartz grains form monocrystalline lenses and ribbons with a moderate to strong crystallographic preferred orientation. The general lack of recrystallized quartz and the abundance of brittle microstructures in feldspar are consistent with greenschist-facies deformation conditions (T ~300–400°C). Undeformed charnockite, protomylonite, and mylonite are composed of approximately 61 percent SiO_2 and have nearly identical concentrations of other major elements. Although significant mineralogical changes occurred between the undeformed charnockite and mylonitic rocks, volume loss appears to be minimal (Bailey and others, in press).

Strain was estimated from monocrystalline quartz lenses and ribbons using standard R_f/f techniques: 16 to 40 grains were measured per sample, and strain in *XZ* sections averaged 3.8 (3.6–4.0, n=2) for the protomylonites and 5.8 (5.5–6.2, n=3) for the mylonites. Three-dimensional strains for all samples plot in the field of apparent flattening on a Flinn diagram, and mylonitic samples consistently have lower K-values than protomylonites (K=0.6 versus 0.8). In the *YZ* section (which approximates the outcrop surface), both metabasalt and epidotized leucocharnockite dikes exhibit pinch-and-swell structure or form boudins, consistent with true flattening strains and elongation parallel to *Y*. The kinematic vorticity number was estimated using the R_s/Q method. In both the protomylonite and mylonite, W_m=0.65. Integrating shear strains across the Kinsey Run high-strain zone yields a total displacement of 60±10 m (197±33 ft). These results indicate that the Kinsey Run high-strain zone experienced a weak triclinic flow characterized by flattening strains that developed under general shear conditions (Bailey and others, in press).

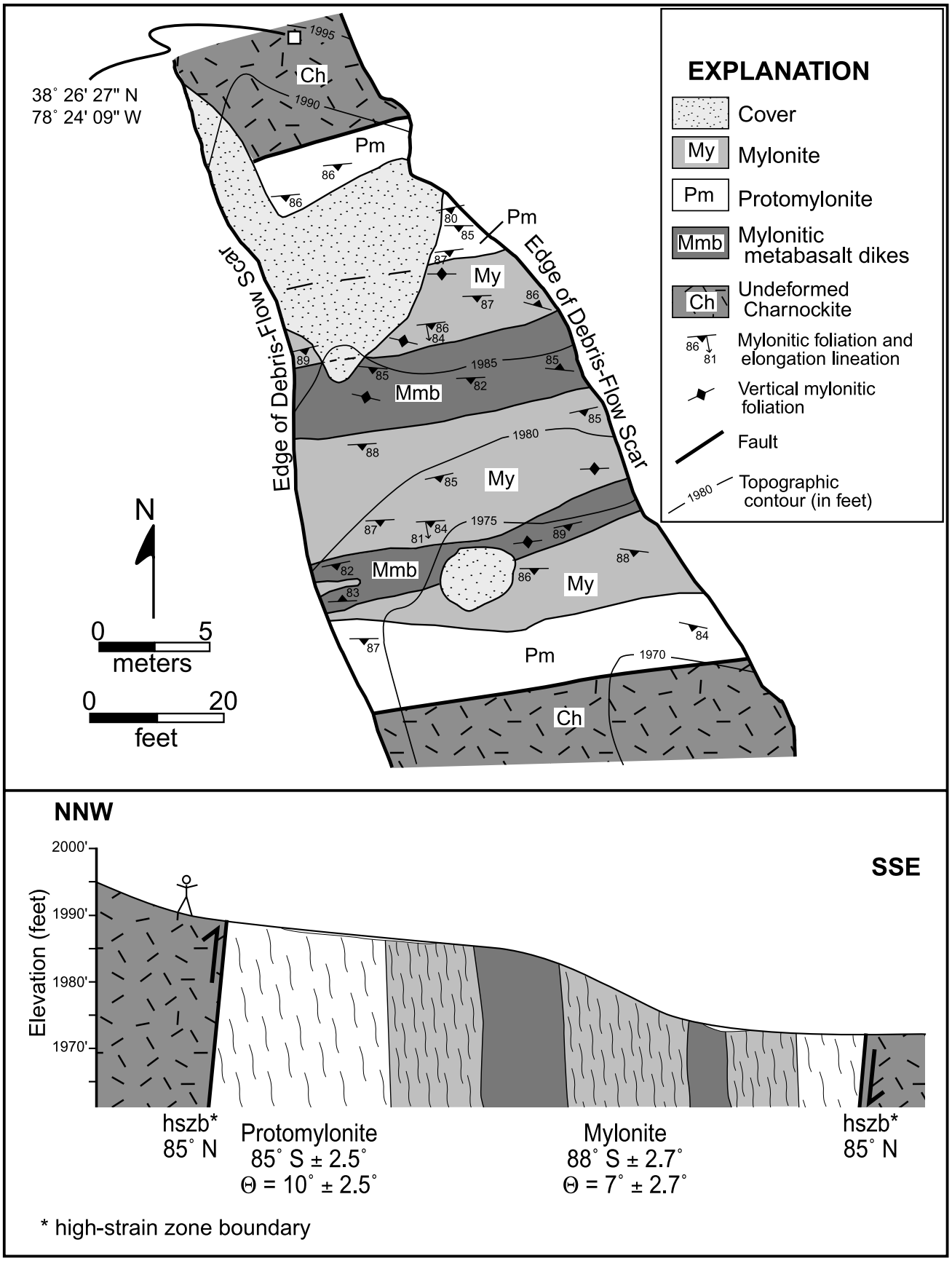
38° 26' 27" N
78° 24' 09" W
Ch
Pm
My
Mmb
1995
1990
1985
1980
1975
1970
Edge of Debris-Flow Scar
Edge of Debris-Flow Scar
N
0 5
meters
0 20
feet
EXPLANATION
Cover
Mylonite
Protomylonite
Mylonitic metabasalt dikes
Undeformed Charnockite
Mylonitic foliation and elongation lineation
Vertical mylonitic foliation
Fault
Topographic contour (in feet)
NNW
SSE
Elevation (feet)
2000'
1990'
1980'
1970'
hszb* 85° N
Protomylonite 85° S ± 2.5° Θ = 10° ± 2.5°
Mylonite 88° S ± 2.7° Θ = 7° ± 2.7°
hszb* 85° N
* high-strain zone boundary

Stop 19. Kinsey Run, east branch: Quaker Run high-strain zone.

This debris-flow scar, which exposes the base of the Quaker Run high-strain zone, is one of the largest created by the rainstorm in June 1995 (Morgan and others, 1999). Medium- to coarse-grained, massive to weakly foliated, low-silica charnockite (Yfqj) passes uphill into protomylonite and mylonite. The contact between undeformed charnockite and mylonitic rocks strikes to the northeast and dips moderately to the southeast. The angle between the foliation and high-strain-zone boundary is <10°. Mylonitic rocks are characterized by a southeast-plunging, downdip elongation lineation. Kinematic indicators, especially visible at this outcrop because of the vertical exposure, are plentiful and record top-to-the-northwest sense of shear. There are, however, numerous back-rotated porphyroclasts (mostly feldspar megacrysts), suggesting that this zone experienced general rather than simple shear. Leucopegmatite dikes are commonly oriented subparallel to foliation and exhibit pinch-and-swell structures along their margins. These competent dikes are cut by fibrous quartz-filled extension fractures. A 2- to 4-m (6.5–13.1-ft)-wide zone of fine-grained chlorite-bearing mylonite may be derived from a Neoproterozoic metabasalt dike.

The Quaker Run high-strain zone was defined by Berquist and Bailey (2000) for exposures a few kilometers to the north. At this latitude, the Quaker Run high-strain zone is the thickest (0.5–1.5 km; 0.3–0.9 mi) Paleozoic mylonite zone in the north-central Blue Ridge and can be traced for over 30 km (19 mi) parallel to the regional trend. Strain throughout the zone is very heterogeneous. On the basis of estimates of shear strain using values determined from other Blue Ridge mylonite zones, Berquist and Bailey (2000) estimated a total displacement of 1.5±0.5 km (4,900±1,650 ft) across the Quaker Run high-strain zone.

Mileage

Trip Cumulative	Stop-to-Stop Cumulative	
	0.0	Turn around and proceed east and south on Va. 615.
172.6	1.2	Intersection with Va. 622; continue south on Va. 622.
176.5	5.1	Bridge across the Rapidan River.
177.9	6.5	Turn right onto Va. 230 (Wolftown-Hood Road) and proceed west.
179.2	7.8	Bridge across the Rapidan River.
181.5	10.1	Bridge across the Conway River.
181.9	10.5	Turn right onto Va. 667 (Middle River Road) and proceed northwest.
185.2	13.8	*View on the right of home built in flood plain.*
185.6	14.2	Kinderhook.
		View on the right of the dredged riverbed and rocks piled on the embankment. Dredging was undertaken after the June 1995 flooding in order to deepen and widen the debris-choked channels.
187.5	16.1	Va. 667 becomes unpaved; continue north.
187.9	16.5	*Large outcrops in Conway River are leucogranite gneiss (Ylgg).*
188.4	17.0	Stop 20.
		Follow Trip Leaders
		PRIVATE PROPERTY

Stop 20. Leucogranite gneiss (Ylgg) xenoliths enclosed within nonfoliated low-silica charnockite (Yfqj).

Outcrops exposed at the base of the hill within the scoured channel of the Conway

Figure 15 (opposite page). Detailed geologic map showing ~30-m (100-ft)-wide high-strain zone exposed in debris-flow scar at Stop 18. Cross section shows structural relations approximately perpendicular to strike of units.

Figure 16. Photograph of strongly foliated leucogranite gneiss (Ylgg) xenolith within nonfoliated low-silica charnockite (Yfqj) at Stop 20. Hammer handle, oriented parallel to foliation in the leucogranite gneiss, is 82 cm (32 in) long.

River provide critical field relations and age information bearing on the timing of local Grenvillian deformation. The hill located on the east side of the river is underlain by light-greenish-gray, strongly foliated leucogranite gneiss (Ylgg) that defines an isolated screen within low-silica charnockite (fig. 3) (Tollo and others, in press a,b). The coarse- to very coarse-grained, inequigranular, strongly foliated leucogranite gneiss is composed of 80 percent alkali feldspar mesoperthite (chiefly microcline), <1 percent plagioclase, and 20 percent gray quartz with <1 percent biotite. Accessory minerals include ilmenite, magnetite, zircon, epidote, and muscovite. Locally prominent gneissic layering is defined by interlayered quartz+feldspar-rich and quartz-rich domains ranging from less than 3 cm (1.2 in) to greater than 13 cm (5 in). Foliation is locally defined by planar alignment of tabular mesoperthite megacrysts. Subhedral to euhedral, monocrystalline mesoperthite megacrysts range up to 10 cm (4 in) in length. Chemical analyses of the leucogranite gneiss collected from this riverside exposure indicate very high SiO_2 contents (74–75 weight percent) (table 4); however, low Y+Nb concentrations in one sample suggest that chemical alteration resulting from interaction between the xenoliths and surrounding charnockitic magma likely occurred. Although extensively altered in the outcrop, the nonfoliated charnockite contains the same mineral assemblage that is typical of the Yfqj lithologic unit. Two samples of charnockite collected from this exposure (samples SNP-99-91 and SNP-99-92 in table 4) generally plot with other data points from the Yfqj lithologic unit but are characterized by significantly different SiO_2 contents (table 4) that suggest that local chemical exchange occurred between the charnockite magma and leucogranite gneiss xenoliths.

The outcrops along the river channel display a crosscutting relation that is similar to the map pattern: xenoliths of strongly foliated leucogranite gneiss are enclosed within dark-gray-green, nonfoliated to weakly foliated, amphibole-bearing charnockite (Yfqj) that locally truncates the foliation of the leucogranite gneiss at the contacts of individual xenoliths (fig. 16). This relation is confirmed by U-Pb SHRIMP isotopic analyses of zircons. Subhedral, typically prismatic zircons in the leucogranite gneiss have broad cores charac-

terized by concentric, oscillatory zoning surrounded by distinct, unzoned rims. Thirteen analyses of cores yield a weighted average of the $^{207}Pb/^{206}Pb$ ages of 1,078±9 Ma, which is interpreted as the crystallization age of the igneous protolith (table 3) (Tollo and others, in press a). Analyses of a limited number of overgrowths suggest two periods of metamorphism at 1,028±10 Ma and 997±19 Ma (table 3). The occurrence of these foliated leucogranite gneiss xenoliths within the 1,050±8-Ma charnockite indicates that local deformation took place within the interval 1,078 to 1,050 Ma. The age of this Blue Ridge deformation partly overlaps the period of tectonomagmatic activity associated with Ottawan orogenesis in the Adirondacks that was constrained to the interval 1,090 to 1,035 Ma by McLelland and others (2001). As a result, ductile fabrics and gneissosity developed in the leucogranite gneiss and older units are interpreted to result from a possibly correlative period of orogenesis in the Blue Ridge.

End of Field Trip.